Lancaster University

Analysis of the Impact of GPX1 on Cancer and the Effect of GPX1 Stimulation and Inhibition in Human Cell Lines

Ruth Simpson

A thesis submitted to Lancaster University in fulfilment of the requirements for the degree

MSc by Research Biomedical Sciences

October 2021

Declaration

This dissertation is entirely my own work and has not been submitted in full or in part for the award of a higher degree at any other educational institution.

Word Count: 31648

Acknowledgements

First and foremost, I would like to thank my supervisors Sarah Allinson and Mike Coogan for their support in a most challenging academic year. I would also like to thank the Allinson, Copeland and Gadd lab groups for their help and advice.

I would finally like to thank Olivia Dunphy for being the most wonderful friend during this degree.

List of Figures

List of Tables

List of Abbreviations

ABL2	Abelson Homolog 2
LAML	Acute Myeloid Leukemia
ACC	Adrenocortical Carcinoma
BLCA	Bladder Urothelial Carcinoma
LGG	Brain Lower Grade Glioma
BRCA	Breast Invasive Carcinoma
COSMIC	Catalogue Of Somatic Mutations In Cancer
CESC	Cervical Squamous Cell Carcinoma and Endocervical Adenocarcinoma
CHOL	Cholangiocarcinoma
CLL	Chronic Lymphocytic Leukaemia
CTC	Circulating tumour cells
COAD	Colon Adenocarcinoma
COREAD	Colorectal Adenocarcinoma
CTSD	Cathepsin D
DNA	Deoxyribonucleic acid
DOX	Doxorubicin
DMEM	Dulbecco's Modified Eagle's Medium
EGFR	Epidermal growth factor receptor
ESCA	Esophageal Carcinoma
EXOSC2	Exosome component 2
FAK	Focal adhesion kinase
GEPIA	Gene Expression Profiling Interactive Analysis
GDC	Genome Data Commons
GDSC	Genomics of Drug Sensitivity in Cancer
GCTB	Giant Cell Tumour of Bone
GBM	Glioblastoma Multiforme
GSH	Glutathione
GPX	Glutathione Peroxidase
GR	Glutathione Reductase
HNSC	Head And Neck Squamous Cell Carcinoma
H_2O_2	Hydrogen Peroxide
HIF-1α	Hypoxia inducible factor 1α

ICGC	International Cancer Genome Consortium
KICH	Kidney Chromophobe
KIRC	Kidney Renal Clear Cell Carcinoma
KIRP	Kidney Renal Papillary Cell Carcinoma
KO	Knockout
LIHC	Liver Hepatocellular Carcinoma
LUAD	Lung Adenocarcinoma
LUSC	Lung Squamous Cell Carcinoma
DBLC	Lymphoid Neoplasm Diffuse Large B-Cell Lymphoma
KARS	Lysyl-tRNA synthetase
MB	Medulloblastoma
MSA	Mercaptosuccinic acid
MESO	Mesothelioma
mRNA	Messenger Ribonucleic Acid
MAPK	Mitogen-activated protein kinase
MDR	Multidrug Resistant
MM	Multiple Myeloma
NB	Neuroblastoma
NSCLC	Non-Small-Cell Lung Cancer
NFκB	Nuclear factor kappa B
OV	Ovarian Serous Cystadenocarcinoma
PAAD	Pancreatic Adenocarcinoma
PDA	Pancreatic Ductal Adenocarcinoma
PP	PeroxiPlat
PCPG	Pheochromocytoma And Paraganglioma
PI3K/AKT	Phosphatidylinositol-3-Kinase and Protein Kinase B
PRAD	Prostate Adenocarcinoma
RHOA	Ras Homolog Family Member A
ROS	Reactive Oxygen Species
READ	Rectum Adenocarcinoma
POLR2L	RNA Polymerase II Subunit L
SARC	Sarcoma
SECIS	Sec insertion sequence

SBP	SECIS binding protein
SKCM	Skin Cutaneous Melanoma
SCLC	Small Cell Lung Cancer
SDS-PAGE	Sodium Dodecyl Sulphate–Polyacrylamide Gel Electrophoresis
Na_2SeO_3	Sodium selenite
STAD	Stomach Adenocarcinoma
TGCT	Testicular Germ Cell Tumours
TGCA	The Cancer Genome Atlas
TXN	Thioredoxin
TxnRD	Thioredoxin reductase
THYM	Thymoma
THCA	Thyroid Carcinoma
TPM	Transcripts Per Million
tRNA	Transfer Ribonucleic Acid
TME	Tumour microenvironment
P53	Tumour Protein 53
UTR	Untranslated region
UCS	Uterine Carcinosarcoma
UCEC	Uterine Corpus Endometrial Carcinoma
UVM	Uveal Melanoma
VEGF	Vascular endothelial growth factor
VAMP8	Vesicle-Associated Membrane Protein 8
HSD17B10	β-Hydroxysteroid 17-Beta Dehydrogenase X

Abstract

GPX1 is a selenoprotein which protects cells from damage by removing H_2O_2. GPX1 has a complex role in cancer development, both in promoting and protecting against cancer, and is therefore of great interest in cancer research.

Bioinformatic analyses of cancer databases were used to investigate the expression of *GPX1* and GPX1-interacting proteins across cancer types, as well as the effect of *GPX1* expression on prognosis and chemoresistance.

GPX1 production was stimulated in HaCaT, A431 and HeLa cells using sodium selenite (Na_2SeO_3) and measured at various timepoints using western blotting and flow cytometry. Na_2SeO_3-treated cells were treated with chemotherapeutic agents (cisplatin, doxorubicin, docetaxel) and H_2O_2, and changes to chemoresistance were measured using CyQuant and XTT assays.

The interaction of a new platinum agent, PeroxiPlat, *in vivo* with GPX1 was investigated using flow cytometry and its inhibition of GPX1 was measured using two biochemical activity assays.

GPX1 was overexpressed in the majority of cancers, and worsened prognosis for UVM, LGG, ACC, KICH and LAML patients. *GPX1* was commonly overexpressed *with GPX4*, *TP53*, *POLR2L*, *HSD17B10*, *and CTSD*, many of which were involved in leukocyte activation. No significant correlation between *GPX1* expression and chemoresistance was identified. Na_2SeO_3 supplementation significantly but transiently increased the level of GPX1, and increased chemoresistance, although results were inconsistent between assays. It was also found that PeroxiPlat may weakly penetrate cells and exerts a low level of GPX1 inhibition.

GPX1 is clearly an important factor in cancer development and progression, and a potential target for therapy. Further research is needed to clarify the role of GPX1 in chemoresistance, although these results support existing evidence that GPX1 promotes multidrug resistance. Although PeroxiPlat does not appear to be a potent GPX1 inhibitor, its use as a fluorescent molecule warrants further investigation into the uptake and uses of PeroxiPlat.

Contents

Chapter 1 – General Introduction

1.1 Introduction

Glutathione peroxidase 1 (GPX1) is a well-characterised selenoprotein with the primary function of removing intracellular ROS, in particular H_2O_2. Although there are many GPX family members with similar roles in antioxidant defence, and there is some functional redundancy, their structural differences afford each of them important and unique functions. As the primary detoxifier of H_2O_2, GPX1 is essential in the defence against biomolecular damage, such as protein oxidation, DNA oxidation and lipid peroxidation. This damage can accumulate over time, and is linked to many age-related diseases, including cancer. However, the role of ROS, particularly H_2O_2, in cell signalling makes the relationship between GPX1 and cancer more complex. GPX1 can protect against or promote cancer, depending on the tissue and the signalling pathways stimulated. As will be discussed, *GPX1* overexpression is a negative indicator for cancer progression, often leading to more aggressive, more chemoresistant cancers, and lowering survival rates for cancer patients. This makes GPX1 a particularly promising target, and inhibitors are currently being developed with the aim of sensitising cancer cells to treatment and improving patient prognosis.

1.2 GPX1 and the GPX Family

GPX1 was first discovered in erythrocytes, where it was found to reduce hydrogen peroxide (H_2O_2) using GSH (Mills, 1957). It was later found that this function was not specific to GPX1, and that GPX1 was just one of eight proteins in the glutathione peroxidase family (GPX), a group of proteins with peroxidase activity (Jiao et al., 2017). Almost all members of this family share a conserved catalytic tetrad, containing Sec/Cys, Gln, Trp and Asn, aside from in three exceptions (Toppo et al., 2009; Toppo et al., 2008). Despite this key similarity, it is the differences in structure between the GPXs, especially within the catalytic tetrad, that can dictate the differences in function. From different reaction rates, substrates and localisations, the GPX family spans a wide range of variation within the core function of metabolising peroxides and ultimately managing oxidative stress in an organism.

GPX1 was the first of the GPX family to be discovered, and crystal structures of GPX1 taken from bovine erythrocytes gave us insights into its arrangement (Epp et al., 1983). The monomers consist of a thioredoxin fold structure with seven β-strands and four α-helices (figures 1.1 and 1.3). Four of these β-strands (figure 1.1), β3, β4, β6 and β7) form a β-sheet, which runs through the centre, while the α-helices cover the surface. From the structure, we learned that GPX exists as a homotetramer, with an active site consisting of a glutamine (Gln-84), tryptophan (Trp-162) and selenocysteine (Sec-49) catalytic triad. Mutational studies on

the *Drosophila melanogaster* GPX showed that an asparagine adjacent to the tryptophan (Asn-163 in humans, Asn-136 in *drosophila*) was also essential for function of the active site. This residue is highly conserved across *dm*GPX and human GPXs - GPX1-7 specifically (Tosatto et al., 2008; Toppo et al., 2008). Tosatto also demonstrated that substitution of Asn-136 for His, Ala or Asp in these experiments reduced the rate of oxidation for GPX1 by 2-3 orders of magnitude, implicating Asn as a key contributor to the catalytic activity. As the *dm*GPX is not a selenoprotein, there was a large amount of debate surrounding whether Asn-163 formed part of a catalytic tetrad in human GPX1. This is now accepted to be the case, as mutational studies showed that Q84A, W162A, and N163A variants of human GPX1 had a similarly detrimental effect on activity (Cheng and Arnér, 2017).

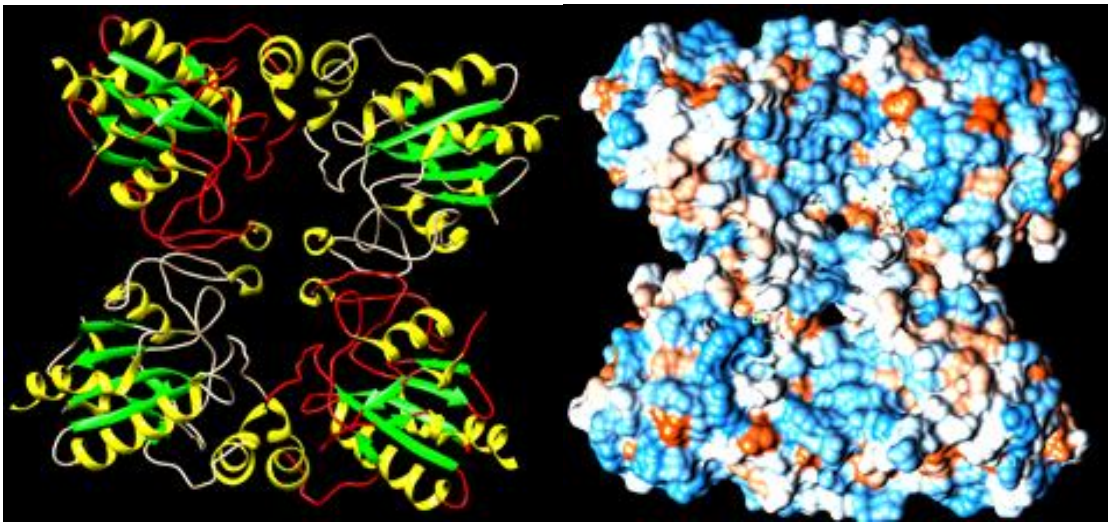

Figure 1.1: Structure of the GPX1 tetramer. *Ribbon structure of GPX1 showing α-helices (yellow) and β-sheets (green) (left) and a space-filling model, showing the binding pocket and cleft (right). resolution: 1.5 Å, PDB ID: 2f8a.*

1.2.1 Substrate Specificity in the GPX family

Despite sharing a similar overall structure and identical active site, GPXs gain substrate specificity through other means. Early research showed that GPX1 can reduce a variety of simple soluble lipid hydroperoxides (Little and O'Brien, 1968; Christophersen, 1969). Other GPXs can act on a range of substrates, and each member of the GPX family has a preference to certain hydroperoxides over others (figure 1.2), which is reflected in their kinetics (Toppo et al., 2009). Human GPX1 processes hydrogen peroxide at an extraordinarily fast rate and is reliant on Lys-114 for H_2O_2 binding, the rate of which is further increased by carbonylation of this residue (Sultan et al., 2018). GPX1 metabolises fatty acid hydroperoxides at a slower rate (Takebe et al., 2002). However, it cannot act upon complex lipids, such as phospholipids.

GPX3 can metabolise these, as well as phospholipid hydroperoxides, and may use donor substrates other than GSH. GPX4 is even more promiscuous *in vitro*, and its substrate range does indeed overlap with that of GPXs 1-3. GPX4 can not only reduce hydrogen peroxide, lipid hydroperoxides and phopholipid hydroperoxides (Maiorino et al., 1991), but can also reduce cholesterol ester hyperoxides (Sattler et al., 1994), and can use substrates other than glutathione to do so (Bjornstedt et al., 1994; Ursini et al., 1999). Interestingly, as subtrate specificity decreases, so does reaction rate, which helps GPX enzymes to set up a reaction gradient whereby hydrogen peroxide is more likely to be turned over by GPX1, and more complex lipids by GPX4 (figure 1.2) (Takebe et al., 2002). These differences allow GPXs to have some redundancy, while maintaining enough specificity to ensure the functions of each GPX family member can be both performed and regulated.

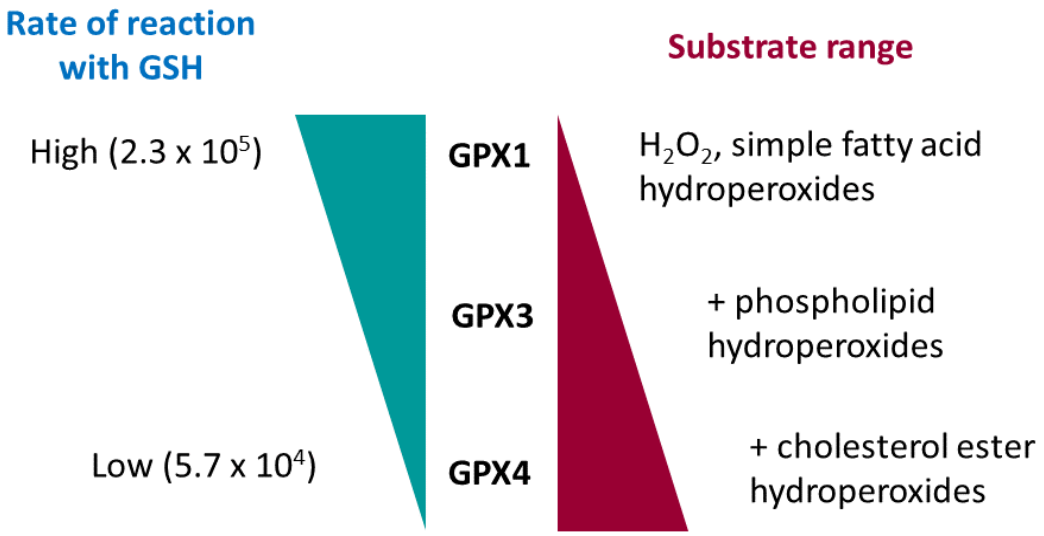

Figure 1.2: Rate of reaction and substrate range within the GPX family*. The inverse relationship between increased substrate range of a GPX enzyme and reaction rate with GSH.*

One contributing factor to the difference in specificity is the slight changes in amino acid sequence near the GSH binding pocket. GPX1 has high specificity and affinity for GSH, which is owed to the positive charges on the surface of the binding site. These charges are contributed by four arginines (positions 57, 103, 184, 185) and one lysine residue (position 91; Epp et al., 1983). From this structure, it was predicted that the electrostatic charge pushes the GSHs into a conformation which facilitates the reaction in the catalytic centre (Flohé et al., 2003). Variation in this surface structure does appear to be somewhat responsible for donor specifity. GPX1 and GPX2 are the most structurally similar, and have a similar specifity for GSH. GPX2 has a glutamine substitution in the Lys-91 position, and threonine at Arg-185, and so while some electrostatic charge is lost, it maintains a fairly good

surface for GSH binding (Toppo et al., 2008). Of these 5 basic residues, GPX3 only has Arg-103 and Arg-185 (Toppo et al., 2008), which may explain the lower specificty of GPX3 for GSH, and why it is able to accept glutaredoxin and thioredoxin in its place (Bjornstedt et al., 1994). GPX4 has none of the residues which form this basic pocket (Toppo et al., 2008). Instead, GPX4 uses Lys-48 and Lys-125 to orientate GSH, which also allows it to utilise a greater range of donor substrates (Mauri et al., 2003).

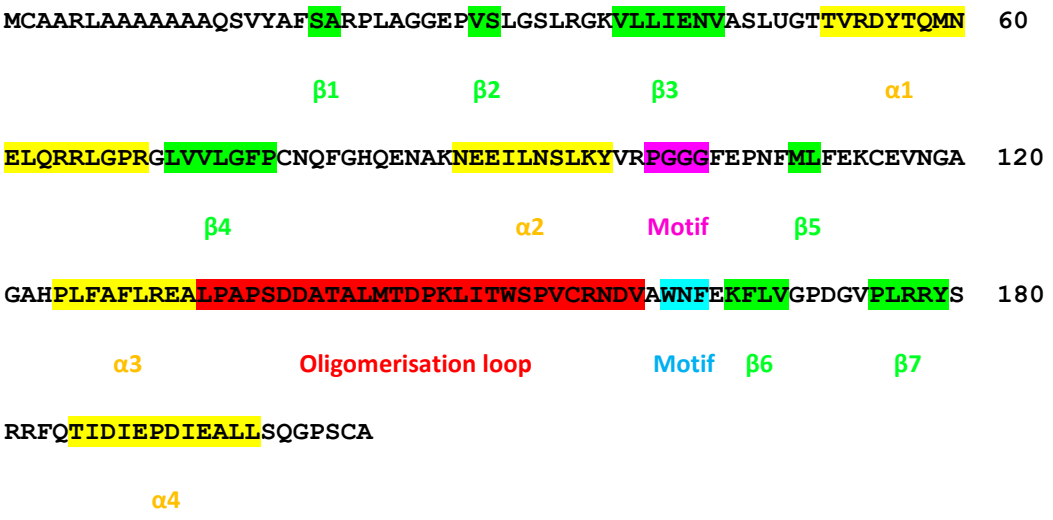

Figure 1.3: Human GPX1 sequence (GPX1_HUMAN). *Labelled amino acid sequence of GPX1, showing α-helices (yellow), ß-sheets (green), PGGG tetramerisation loop (pink), oligomerisation loop (red), WNF motif (blue).*

The oligomerisation state of GPXs can also affect substrate binding. GPX1, along with tetrameric GPXs GPX2, 3, 5 and 6, contains an oligermerization loop and PGGG motif, which allows them to form a homotetramer (figure 1.3). Homotetrameric GPX enzymes contain a groove where the subunits meet, which potentially shields the catalyic core from lipid surfaces, and so hinders the access of complex lipids (Epp et al., 1983). While this promotes some hydroperoxide selectivity in GPX1, it also explains why GPX4 has such broad specificity; it exists as a monomer. Therefore, there is easier access to the active site, as the selenocysteine residue is more exposed, and the surface is better suited to facilitate lipid interactions (Aumann et al., 1997; Scheerer et al., 2007). However, it not just the oligomerisation state of the enzyme that can affect substrate specificity, as the oligomerisation loop itself may sterically block entry to the site for larger substrates. This loop consists of around 20 residues, between the second and third alpha helix, near the conserved WNF motif, and sits near the active site (figure 1.3) (Toppo et al., 2008). A study of a monomeric GPX3 mutant that closely resembled GPX4, apart from the continued presence of this oligermerisation loop, showed that while it maintained activity, it also retained its

selectivity for substrates (Song et al., 2014). Song et al explained this by theorising that the electrostatic charge of the loop alone may be responsible for monomeric GPX3 remaining unable to catalyse the same range of substrates as GPX4, despite its structural similarity.

The difference in specificity for GSH establishes some functional niches for each GPX, and so although there is some functional overlap, each GPX can perform their own distinct functions based on the enviroment. Therefore, while low GSH enviroments prove hostile for GPX1, they allow GPX4 to perform separate and unique functions. For example, GPX4 has been shown to be essential in ferroptosis, lipid homeostasis and sperm maturation (Forcina and Dixon, 2019). In the late stages of sperm maturation, GSH levels are low, and so the less selective, more flexible GPX4 enzyme is primarily used in the testes, where it also plays a structural role (Ursini et al., 1999). Conversely, in most tissues, GSH is in good supply, and as GPX1 is more selective for GSH and more efficient than other GPXs, it can rapidly turn over hydrogen peroxide as a major protector of tissues from oxidative stress. In mammals, GPX1 and GPX4 are ubiquitous (although GPX4 is expressed highly in the testes), GPX2 is found primarily found in the gastrointestinal region, and GPX3 in plasma (but is secreted from the lung and kidney) (Lubos, Loscalzo and Handy, 2011). The differential expression of GPXs compounds the formation of functional niches, and may have some effect on the substrates used, and the function performed.

The subcellular location can act in a similar way, as GPXs are not evenly distributed within the cell. GPX1 is found in the cytoplasm, mitochondria and peroxisomes. Given its preference for hydrogen peroxide, the mitochondrial and peroxisomal environments are ideal for GPX1, as they generate a large amount of hydrogen peroxide. In contrast, GPX4 is localised to the lipid bilayer in the cellular membrane (Cozza et al., 2017). This allows it to process lipid hydroperoxides, especially those within the membrane that may have become damaged during times of oxidative stress. Despite existing in many of the same cells, GPX1 and GPX4 can work in parallel to protect the cell from different types of oxidative damage, and in different areas, so as not to compete for substrates and maintain a higher overall efficiency.

It should be noted, however, that while this is true for GPX1 and GPX4, some GPXs, like GPX1 and GPX2, do in fact share a greater amount of functional redundancy. For this reason, lowering expression of GPX1 in models is often non-lethal, as *GPX2* can be overexpressed to compensate for lost GPX1 function. Transgenic mice that were knockouts for GPX1 or GPX2 were able to survive but GPX1 knockouts had increased sensitivity to damage induced by paraquat (Cheng et al., 1998). In a later experiment using gamma radiation as the stress-

inducer, the ability to cope without GPX1 was found to be a direct result of increased *GPX2* expression (Esworthy et al., 2000). In areas such as the lungs, having GPX1 and GPX2 working together can aid in scaling up the response to oxidative stress. While *GPX1* is constitutively expressed at high levels, during times of increased oxidative stress, *GPX2* expression can be switched on, allowing for a tightly regulated response that remains specific for the target substrate - hydrogen peroxide (Singh et al., 2006).

1.2.2 GPX1 Mechanism

Although there are differences in substrate specificity and in the composition of the active site, all members of the GPX family use a common mechanism for catalysis (Tosatto et al., 2008; Toppo et al., 2009). For GPX1 and other selenocysteine-containing GPXs, the selenocysteine residue is the centre of this mechanism (figure 1.4). This is a ping-pong mechanism, detoxifying hydrogen peroxide via selenocysteine, using two reduced glutathiones as substrates. A similar mechanism is utilised by members of the GPX family with a cysteine in the active site, however other amino acids within the active site, such as a second resolving cysteine, are used to enhance the reaction rate (Tosatto et al., 2008; Toppo et al., 2009). As will be discussed, small differences in the active site of members of the GPX family can allow some members to catalyse reactions significantly quicker than others.

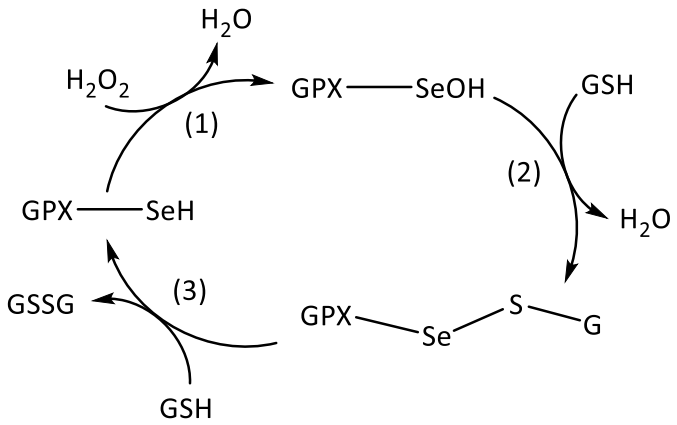

Figure 1.4: The reaction of Sec-GPXs with hydrogen peroxide (H_2O_2). *(1) The active site selenocysteine becomes oxidised via reaction with a peroxide, changing from the selenol (GPX-SeH) form to the selenic (GPX-SeOH) form, and producing an ROH compound. (2) Selenic GPX1 is then reduced by GSH in a dehydration reaction, forming a selenenyl sulphide intermediate (GPX-SeSG) and releasing water. (3) Finally, this intermediate is reduced by a second GSH substrate to release an oxidised GSSG product and regenerate the original form of the enzyme*.

1.2.3 GPX as a Selenoprotein

Although they are phylogenetically and functionally related, there is a key structural difference between many GPX enzymes. In humans, GPX1-4 and 6 are selenoproteins, and contain a selenocysteine (Sec) residue in the catalytic centre, while GPX5, GPX7 and GPX8 use a cysteine in place of this selenocysteine (Brigelius-Flohé and Maiorino, 2013). While the cysteine substitution corresponds with a lower reaction rate, the cysteine motifs were later revealed to be present in the majority of GPX enzymes across all lifeforms (Brigelius-Flohé and Maiorino, 2013). It is now believed that all GPX enzymes evolved from a cys-containing ancestor (Toppo, 2008), and while this explains the prevalence of cysteine, it does not explain why selenocysteine is not selected for despite its obvious advantage in reaction rate. To understand why GPX1 is one of a minority of enzymes across all kingdoms containing selenocysteine, we must examine the properties of selenocysteine which make it so vital for GPX1, and the limitations this amino acid may confer to the enzyme.

1.2.3.1 Structural Differences in Sec and Cys

Selenium is incorporated into GPX via selenocysteine, a rare amino acid structurally similar to cysteine, but with selenium replacing sulphur (figure 1.5) (Ren et al., 2018). This small difference has a remarkable effect on the amino acid, and indeed its role within GPX enzymes. An obvious difference is that the atomic radius is slightly greater in selenium than in sulphur. This affords a longer bond radius in the selenolate (Se-H group), and increases the polarity of this bond, thereby decreasing its dissociation energy (Reich and Hondal, 2016). Selenolates are also more nucleophilic, and so are readily oxidised by H_2O_2 and other peroxides (figure 1.4). This added nucleophilicity increases the rate of the rate-limiting step of the reaction with hydrogen peroxides in GPX enzymes containing selenocysteine in their active site, as opposed to cysteine.

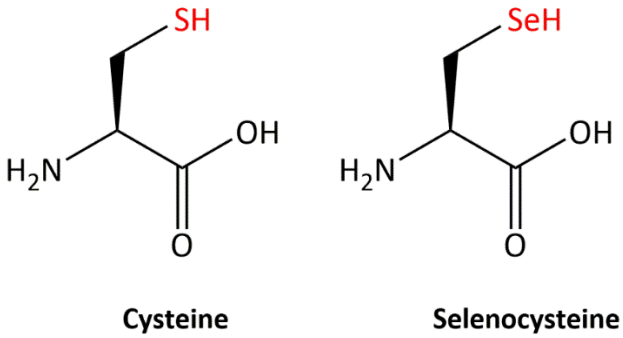

Figure 1.5: Comparison of cysteine (left) and selenocysteine (right) structures. *Red text indicates the difference in structure between the two amino acids, which results in changes to pKa, atomic radius size and redox potential (E_0).*

Characteristic	Cysteine (Cys)	Selenocysteine (Sec)
pKa	8.3	5.2
Atomic radius (pm)	105	120
E_0 (mV)	-220	-338

Table 1.1: Comparison of the biochemical properties of the cysteine and selenocysteine.

The difference in biochemical characteristics between these amino acids becomes greater when we consider their state in a physiological context. The pKa of cysteine is approximately 8.3 units, however this drops to 5.2 units with the selenolate group (Reich and Hondal, 2016) (Table 1.1). This difference in acidity is owed to the larger atomic size of selenium, which results in increased polarizability and generally weaker bonds. Consequently, selenocysteine is a better proton donor, and so becomes almost fully ionized at physiological pH. This greatly improves its ability to attack hydroperoxide in the initial stage of the reaction, as it more likely to be in a more nucleophilic state than cysteine (Table 1.1). Although this is generally true, the microenvironment in the active site can also impact the pKa of cysteine. Adjacent amino acid side chains, especially those that are polar, can balance the negative charge on sulphur, weakening its interaction with hydrogen and increasing its acidity (Roos, Foloppe and Messens, 2013). This may explain why other organisms can still maintain redox homeostasis with cysteine, despite the redox advantage of using selenium for this reaction. The importance of selenium in GPX1 and in the systems responsible for oxidative stress management is therefore still to be determined.

1.2.3.2 Sec incorporation via SBP2

Many modified amino acids result from post-translational modification, and they too can affect the activity of enzymes. For example, the phosphorylation of a tyrosine can be used to

activate entire pathways and can regulate both DNA damage responses (Cook et al., 2009) and innate immune responses (Okabe, Sano and Nagata, 2009) among other key physiological pathways. However, selenocysteine is not a post-translationally modified amino acid. Uniquely, Sec is incorporated at the translational stage, and utilises a UGA codon, normally a stop codon. The change in recognition from stop to Sec is mediated by a section of the 3'UTR of mRNA that sits around 40 bases downstream of the UGA codon defined as the selenocysteine insertion sequence (SECIS) element (figure 1.6) (Zinoni, Heider and Bock, 1990; Howard and Copeland, 2019).

The SECIS element structure was found to be key in selenoprotein synthesis through transfection experiments using *5' deiodinase* (5'DI) and *GPX1* (Berry et al., 1991). Berry found that the 3'UTR SECIS element was only required for synthesis of Sec-containing 5'DI, and not for the Cys-mutant. The SECIS elements in 5'DI and GPX1 mRNA have little sequence homology but both were likely to form stem-loop structures of varying size but similar structures (as both contained an AAA sequence in the loop and an unpaired UGAU in the stem). When the GPX1 mRNA 3'UTR sequence was substituted for the 3'UTR of 5'DI, Berry et al found that it could direct the inclusion of a Sec residue, despite them having a different 3'UTR primary sequence. These experiments demonstrated clearly that it was the stem-loop secondary structure specifically that was critical for Sec incorporation.

The SECIS element is central to Sec incorporation as, once the stem-loop structure is formed, it recruits the proteins required for Sec-tRNA binding (Howard and Copeland, 2019). The first of these proteins to be discovered was SECIS binding protein (SBP2), which was found to interact with the AUGA motif in the 5' stem of the SECIS element (Lesoon et al., 1997). SBP2 contains a regulatory domain in the N terminus (NTD), a Sec incorporation domain (SID), and an RNA binding domain (RBD) at the C-terminus. The SID and RBD are known to be essential for Sec incorporation and recoding the stop codon. The function of the NTD, however, is not well understood.

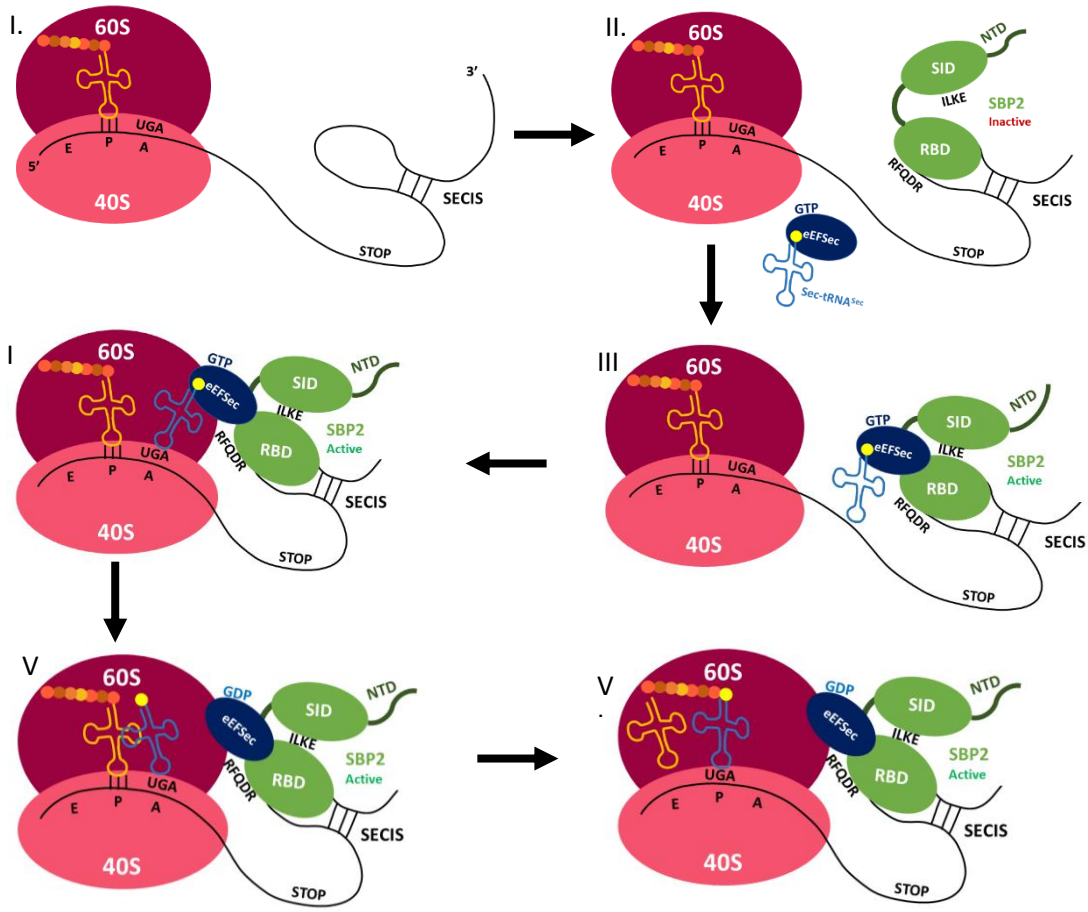

Figure 1.6: Incorporation of selenocysteine using a SECIS element*. I. During translation of the selenoprotein mRNA, a stem-loop structure is formed at the 3' end (the SECIS element). II. This structure is recognised by the RBD domain of SBP2, which forms an unstable structure with the SECIS. III. The SID domain of SBP2 stabilises the structure by interacting with the RBD via an ILKE motif. eEFSec-bound Sec-tRNA^{Sec} binds to the NES of SBP2 before its contact with the ribosome, which signals the beginning of its own delivery to the ribosome via SBP2. IV. The RFQDR motif in the RBD of SBP2 binds to the ribosome, delivering with it eEFSec bound to GTP and Sec-tRNA^{Sec}, and allowing it to enter the A site. V. GTP hydrolysis by eEFSec causes the release of the Sec-tRNA^{Sec}. VI. Sec-tRNA^{Sec} moves into the P site, adding the Sec to the chain. Both the previous tRNA and the Sec insertion machinery have been released.*

The NTD is only present in higher eukaryotes; the N-terminus appears to be dispensable for Sec incorporation *in vitro* (Takeuchi et al., 2009). Mutations in the N-terminal domain of SBP2 can cause pathology in humans, as selenoenzyme synthesis is reduced, leading to increased photosensitivity, as an increase in ROS following UV exposure cannot be effectively managed by the GPXs (Schoenmakers et al., 2010). Other biochemical impacts of these mutations included increased insulin sensitivity and a higher ROS level, which are also seen

in mice lacking GPX1, suggesting that GPX1 deficiency as a result of defective SBP2 has a significant impact on overall health. While this would also suggest a novel function for the SBP2 NTD, it was found that rather than altering the NTD function, patients with SBP2 NTD mutations had fully dysfunctional SBP2 due to a frameshift (introducing an early stop codon) or the creation of an alternative start site (Schoenmakers et al., 2010; Di Cosmo et al., 2009). Despite mutations in the NTD, the truncated protein retains some functionality, as the SID and RBD remained somewhat intact.

The RBD is important for binding with the SECIS RNA stem-loop structure and the ribosome to begin the Sec incorporation (figure 1.6). This domain was first characterised in rat SBP2, and owes its function to an L7Ae motif, which allows both SECIS and ribosome binding (Bubenik and Driscoll, 2007; Caban, Kinzy and Copeland, 2007). L7Ae motifs are known to bind RNA kink-turns, commonly found in ribosomes, but also seen in the SECIS (Shi et al., 2016). While both the ribosome and the SECIS rely on this motif for binding, it was found that a G669R mutation in rat SBP2 abolished SECIS binding, but not ribosome binding (Copeland, Stepanik and Driscoll, 2001). This indicates that within the RBD, there are regions mediating selectivity for RNA binding. Further mutational experiments showed that the α-helix and loop region of the L7Ae motif formed an interaction surface essential for ribosome binding and Sec incorportation, but not SECIS binding, further substantiating the argument for multifunctionality within the RBD (Caban, Kinzy and Copeland, 2007).

Not only is the RBD able to bind to the SECIS and ribosomal kink turns differently, its interaction with the SECIS modulates ribosome binding. RBD binding to the SECIS causes a conformational change in the RBD structure, which allows for the recruitment of the SID, forming a stable RBD-SECIS-SID complex, using the IILKE motif of SID (Donovan and Copeland, 2010) (figure 1.6). The RBD then binds to the 28S rRNA via a RFQDR motif, which is essential for the recruitment of the ribosome and subsequent Sec incorporation (Caban, Kinzy and Copeland, 2007). This interaction causes a conformational change in Helix 89 of the ribosome, promoting Sec incorporation (Caban and Copeland, 2012). Sec-tRNA^{Sec} delivery to the ribosome is mediated by eEFSec, a specialised elongation factor for Sec-tRNA^{Sec}, and is recruited to the site by the SID (Fagegaltier, 2000; Gonzalez-Flores et al., 2012). It is thought that the ribosomal conformational change promotes Sec incorporation by allowing eEFSec-bound Sec-tRNA^{Sec} to move into the A-Site and/or by stimulating the ribosome-dependent GTPase activity of eEFSec (Caban and Copeland, 2012). A recent review has proposed a mechanism for this, in which the GTPase activity of eEFSec causes a non-canonical structural

change in the eEFSec domains, which releases Sec-tRNA^{sec} into the peptidyl-transferase centre of the ribosome (Simonović and Puppala, 2018).

1.2.3.3 The Selenium Hierarchy

GPX1 is one of many genes encoding selenoproteins that uses this SBP2-dependent system for Sec incorporation. However, when limited, selenium is preferentially retained in some proteins over others (Berry, 2005; Touat-Hamici et al., 2018). This was first observed in rats, where selenium depletion lowered GPX1 activity far more than that of GPX4 in the heart, liver, kidney and lung (Lei et al., 1995). Another study indicated that the selenoprotein iodothyronine deiodinase (IDI) activities decreased along with GPX4 during selenium deficiency, compared with GPX1 in both the thyroid and the liver (Bermano et al., 1996). Bermano found that GPX1 mRNA levels correlated with activity change during selenium repletion in the liver, whereas GPX4 had steady levels of mRNA and activity through depletion and repletion. This indicated that mRNA stability was able to dictate the production of enzymes in selenium-limited environments, and therefore the position in the selenium hierarchy.

It was later found that the ranking of a selenoprotein in the hierarchy was indeed based upon the instability of the mRNA, but particularly of the 3'UTR. Early experiments exchanging the 3'UTR of GPX mRNAs showed that the more stable GPX2 and GPX4 could exchange 3'UTRs without losing stability in selenium-limited conditions (Müller, Wingler and Brigelius-Flohé, 2003). However, the GPX2 and GPX4 3'UTRs could not increase the stability of GPX1 mRNA. These experiments also revealed that the GPX1 3'UTR, however, could decrease the stability of GPX2 and GPX4 mRNA. This implied that 3'UTRs were not only important for GPX1 production and selenium incorporation, but also that there is a hierarchy of stability, and therefore of selenium distribution across selenoproteins. Structural studies of SECIS kink-turn loop structures across selenoproteins proved that specific bases in the flanking sequences can determine whether the SECIS is 'weak' or 'strong' in terms of translatability (Latrèche et al., 2009). This supports the argument that each SECIS contains information that can determine the ranking of a selenoprotein in the hierarchy.

In 2007, further evidence of the hierarchy being controlled at the post-transcriptional level emerged, this time involving SBP2. Experiments using the SBP2 C-terminus showed that this alone could differentiate between different SECIS elements, as it had a higher affinity for the GPX4 than for the GPX1 SECIS *in vitro* (Bubenik and Driscoll, 2007). Additionally, a selenoprotein's placing in the hierarchy can be determined by the ability of the SECIS to recruit other RNA-binding proteins for selenocysteine incorporation. For example, eIF4a3 can

bind to the SECIS to inhibit SBP2 binding, and subsequently, selenocysteine incorporation. Not only are eIF4a3 levels regulated by selenium level, but as an added layer of control, eIF4a3 binds with different affinity to different SECIS elements (Budiman et al., 2009). By siRNA knockdown, the group demonstrated that high eIF4a3 levels were necessary for lowering *GPX1* expression in selenium-deficient cells, and using transfection experiments, found that overexpression of eIF4a3 could produce a similarly suppressive effect on *GPX1* expression even in selenium-rich conditions. Nucleolin has been shown to regulate *GPX1* expression at the translational level, however in this case, it binds preferentially to the GPX4 SECIS as opposed to the GPX1 SECIS, positively regulating translation (Miniard et al., 2010). While nucleolin levels are independent of selenium availability, they fluctuate with cell stress, and this allows for modulation of GPX activity in response to environmental cues. The combined actions of these modulators establish GPX4 as higher in the hierarchy than GPX1 and create a complex system of selenium-regulated and selenium-independent regulation of GPX expression.

Nonsense-mediated decay (NMD) is also an important contributor to hierarchical ranking, as it promotes the degradation of some mRNA transcripts above others (Seyedali and Berry, 2014). NMD was predicted to be effective on around half of the selenoprotein transcriptome, with the other half being resistant, and those able to be targeted by NMD were also responsive to changes in selenium level. NMD operates in conjunction with the modulators previously discussed to regulate translation of low-ranking selenoprotein mRNA in times of selenium-deficiency. However, as this study did not address the effect of this on protein level, the effectiveness and latency of this regulatory mechanism on selenoprotein level and activity needs further research.

More complex still, this hierarchy, as well as these methods of regulation, do not just exist for the GPX family, but largely extend to the 25 selenoprotein genes in humans, such as thioredoxin reductases (TxnRDs). While they all utilise SECIS elements for selenocysteine incorporation, these selenoproteins perform different functions within the cell. GPX1, for example, is an oxidative stress-related enzyme, while enzymes like TxnRD1 perform 'housekeeping' roles (Zoidis et al., 2018). Housekeeping genes need to remain at constant levels regardless of selenocysteine availability, putting them at the top of the hierarchy, in theory. In reality, the hierarchy is cell-line specific, and rankings vary depending on each cell's regulatory machinery, and varies between cancerous and non-cancerous cell lines (Touat-Hamici et al., 2018). Furthermore, this comprehensive study tested selenium absorption, selenoprotein mRNA level, protein level and enzymatic activity, and found that

previous studies using mRNA data to determine the hierarchical position may be incomplete. In fact, greater increases are observed at the protein level than at the mRNA level following the addition of selenium. This demonstrates the necessity for observing the relationship between selenium supplementation and selenoproteins across multiple cell types in subsequent experiments, and the need for further work understanding regulation of selenoproteins beyond the translational level.

The fact that *GPX1* expression is highly dependent on selenocysteine levels and ranks low in the hierarchy in many tissues makes it an interesting target for therapy, as a small change in selenium availability would make a large impact on expression levels, and therefore on the cell. Failing to meet the required threshold would disadvantage cells which are highly reliant on *GPX1* for survival, such as multi-drug resistant cancer cell lines, while maintaining appropriate levels of the vital selenoproteins for healthy, non-cancerous cells to survive. However, the variation of the ranking of GPX1 (and indeed other selenoproteins) poses challenges for systemic therapies such as selenium supplementation or restriction in humans, or the use of an oral drug, as the effect may cause unpredictable and unintended responses outside of the target tissue or target selenoprotein.

1.3 Role of GPX1 in Managing Oxidative Stress

GPX1 works alongside other enzymes, such as catalase, to detoxify hydrogen peroxide and maintain a tolerable redox level for the cell, preventing oxidative stress and damage (figure 1.7). Despite its inherent oxidising ability, low levels of H_2O_2 are tolerated well by the cell, and a small amount is required to maintain what is termed 'oxidative eustress' (Sarsour, Kalen and Goswami, 2014). These low levels of hydrogen peroxide can be produced as a by-product of aerobic metabolism (Loschen and Flohé, 1971). Mitochondria are known to generate peroxides, which often happens due to electron leakage and the subsequent reaction of these electrons with oxygen. For example, hydrogen peroxide production can be caused by reaction of redox-active groups, such as Flavin, with O_2 or by the release of electrons following reduction of ubiquinone in the electro transport chain (Wong et al., 2017). While electron leaks are common, they can lead to severe damage to proteins, lipids and DNA via reactive oxygen species such as H_2O_2. ROS levels are also increased by external factors, such as exposure to UV radiation, plasma, chemotherapeutics, such as cisplatin (Rhie et al., 2001; Mitra et al., 2019; Marullo et al., 2013).

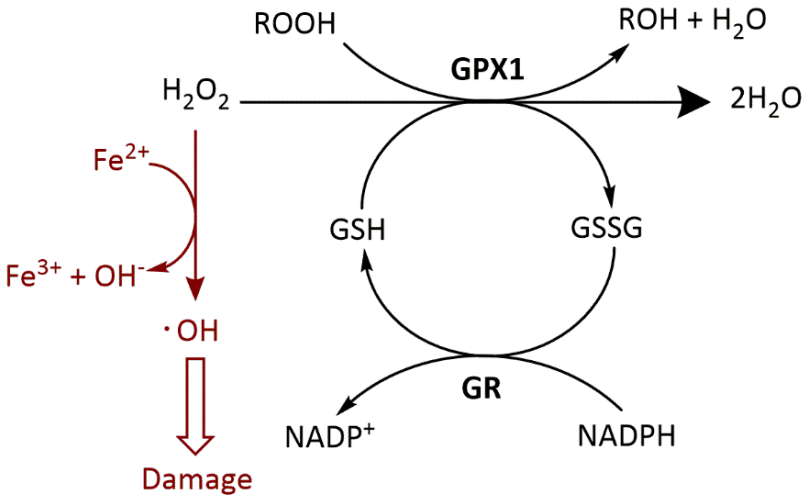

***Figure 1.7: The role of GPX1 in H_2O_2 removal**. GPX interacts with the hydroperoxides (ROOH) and hydrogen peroxide (H_2O_2) using two reduced glutathione molecules (GSH) as antioxidants, forming water and alcohols. This process produces oxidised glutathione in the form gluthathione disulphide (GSSG). This is then reduced by glutathione reductase (GR), which uses NADPH as a proton donor. This ensures the GSH is regenerated in the cell to continue peroxide detoxification. The alternative fate of H_2O_2 is shown in red, where the Fenton reaction produces hydroxyl radicals that cause damage to biomolecules.*

1.3.1 GPX1 managing H_2O_2

The primary role of GPX1 is to detoxify the ROS and prevent damage to biomaterials. This was recently demonstrated in pancreatic ductal adenocarcinoma (PDA) cells, where knockdown of GPX1 with siRNA increased ROS and H_2O_2 levels (Meng et al., 2018). The converse was also seen; overexpression of GPX1 in the PDA cells caused a significant decrease in the ROS and H_2O_2 level. This exemplifies the importance of the function of GPX1 in maintaining cellular redox homeostasis. However, the full impact of preventing oxidative stress cannot be measured until much later - once ROS have been able to cause damage to cellular materials. While the immediate effect can be quantified in these experiments, the long-term benefits of GPX1 are more complex.

GPX1 detoxifies hydrogen peroxide and lipid hydroperoxides using two glutathione molecules per one molecule of the peroxide (figure 1.4). As discussed in section 2.2, GPX1 is one of the fastest working enzymes in the body as it works to remove the most abundant endogenous ROS, H_2O_2, and therefore manage oxidative stress. This is a necessity, as the alternative fate for hydrogen peroxide if not detoxified, is to react and form hydroxyl radicals, which are highly reactive and easily damage biomaterials. The formation of this radical can occur through two pathways (Moldovan and Moldovan, 2004); (1) the Fenton

reaction ($Fe^{2+} + H_2O_2 \rightarrow Fe^{3+} + OH^- + OH$), which requires transition metals such as iron and copper, which are both present in the peroxisome, and (2) the Haber–Weiss ($O_2- + H_2O_2 \rightarrow O_2 + OH + OH^-$), which occurs in the presence of superoxide, often produced by peroxisomal enzymes themselves (Fransen et al., 2012).

1.3.2 ROS damage

A range of cellular biomaterials are vulnerable to damage by ROS. For example, these radicals can react with DNA in many ways. Hydroxyl radicals can perform proton abstraction at the sugar moiety on the DNA backbone, which results in DNA strand breaks or, in the case of a reaction at the C1', 2-deoxyribosyl radical formation (figure 1.8). This radical can then form a 2-deoxyribonolactone abasic site, causing a DNA lesion (Pogozelski and Tullius, 1998; Chan et al., 2010). These lesions require repair by the base excision DNA repair pathway (BER). However, 2-deoxyribonolactone sites require excision by a specific pathway, called long-patch BER (Sung, DeMott and Demple, 2005). If this form of BER is not initiated, and instead short-patch BER is used, the DNA can covalently bond with proteins such as Polymerase β, topoisomerase I and topoisomerase IIα (Quiñones et al., 2015). This traps these repair proteins at the DNA, causing DNA-protein crosslinks, which can be toxic if allowed to accumulate (Quiñones et al., 2015).

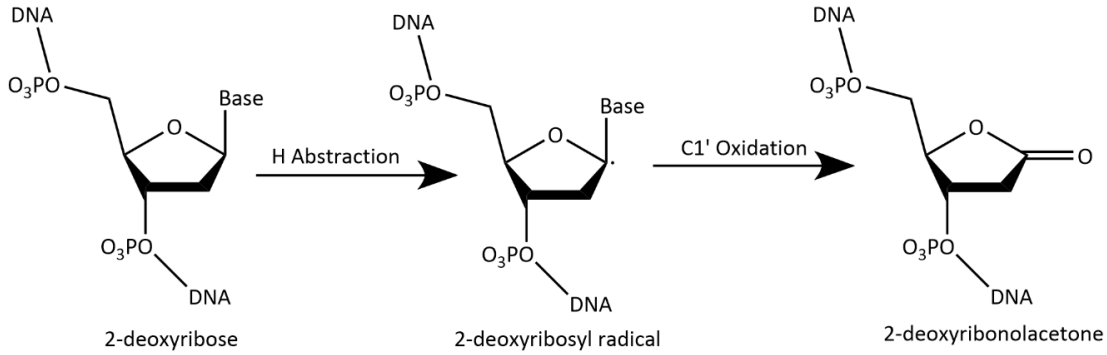

Figure 1.8: DNA backbone damage following attack by a hydroxy radical. *The formation of 2-deoxyribonolacetone from 2-deoxyribose by proton abstraction and oxidation at C1.*

Radicals can also interact with bases within DNA, or in the nucleotide pool, to oxidise them. This is most frequent in guanine, which can be attacked at multiple sites by hydroxyl radicals to form different oxidised products. Attacking at C4 or C5 forms an adduct which is short-lived. This process is also easily reversible, and unlikely to cause DNA damage (Breen and Murphy, 1995). Attacking at C8, however, forms an intermediate with a long half-life, allowing it time to oxidise again to form 8-oxyguanosine (8-oxo-G) or fragment and reduce to form formamidopyrimidine (FAPy-dG) (Greenberg, 2011; Singh et al., 2019) (figure 1.9). In

DNA, these bases can hydrogen bond to either adenine or cytosine bases; the former causes G:C-T:A transversions (Grollman and Moriya, 1993). Failure of DNA repair machinery to recognise and excise the oxidised base leads to permanent mutations, particularly in G-rich sequences. Highly G-rich sequences can form G-quadruplex structures, and many of these are found in the promoters of oncogenes, increasing the risk of carcinogenesis (Singh et al., 2019). Furthermore, it was recently found that 8-oxo-G can affect base pairing at the translational level, with oxidised mRNA producing a higher level of abnormal protein (amyloid-β) (Dai et al., 2018).

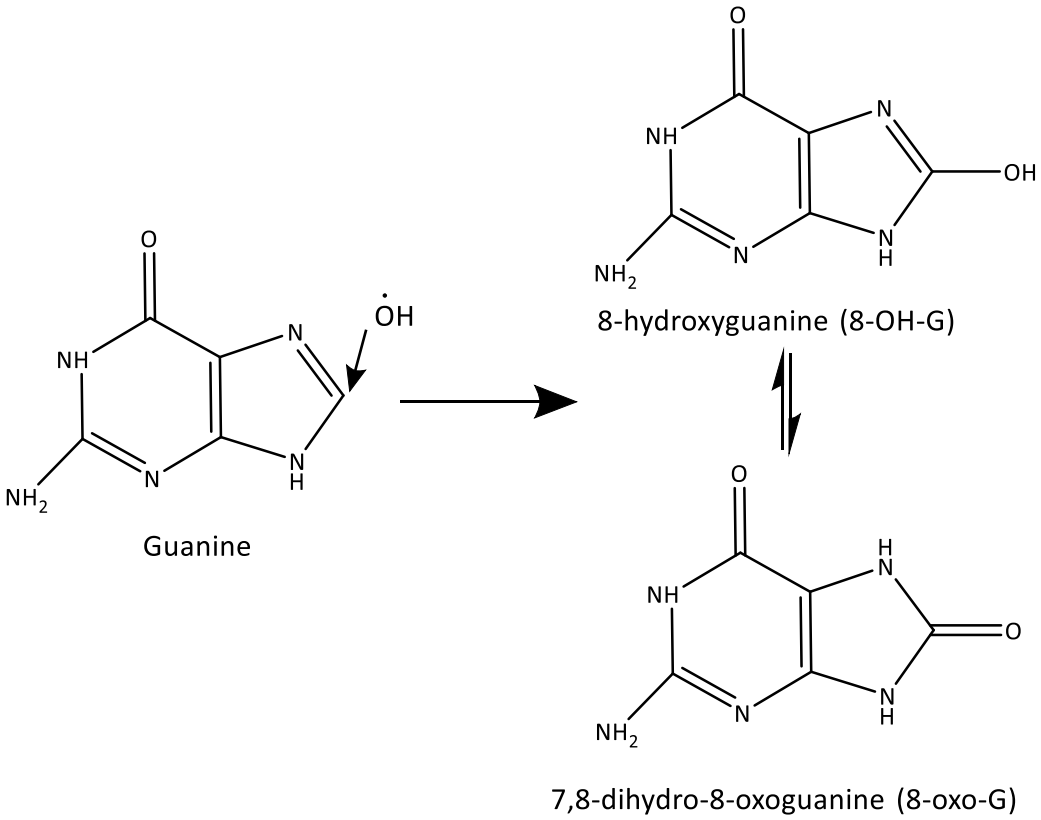

Figure 1.9: Guanine base damage following attack by a hydroxyl radical. *Tautomeric forms of 8-oxo-G (right) formed following oxidation of guanine (left) by a hydroxyl radical.*

Proteins are also vulnerable to attack by hydroxyl radicals. They represent a major group of molecular targets for ROS, and hydroxyl radicals can react through proton abstraction, addition or electron transfer, and can attack amino acid side chains as well as the peptide backbone itself (Davies, 2016). In the backbone, as in DNA, proton abstraction is the most common reaction, occurring at the α-carbon, forming a carbon-centred radical. When this is further oxidised with O_2, a peroxyl radical is formed, which causes cleavage of the backbone and protein fragmentation. In the absence of O_2, two radicals can instead dimerise and disproportionate rapidly, as well as fragmenting.

Protein peroxides can interact with other proteins in a chain reaction, forming carbonyls and alcohols as products, and the damage can propagate to as many as 15 amino acids after the original hydroxyl radical has been used up (Neužil et al., 1993). Despite many protein radicals being more reactive than H_2O_2, the apparatus to remove peroxyl radicals and protein peroxides are much slower than the systems for detoxifying H_2O_2 (Morgan et al., 2004). While GPX family enzymes were shown to rapidly remove peptide peroxides, the steric hinderance of protein peroxides prevents their detoxification by antioxidant enzymes. Instead, the cells relied upon thiols and ascorbate for protein peroxide removal, and scavengers such as Trolox to remove radicals. These compounds work slower than antioxidant enzymes, allowing time for accumulation or dysfunction, and in the case of radicals, allowing time for chain reactions to occur. This establishes the H_2O_2-managing function of GPX family members, as well as catalase and superoxide dismutase, as the first line of defence against oxidative damage. These antioxidant enzymes remove H_2O_2 before radicals can propagate and cause large amounts of protein damage (Ighodaro and Akinloye, 2018).

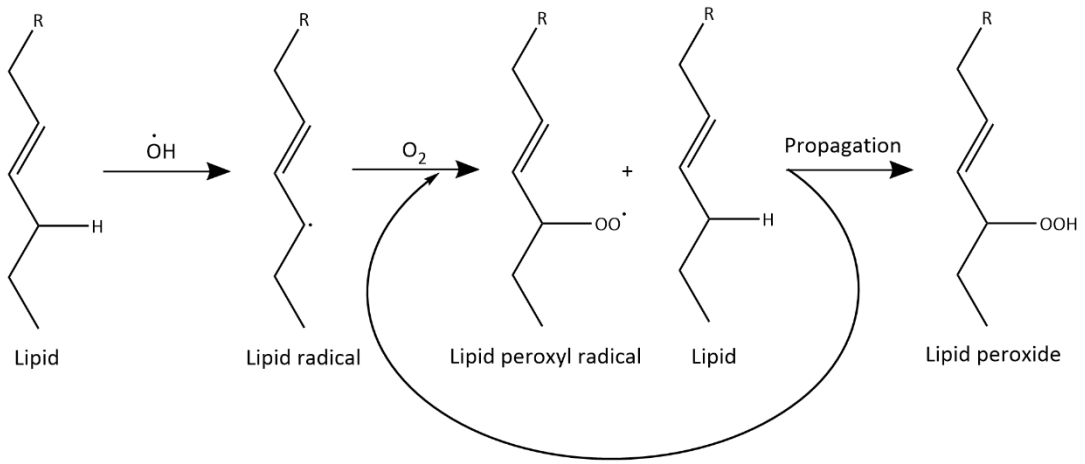

Figure 1.10: Mechanism for lipid peroxidation after initiation from a hydroxyl radical attack. *The lipid radical formed reacts with oxygen to form a lipid peroxyl radical, which abstracts the hydrogen from another lipid to form a lipid peroxide product and a lipid radical that can propagate the reaction.*

Finally, hydroxyl radicals from H_2O_2 are able to attack lipids (figure 1.10). The mechanisms for attack are similar to those previously stated for proteins. The hydroxyl radical abstracts hydrogen from the lipid, creating a lipid-peroxyl radical, which abstracts another hydrogen to form a lipid hydroperoxide and another radical to propagate the chain reaction. Unlike in protein oxidation, lipid hydroperoxides can be managed by antioxidant enzymes such as

GPXs (GPX4 in particular) and SeP, however, these chain reactions can have wide-ranging impacts on the cell (Takebe et al., 2002). Lipid peroxidation can have such significant effects on cellular function that it has been linked to many age-related diseases and can be used as a predictor for longevity in mammals (Jové et al., 2013). Peroxidation of lipids in the membrane can affect membrane function through changes to the physical properties of lipids, altering permeability and membrane integrity (Volinsky and Kinnunen, 2013).

The products of these chain reactions cause a range of damage to biomaterials. The most common product, Malondialdehyde (MDA), can damage DNA in many ways. MDA can react with DNA (dG) to form an adduct, leading to base pair substitutions and frameshifts in both nuclear and mitochondrial DNA (VanderVeen et al., 2003; Wauchope et al., 2018). MDA is also able to cause interstrand crosslinks within DNA (Niedernhofer et al., 2003), or mediate DNA-protein crosslinks (Voitkun and Zhitkovich, 1999). Another cytotoxic product, 4-HNE, is highly reactive, particularly to thiols and amino groups, meaning it primarily causes damage to proteins (Schaur, 2003). Its ability to form adducts with ATPases and kinases can allow it to interact with many signalling processes in a physiological and pathophysiological manner, impacting proliferation, apoptosis, cytokine production and mitochondrial membrane potential (Breitzig et al., 2016; Dalleau, et al., 2013; Zarkovic et al., 2013). Similarly, MDA was found to modify over 30 proteins involved in processes such as energy metabolism, cytoskeletal integrity and transport (Zarkovic et al., 2013).

1.4 GPX1 in cancer

Far from being just a harmful by-product from cellular metabolism, hydrogen peroxide has many uses as a signalling molecule, and as such, the levels are tightly controlled in the cell. This implicates GPX1 and other GPX enzymes in having a key regulatory role in redox homeostasis. This redox homeostasis is essential for monitoring stress and stimulating the cell to activate stress response machinery. As Sies stated in their recent review, oxidative stress is a broad term which can be split into two states: oxidative eustress, which describes low levels of hydrogen peroxide which can be managed by stress machinery, and oxidative distress, which describes hydrogen peroxide levels high enough to overwhelm stress response machinery and cause damage (Sies, 2017). At any one time, most cells will exist in oxidative eustress, where normal cell function is maintained. By contrast, oxidative distress can be characterised by growth arrest and apoptosis. The way in which cells initiate their response, towards apoptosis or recovery, is chiefly dictated by the central signalling molecule: hydrogen peroxide.

This balance is determined by both the production of hydrogen peroxide, and its clearance or detoxification. As discussed previously, hydrogen peroxide is produced from metabolic processes in the mitochondria and peroxisome. As well as this, 31 enzymes (Go et al., 2015), including NOX enzymes (Bedard and Krause, 2007), xanthine oxidoreductase (XOR) (Pritsos, 2000) and many other oxidases, generate H_2O_2, either directly or through superoxide formation. These enzymes, alongside metabolic systems, work antagonistically to the action of antioxidant enzymes such as the GPXs, peroxiredoxins and catalase. To add a layer of complexity, the local concentration of hydrogen peroxide can also be altered by its transport across membranes by aquaporins (AQP) (Bienert et al., 2006) - the rate of which can vary between isoforms (Wang et al., 2020). Depending on the tissue and compartment, the enzymes involved in the production, transport and removal of hydrogen peroxide can vary (Sies et al., 1972; Jones et al., 1981; Antunes et al., 2002). This allows for the maintenance of different resting levels of hydrogen peroxide, which allows for different inter- and intra-cellular signalling pathways to be utilised effectively.

As a peroxidase, GPX1 has an important role in protecting the cells from oxidative damage, which also implicates it in protecting cells from age-related diseases, such as cancer. Based on this understanding alone, it may be assumed that GPX1 is purely beneficial for preventing cancer development. However, the prevalence of H_2O_2 and ROS in many signalling pathways has particularly interesting ramifications in the context of cancer development and lends GPX1 a role in many of the hallmarks of cancer (figure 1.11) (Hanahan and Weinberg, 2011). By controlling the level of H_2O_2, GPX1 can play a protective role against cancer, as it interacts with pathways controlling immune cell development and inflammation, which works to prevent cancer development and growth. However, the role of GPX1 as a modulator can work in the opposite fashion, promoting pro-carcinogenic signalling. Therefore, GPX1 has a complex relationship with cancer, whereby it acts as a tumour suppressor and an oncogene, depending on the cell context.

For many cancer cells, high levels of GPX1 activity can be advantageous, activating many of the other hallmarks (figure 1.11). In fact, meta-analyses show that *GPX1* expression is often upregulated in cancer (Wei et al., 2020). As discussed below, one explanation for this finding is that GPX1 can promote invasion and metastasis, angiogenesis, proliferative signalling, and can protect cancer cells from cell death. This not only allows cancer to progress quicker, but, as many chemotherapeutic agents rely on apoptosis to kill cancer cells, it also promotes resistance to treatment. These effects are often compounded in patients with high *GPX1* expression, giving patients with high GPX1 worse prognoses (Wei et al., 2020). This is

perhaps the most clinically relevant aspect of GPX1, as our understanding of this relationship can aid us in designing more effective cancer therapies.

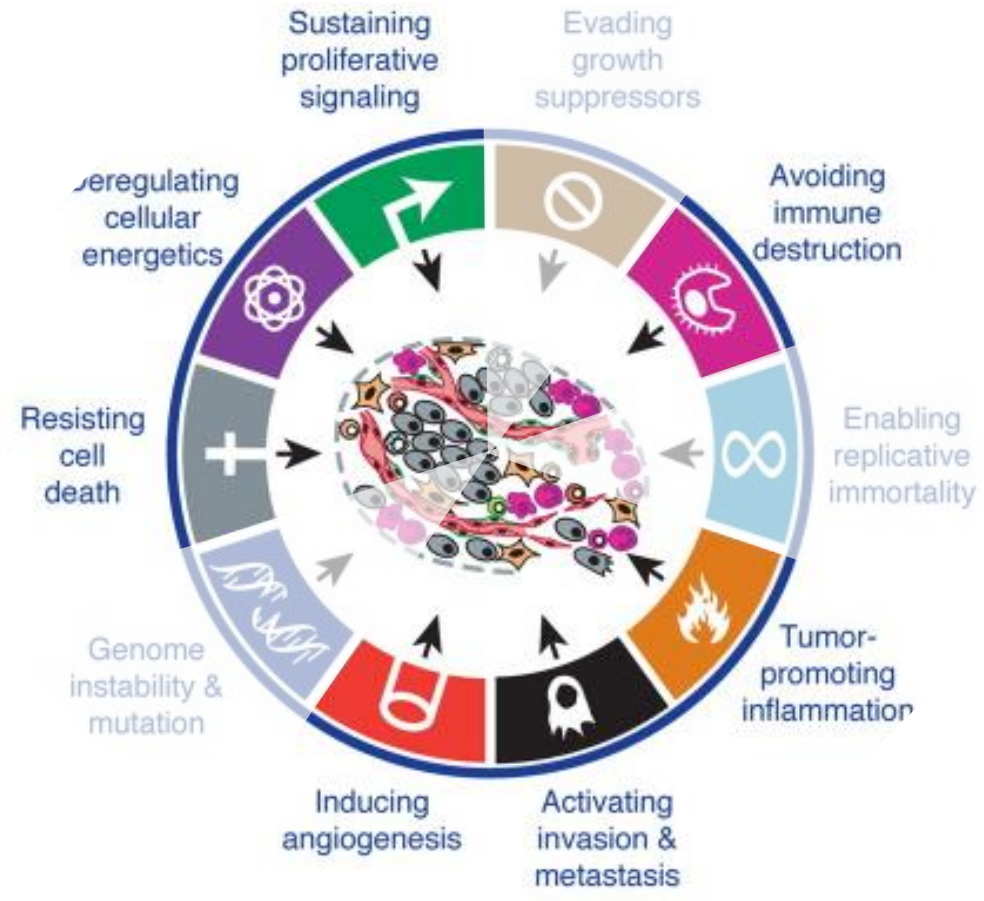

Figure 1.11: The hallmarks of cancer. *Bolded sections are those in which GPX1 and/or H_2O_2 play an important role. Adapted from Hanahan and Weinberg, 2011.*

1.4.1 GPX1 as a protector

Protecting against cancer is arguably the primary function of GPX1. Its role in detoxifying H_2O_2 contributes to the maintenance of redox homeostasis and prevents the formation of radicals. As discussed in section 3.2, these radicals can damage DNA and cause mutations if the DNA damage is not repaired by maintenance machinery. Knockouts of GPX1 in mice showed increased susceptibility to oxidative damage produced by paraquat, hydrogen peroxide (de Haan et al., 1998) and diquat (Fu et al., 1999), leading to early death. Conversely, overexpression of *GPX1* in mouse fibroblasts can protect against UV-induced damage (Baliga et al., 2007). In human cells (HaCaT keratinocytes (Hazane-Puch et al., 2013) and fibroblasts (Hazane-Puch et al., 2014)) supplementation with selenium causes overexpression of *GPX1*, which is protective against UV-A. In addition, cell death was

reduced following UV-A treatment at non-toxic doses of the selenium supplement. Not only is GPX1 protective against UV and subsequent ROS, but its expression is also easily manipulated by selenium supplementation, which offers an easy route of investigation for determining the anti-cancer ability of GPX1. It is not just the direct reduction in ROS that confers the anti-cancer ability of GPX1; GPX1 and hydrogen peroxide are involved in many other pathways which can influence the cellular defence against cancer.

One of the easiest ways to illustrate the protective relationship of GPX1 against cancer is through looking at a common polymorphism of GPX1 which reduces antioxidant activity, and how this can affect cancer risk. The Pro198Leu polymorphism is fairly common (Forsberg et al., 2000) and is associated with lower GPX1 activity, which was shown to correlate with reduced sensitivity to selenium supplementation (Hu and Diamond, 2003; Jablonska et al., 2009). The presence of this polymorphism in a cohort is associated with an increased cancer risk in many cancer types including bladder cancer (Zhao et al., 2005; Paz-y-Miño, 2009; Cao et al., 2013), and breast cancer (Méplan et al., 2013; Jablonska et al., 2015; Ravn-Haren et al., 2005), among others (Bănescu et al., 2016; Krhin et al., 2016; Trifa et al., 2016). While a meta-analysis study has supported the link between the Pro198Leu polymorphism and increased cancer risk (Chen et al., 2011), many studies have failed to support these findings (Hansen et al., 2005; Goerlitz et al., 2011; Arsova-Sarafinovska et al., 2008). To an extent, discovering a consistent relationship seems unlikely given our understanding that the expression of GPX family proteins varies between tissues and with selenium level (see section 2.2.3), and that some GPXs in some tissues can compensate for the loss of GPX1 activity. Not only this, but GPX1 operates within many other pathways involved in carcinogenesis, making the protective capabilities of GPX1 more complex and likely to vary between cohorts and cancer types.

1.4.1.1 Inflammation

Hydrogen peroxide acts as a redox sensor for oxidative stress and can stimulate a wide range of signalling pathways. It is not an on/off response, and is finely tuned to modulate the signalling of some stress pathways even during oxidative eustress. Inflammation for example, is stimulated by H_2O_2 through the PI3K/AKT pathway, which causes the NF-κB transcription factor to promote the expression of interleukins and TNF-α to induce inflammation. This can also induce the response in adjacent cells, regardless of their redox state. Overstimulation of inflammation leads to apoptosis in hydrogen peroxide-rich cells. As these cells are also likely to have a greater risk of damage to biomaterials, this can also be a

protective action, as these cells would be more likely to adopt abnormal phenotypes and become cancerous.

GPX1 can compensate for changes to inflammatory signalling caused by GPX2 loss. Such events have been observed in the intestinal crypts, where GPX2 is normally expressed. In GPX2 KO mice, GPX1 levels were increased in the crypt bottom, and this was able to partially compensate for loss of GPX2 when selenium was sufficiently available, as it was regulated at the transcriptional level (Florian et al., 2010). However, in a double KO of both GPX1 and GPX2, mice develop ileocolitis and intestinal cancer, as they have a greater level of peroxidative stress and are far more susceptible to bacteria-associated inflammation (Chu et al., 2004; Florian et al., 2010). This phenotype could be rescued by restoring GPX2 but not GPX1 (Chu et al., 2004). Furthermore, when colitis was induced through dextran sodium sulphate, GPX2 levels increased greatly during inflammation, as inflammatory mediators upregulated GPX2, whereas GPX1 increased only slightly during the acute inflammatory phase (Hiller et al., 2015). GPX1 is therefore protective against cancer in this context, and these findings indicate that GPXs have specific roles within the inflammatory signalling network.

Inflammatory signalling can be modulated by H_2O_2. Nuclear factor κB (NF-κB) is a key downstream effector for H_2O_2 (figure 1.12). This transcription factor is responsible for the upregulation of genes involved in inflammatory and immune responses to oxidative stress. These target genes encode for cytokines (TNF-α, IL-1β, and IL-6), as well as inflammatory enzymes such as cyclooxygenase-2 (COX-2) and inducible NO synthase (iNOS) - all of which promote inflammation (Ogata and Hibi, 2003; Itzkowitz, 2006; Piotrowski et al., 2020). Although H_2O_2 was once believed to an inducer of NF-κB, this relationship has since been found to be more complex (Oliveira-Marques et al., 2009; Lingappan, 2018). H_2O_2 acts instead as a modulator and fine-tunes NF-κB activation in response to oxidative stress by stimulating both activating and inhibitory pathways to control NF-κB induction (Lingappan, 2018). This promotes a proportionate response to stress, allowing for pro-inflammatory pathways to be activated briefly in order to prevent prolonged inflammation and carcinogenesis (de Oliveira-Marques et al., 2007). GPX1 itself is also upregulated by NF- κB, which creates a negative feedback loop to further modulate this response (Gan et al., 2014).

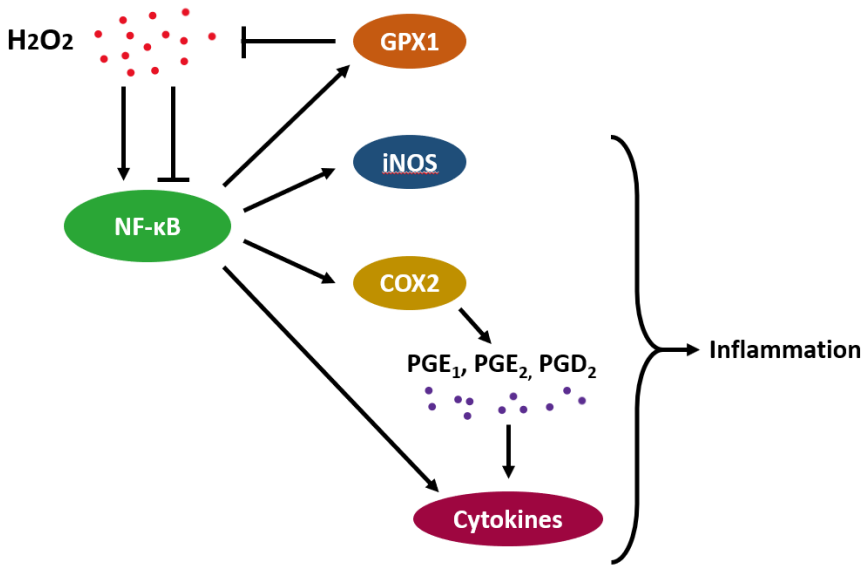

Figure 1.12: NF-κB modulation by H_2O_2 and the subsequent impact on inflammation. *H_2O_2 can activate or inhibit NF-κB. NF-κB activation leads to the upregulation of iNOS, COX2 and GPX1, and cytokines, both directly and via prostagladins (PGE_1, PGE_2, PGD_2) produced by COX2.*

This pathway's reliance on H_2O_2 lends itself to modulation by GPX1. Indeed, *GPX1* overexpression has been shown to reduce the activation of NF-κB in response to UV, TNF-α and H_2O_2, and knockdowns show the opposite effect (Li et al., 2001) (figure 1.12). In particular, the expression of *COX-2* and *TNF-α* were increased in GPX1 KD cell lines, as well as the quantity of the prostaglandins produced by COX-2, such as PGE_1, PGE_2 and PGD_2 (Koeberle et al., 2020). These prostaglandins are responsible for many of the biochemical changes involved in inflammation, such as the maturation of immune cells and the release of cytokines (Ricciotti and FitzGerald, 2011). In many tissues, the downregulation of *GPX1* mediates this response through H_2O_2, however this is not always the case, as other selenoproteins are able to compensate for the loss of GPX1 activity. However, knockdown of GPX1 in gut epithelium was associated with a ROS-independent induction of NF-κB (Gong et al., 2011), suggesting that there are more direct mechanisms for GPX1 modulation of NF-κB, unrelated to ROS removal, yet to be elucidated.

1.4.1.2 Deregulating Cellular energetics

GPX1 works against deregulated metabolism in pancreatic ductal adenocarcinoma (PDAC) cells, a particularly aggressive and lethal disease. GPX1 is often downregulated in pancreatic cancer tissues, however it was unclear how this would convey an advantage to PDAC cells (Cullen, Mitros and Oberley, 2003; Kodydkova et al., 2013). PDAC cells rely upon glycolysis

for metabolism, and in glucose-deprived conditions, metabolic stress responses upregulate autophagy in order to provide materials, such as ATP, for cancer growth (Blum and Kloog, 2014). Glucose deprivation downregulates GPX1 by increasing degradation. Lower GPX1 in these cells resulted in high levels of ROS, which activated autophagy (Meng et al., 2018). The reverse was also true, *GPX1* overexpression lowered ROS and prevented autophagy induction, promoting cell death. GPX1 is therefore an antagonist of the cancerous energetic phenotype and offers protection against the development of this hallmark.

1.4.2 GPX1 promoting cancer

Despite protecting cells from DNA damage, GPX1 promotes many of the hallmarks of cancer and in many cases, this leads to more aggressive, more invasive and more chemoresistant cancers. GPX1 can influence cancer to such a degree that *GPX1* expression can be used as a biomarker for prognosis in multiple cancer types (Zhang, Q et al., 2018; Wei et al., 2020). For example, in giant cell tumour of bone (GCTB), *GPX1* expression was higher in patients with recurrent cancer, and patients with high *GPX1* expression were more likely to relapse (Okubo et al., 2013). In renal cell carcinoma, *GPX1* expression is positively correlated with metastasis, tumour stage and overall survival, and could potentially be used a diagnostic and prognostic biomarker for disease severity (Cheng et al., 2019). Therefore, although it can protect against cancer in many ways, high *GPX1* expression is often detrimental for patient outcomes.

To understand how GPX1 can drive cancer progression in many of these cases, we will examine the specific hallmarks that GPX1 is able to promote. *GPX1* expression varies from tumour to tumour, as do the impacts of GPX1, however, as there are many mechanisms of action for promoting tumour development across the hallmarks, opportunities for GPX1 to aid growth are plentiful, and can often be compounded in patients. As we will discuss, GPX1 can promote invasion and metastasis, angiogenesis, proliferative signalling, and protect cancer cells from immune destruction and apoptosis. Moreover, increased *GPX1* expression desensitises cancer cells to chemotherapy, reinforcing the importance of GPX1 in severe cancer cases and the need for our understanding of GPX1 as a biomarker and a chemotherapeutic target to improve efficacy of treatment.

1.4.2.1 Invasion and Metastasis

Managing ROS levels is particularly important for invasion and metastasis. Circulating tumour cells (CTCs) must overcome large amounts of stress, including ROS, in order to establish a metastatic colony in a new tissue. For this reason, this environment is highly selective for GPX1-rich CTCs, which are more able to tolerate the oxidative stress. This has been shown in

prostate cancer, where overexpression of *GPX1* and *SOD2* are strong predictors of metastases (Giesing et al., 2010; Giesing et al., 2012). GPX1 has also been found to be upregulated in brain cancer CTCs and CTC-derived brain metastatic tumour cells (Klotz et al., 2019), as well as in breast cancer CTCs (Beck et al., 2019) and lung micrometastases (Basnet et al., 2019). High *GPX1* expression is advantageous for these circulating cells as it protects them from oxidative stress in the new tissues which they seek to invade. As well as this, GPX1 provides advantage to these circulating cells through upregulation of pathways important for adhesion and invasion.

An example of this is found in the relationship between GPX1, selenium binding protein 1 (SBP1) and hypoxia-inducible factor-1α (HIF-1α). SBP1 is able to inhibit the activity of GPX1 by an unknown mechanism, although there is a physical interaction between the SBP1 and GPX1 (Fang et al., 2010). Conversely, Fang et al also found that GPX1 represses the expression of *SBP1* at the transcriptional and epigenetic level. This relationship has been investigated within the context of cancer development (Jerome-Morais et al., 2011). *SBP1* expression alone can be a powerful predictor of prognosis across many cancer types, as lower expression is associated with poorer prognosis (Li et al., 2008; Kim et al., 2006; Chen et al., 2004; Zhang, X et al., 2018). Inhibiting SBP1 in hepatocellular carcinoma using siRNA led to an increase in GPX1 activity and a downregulation of HIF-1α (Huang et al., 2012). It was found that, in this case, the loss of HIF-1α activity increased tumour invasiveness and metastasis, and therefore negatively impacts patient prognosis (Huang et al., 2012).

Recently, it was found that *GPX1* expression drives invasion via focal adhesion kinase (FAK) signalling in Triple-negative breast cancer (TNBC) cells (Lee et al., 2020). TNBC is a particularly aggressive form of breast cancer, associated with poor prognosis and resistance to treatment. While *GPX1* is silenced in other breast cancer cells, it is expressed in TNBC cells, and aids metastasis by promoting cell adhesion via FAK. GPX1 directly interacts with FAK, and hydrogen peroxide inhibits FAK activation by preventing FAK autophosphorylation, as well as phosphorylation via Src. Loss of GPX1 also represses the expression of genes associated with adhesion, which Lee et al believe may be a result of Src activation in the absence of H_2O_2. This offers a good explanation for the aggressiveness of TNBC cells and demonstrates how GPX1, through its role in redox homeostasis, creates advantageous phenotypes for aggressive cancers.

1.4.2.2 Avoiding immune destruction

GPX1 has a key role in T-cell activation, development and function. As discussed previously, GPX1 is an important modulator of NF-κB activation, which is also a central signalling

pathway in the development of immune cells. For example, NF-κB signalling activates neutrophils and macrophages, both of which are known in cancer cells to promote inflammatory signalling and release other procarcinogenic factors into the tumour microenvironment (TME) (Mantovani, 2014). ROS can decrease NF-κB activation in neutrophils, and so acts as an anti-inflammatory agent in this context (Zmijewski et al., 2007). In these experiments, a higher level of H_2O_2 prevented lipopolysaccharide-induced NF-κB activation. As NF-κB remained inactive, it was not able to promote the expression of proinflammatory cytokines such as TNF-α and macrophage inhibitory protein (MIP)-2. Similarly, in GPX1 deficient ($GPX1^{-/-}$) mice, there were lower levels of TNF-α, MIP-2 and granulocyte-macrophage colony-stimulating factor (GM-CSF) protein, which resulted in fewer macrophages and neutrophils being produced. However, in this case, the level of mRNA expression for TNF-α, MIP-2 and GM-CSF was unchanged by removing GPX1, but instead this reduction in protein was attributed to increased 20S proteasome activation (Bozinovski et al., 2012). GPX1 in this case is clearly essential for the maturation of immune cells. As expected, in renal cell carcinoma patients, high GPX1 was associated not only with higher immune invasion, but also with worse prognosis (Chen et al., 2020).

Both H_2O_2 and lipid peroxides can mediate the activation of T cell receptor (TCR) signalling pathways (Devadas et al., 2002). TCR-induced ROS generation allows for the activation of signalling pathways promoting proliferation, and in GPX1 deficient T helper (Th) cells, the resulting elevation in ROS promoted the production of IL-2 and cell proliferation. GPX1 deficient cells also had favoured development to Th_1 cells over Th_{17} cells, indicating that GPX1 influences T-cell fate (figure 1.13). Similarly, GPX1 works alongside catalase (cat) in managing ROS levels in regulatory T (Treg) cells, which are responsible for promoting tolerance in immune cells and are known to dampen antitumor responses (Ohue and Nishikawa, 2019). In $GPX1^{-/-}$ x $Cat^{-/-}$ mice, production of IL-6 and IL-17A was reduced following aggravation of colitis, and KO mice Tregs were also hypofunctional in suppressing the proliferation of effector T-cells (Kim et al., 2014), and again supressed the differentiation of CD4+ cells to Th_{17}. Expression of GPX1 is also strongly correlated with Treg activation in glioblastoma and lower-grade glioma tumours (Lv et al., 2020)

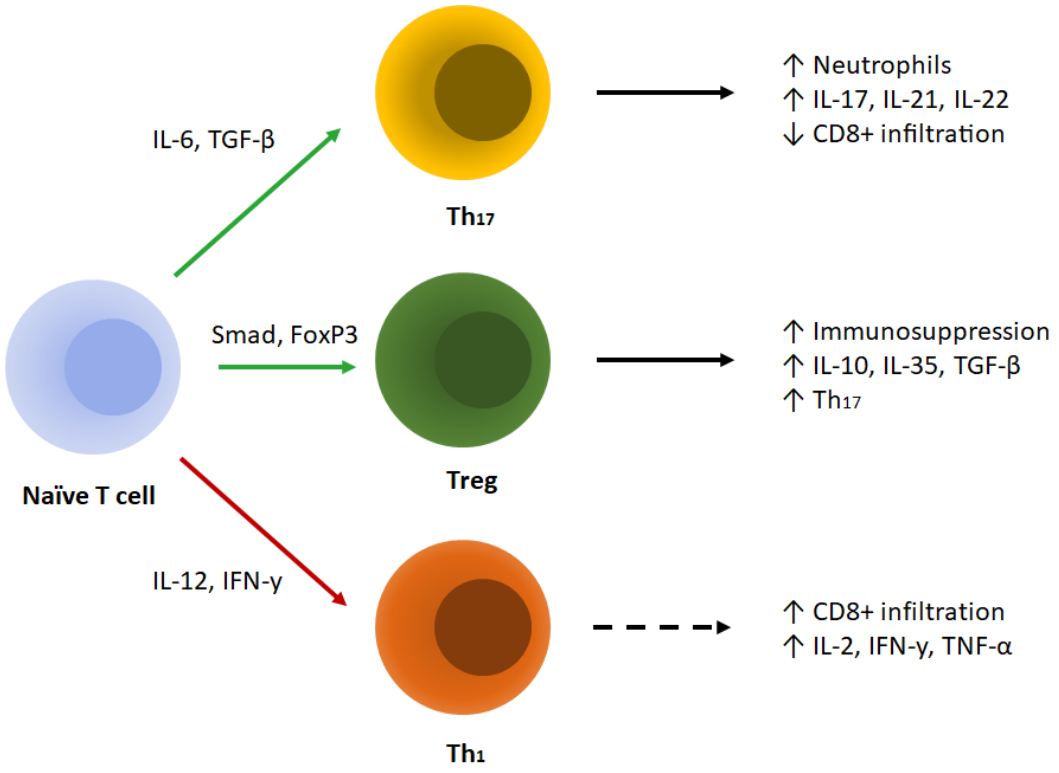

Figure 1.13: Development of T cells from the progenitor naïve T cell. *Green arrows indicate processes which are promoted by GPX1, and red arrows indicate processes which are downregulated by* GPX1 *expression.*

The type of T cells present in the TME can have massive impacts on prognosis, due to the cytokines produced by the T cell (Chraa et al., 2018). It varies greatly between tumour types whether the changes are aid or hinder cancer growth, but some trends can be elucidated. In most cases, Th_1 cells promote anti-tumour immunity, and patients with high levels of Th_1 cells in the TME generally had a better prognosis (Chraa et al., 2018; Fridman et al., 2012). This is thought to be due to their ability to recruit tumour-killing CD8+ cells (Hoepner et al., 2013), as well as their production of IFN-γ, which activates the cytotoxic ability of dendritic cells (figure 1.13) (LaCasse et al., 2011). Conversely, Th_{17} cells in the TME was associated with worse prognosis as they promoted proliferation through IL-17 production, and inhibited infiltration of the tumour by CD8+ cells (Chraa et al., 2018; Wang et al., 2020). As Treg are immunosuppressive, the increased presence of Tregs in the TME is also indicative of worse prognosis in most cases (Chraa et al., 2018). The effect of *GPX1* expression on immune regulation is such that the levels of GPX1 can be used prognostically in GBM and LGG patients to determine patient outcome through predicting the levels of TME infiltrates (Lv et al., 2020). As GPX1 promotes pro-carcinogenic immune infiltrates over tumour-killing

immune cells, higher *GPX1* expression can influence the composition of the TME to provide effective immune protection for tumours.

1.4.2.3 Angiogenesis

GPX1 is linked to angiogenesis in normal cells. In GPX1-deficient mice, loss of GPX1 led to a decrease in revascularisation following injury (Galasso et al., 2006). Not only this, but the number of endothelial progenitor cells (EPCs), which promote neovascularisation, was markedly lower. As expected, these EPCs had higher ROS, and were more susceptible to ROS-induced apoptosis, as elevated levels of ROS led to an inability to stimulate angiogenesis. In endothelial cells, vascular endothelial growth factor (VEGF) signalling was found to promote the expression of GPX1, leading to a decrease in ROS level (Guo et al., 2017). Conversely, the elevated levels of H_2O_2 seen in cancer are able to stimulate VEGF production (Schäfer et al., 2002; Xia et al., 2007; Komatsu et al., 2008). As hydrogen peroxide levels are often elevated in cancer cells (Szatrowski and Nathan, 1991), the linking of these two pathways may allow ROS levels to remain at a tolerable level for promoting angiogenesis without initiating cell death.

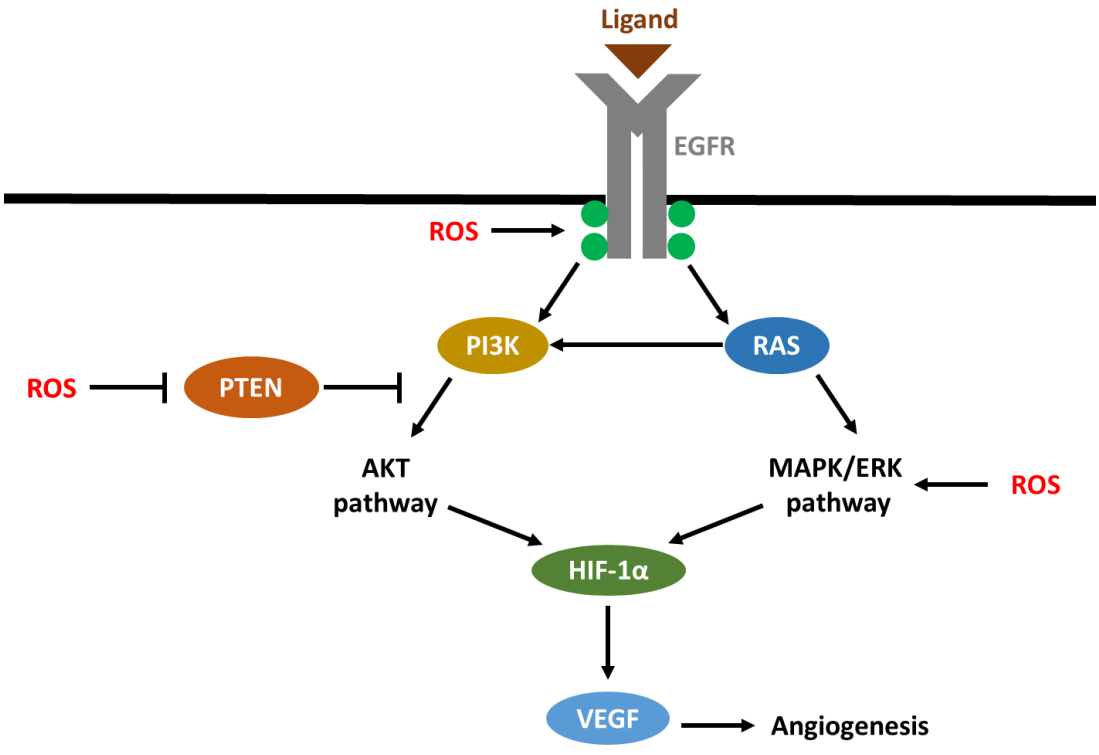

***Figure 1.14: Angiogenic signalling pathways activated following EGFR activation**. ROS stimulates activation of the receptor after ligand binding, activating PI3K and RAS, and stimulating the AKT pathway and MAPK/ERK pathways respectively. Both pathways are promoted by ROS, either directly in the case of MAPK/ERK, or indirectly through inactivation*

of an inhibitor (PTEN) in the AKT pathway. Both pathways stimulate HIF-1α production, which acts as a transcription factor for VEGF, promoting angiogenesis.

ROS, particularly H_2O_2, interact with signalling networks to promote angiogenesis via VEGF (figure 1.14). EGFR-mediated activation of the AKT pathway, for example, was lowered with overexpression of GPX1, as well as EGFR activation itself (Handy et al., 2009). Mitochondrial levels of H_2O_2 were also found to regulate angiogenesis (VEGF production) via inactivation of PTEN in the PI3K/AKT pathway in endothelial cells (Connor et al., 2005; Rodriguez and Huynh-Do, 2012). MAPK can be activated by ROS directly, as well as through interactions with other activating molecules upstream of this pathway (Lee et al., 2020). VEGF production is stimulated via the transcription factor hypoxia-inducible factor-1 (HIF-1α), which is activated by both the MAPK/ERK and AKT/PI3K pathways (Pore et al., 2006). VEGF can also be stimulated through the SPI1 transcription factor, after activation via RAS signalling, subject to redox status (Komatsu et al., 2008).

Hydrogen peroxide is now considered a regulator of angiogenesis-related factors, not only HIF-1α and VEGF, but also tissue inhibitor of metalloproteinase 3 (TIMP3) and thrombospondin 1 (THBS1) in cancer cells (Jerónimo et al., 2017). Its role in mediating angiogenesis, both through the signalling pathways and through interactions with other angiogenesis-related factors makes it a key regulator of the 'angiogenic switch'. The angiogenic switch is the point at which anti- and pro-angiogenic factors are forced out of balance, and cancers adopt an angiogenic phenotype. This makes the cancers more aggressive, as blood supply not only provides oxygen for proliferation and tumour growth, but also presents cancer cells with a means to exit the site of the primary tumour and metastasise in other areas of the body. Hydrogen peroxide is therefore critical in cancer development, and the maintenance of high hydrogen peroxide at tolerable levels contributes through angiogenic signalling to the aggressive cancer phenotype often observed in GPX1-rich cancer cells.

1.4.2.4 Proliferative signalling

The role of GPX1 in sustaining proliferative signalling is conflicted - depending on the cell type, it can either prevent or promote proliferation. Evidence for GPX1 playing a role in suppression of proliferation was discussed in section 1.4.1, however, as mentioned in section 1.4.2.3, overexpression of *GPX1* decreases EGFR signalling (Handy et al., 2009), which also led to decreased replication, indicating that there were lower levels of proliferation in *GPX1*-overexpressing cells. Similarly, lower stimulation of the AKT pathway in the absence of H_2O_2, due to PTEN activation, leads to the suppression of genes for proliferation and survival

(Handy et al., 2009; Connor et al., 2005; Rodriguez and Huynh-Do, 2012). Although in this context GPX1 is clearly antagonistic to proliferative signalling, this is not the case in other cell contexts.

Lack of GPX1 can also attenuate cell growth; fibroblasts from $Gpx1^{-/-}$ mice exhibit a senescent-like phenotype which reduces proliferative capacity and responsiveness to EGF (de Haan et al., 2004). Downregulating GPX1 in oral cancer led to a lower level of proliferation (Huang et al., 2016). In other cell types, such as in oesophageal cancer and skin cancer, *GPX1* overexpression can increase proliferation (Gan et al., 2014; Lu et al., 1997). These effects are thought to be mediated by NFκB signalling, which can modulate the expression of proliferative genes as well as *GPX1* (Huang et al., 2016; Gan et al., 2014). Therefore, cancer cells which are more reliant on NFκB are believed to be more susceptible to GPX1-dependent proliferative signalling. More work is needed to fully determine the extent to which proliferation is affected by GPX1 in different cancer types, however it is currently clear that the role of GPX1 is not universal.

1.4.2.5 Apoptosis

In normal cells, GPX1 works antagonistically to apoptosis, which is mediated through ROS in many ways (figure 1.15). GPX1 knockout mice show a greater susceptibility to apoptosis, with increased ROS stimulating cell death (de Haan et al., 1998; de Haan et al., 2004; Galasso et al., 2006). In certain circumstances, GPX1 is also able to prevent apoptosis in cancer cells. Overexpression of *GPX1* is protective against CD95-induced apoptosis as it blocks activation of key apoptotic machinery, such as caspases (Gouaze et al., 2002). In endothelial cells, overexpression of *GPX1* alters the ratio between Bax (pro-apoptotic) and Bcl-2 (anti-apoptotic) away from apoptosis (Faucher et al., 2005). Overexpression of GPX1 also prevents apoptosis-inducing factor (AIF) from translocating into the nucleus to fragment DNA (Zemlyak et al., 2009). More recently, peptide-Au clusters targeted at GPX1 in tumor cells were able to induce apoptosis through the intrinsic mitochondrial pathway (Liu et al., 2017). This offers proof not only of the importance of GPX1 in tumour cell survival, but also of the potential for GPX1 to be a promising target for anticancer drugs.

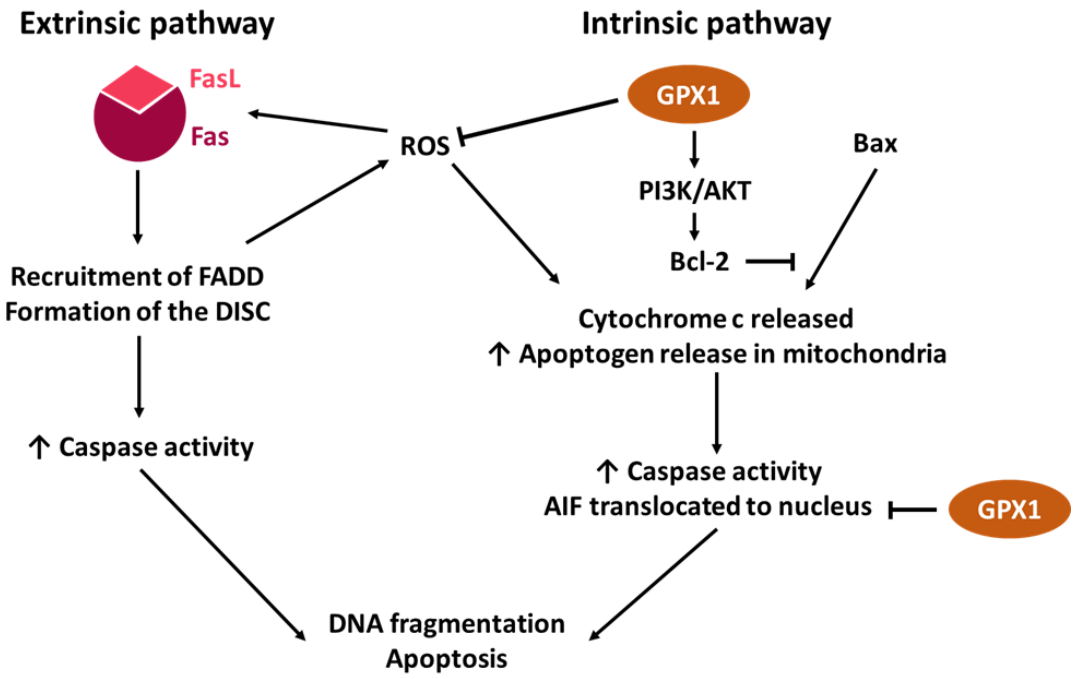

Figure 1.15: The intrinsic and extrinsic pathways of apoptosis*. The extrinsic pathway is initiated through a ligand binding a receptor, in this instance, FasL and Fas respectively. This then recruits the Fas-associated protein with death domain (FADD) along with procaspases 8 and 10 to form the death inducing signalling complex (DISC). These procaspases are then cleaved to become active caspases, and begin a caspase cascade, increasing caspase activity. Caspases can then induce DNA fragmentation which leads to cell death. The intrinsic pathway can be stimulated by ROS and by pro-apoptotic signalling via Bax. Cytochrome c is then released by the mitochondria, along with apoptogens. Cytochrome c binds to apoptotic proteins to form the apoptosome, and activates caspase 9, leading to cell death. GPX1 works in opposition to this pathway by removing ROS, as well as by activating PI3K/AKT signalling, upregulating Bcl-2 and inhibiting Bax. It is also able to inhibit the translocation of AIF to the nucleus, again preventing DNA fragmentation and death.*

1.4.3 Drug resistance

Since many current chemotherapeutic drugs, such as imatinib and erlotinib, aim to generate ROS to trigger apoptosis in the tumour cells (Perillo et al., 2020), overexpression of *GPX1* can substantially impact the success of cancer treatment. The elevated levels of GPX1 observed in some more aggressive tumours (see sections 4.2, 4.2.1, 4.2.5) may protect cancer cells from chemotherapeutic drug-induced cell death and promote multidrug resistance. For example, it has been found in Non-small-cell lung carcinoma (NSCLC) that GPX1 promotes resistance against cisplatin treatment as ROS levels are insufficient to trigger apoptosis via

AKT/PI3K (Chen et al., 2019). Similar experiments in oesophageal cancer found the same trend; GPX1 activity correlated with cisplatin resistance (Gan et al., 2014). In non-Hodgkin B-cell lymphoma cells which were resistant to cisplatin, etoposide, methotrexate and bortezomib, the use of a GPX1 inhibitor resensitises cells to the drug treatment (Schulz et al., 2012).

Increased GPX1 activity conferred greater resistance to doxorubicin (DOX) treatment in breast cancer (Gouazé et al., 2001) and ovarian cancer cell lines (Doroshow and Juhasz, 2019). A similar trend has also been observed in non-cancerous cells (Doroshow, Esworthy and Chu, 2020; Kalivendi et al., 2005). Kalivendi et al suggested that GPX1 can prevent both intrinsic and extrinsic apoptotic pathways from being triggered by DOX. The intrinsic pathway is inhibited as ROS generation is attenuated by GPX1 in response to DOX, which would normally activate cytochrome c and caspases (figure 1.15), leading to apoptosis. The extrinsic pathway is inhibited through the modulation of ROS-dependent calcium/calcineurin signalling. ROS produced by DOX stimulates calcium/calcineurin signalling, which allows nuclear factor of activated T-cells (NFAT) to translocate to the nucleus and upregulate Fas Ligand (Fas L). Fas L binds to the Fas receptor and begins the extrinsic apoptotic signalling cascade, which again activates caspases leading to apoptosis (figure 1.15).

1.4.3.1 Overcoming Multidrug resistance

Due to the central role of ROS in apoptotic signalling, overexpression of GPX can greatly impact response to treatment. Therefore, it is unsurprising that cancer patients with high *GPX1* expression have a worse prognosis and recovery (Wei et al., 2020). GPX1 has immense therapeutic relevance in this sense, as an inhibitor could potentially resensitise cells to chemotherapeutic drugs and improve the efficacy of existing treatments. Indeed, it has already been shown that tiopronin, an agent which selectively targets MDR cancer cells and increases their sensitivity to drug treatment, works via inhibition of GPX1 (Hall et al., 2014). While this is an exciting proof of concept, many available GPX1 inhibitors, including tiopronin, have too low efficacy and specificity *in vivo* for clinical use, and research is ongoing to find a more potent GPX1 inhibitor (Chaudiere et al., 1984; Schulz et al., 2012; Behnisch-Cornwell et al., 2020).

1.4.3.2 Mercaptans

The most potent and widely used inhibitor of GPX1 is mercaptosuccinic acid (MSA). MSA, along with tiopronin, is a mercaptan compound, and uses a thiol to bind to the selenium in the active site of GPX1 (Chaudiere et al., 1984; Hall et al., 2014). The initial binding of the sulphur in mercaptan compounds to selenium allows the inhibitor to oxidise a lysine residue

within the active site, regenerating the selenium but creating a sulfenamide group on the lysine. The sulfenamide can then be irreversibly oxidised to a sulfonamide, occluding further binding of GSH in the active site. Thus, MSA and tiopronin are irreversible competitive inhibitors of GPX1, and were able to attain IC_{50} values of between 42.7 and 149.4μM in human cancer cell lines (Behnisch-Cornwell et al., 2019). This makes them among the most potent inhibitors of GPX1 available; however, this mode of action means that the inhibitors exhibit non-specific binding of other selenoproteins as well as GPX1, as they have similar structures (Lubos et al., 2011). This means that there may some off-target effects associated with its clinical use as a GPX1 inhibitor.

1.4.3.3 Methylmercury

Methylmercury (MeHg) uses a distinct mechanism of inhibition, as it modifies the substrate and the enzyme. MeHg is highly reactive to thiols, and binds directly to GSH, preventing it from entering the active site of GPXs (Kaur et al., 2006; Franco et al., 2009). Although this is not specific to GPX1, as GPX1 has a relatively high affinity for GSH, its activity is severely affected by the reduction in GSH availability (Hirota et al., 1980). It can also bind to selenium or sulphur in the active site of redox proteins (Fujimura and Usuki, 2020). Therefore, in its use as a GPX1 inhibitor, it could have many off target effects, for example in lowering the activity of TxnRDs (Carvalho et al., 2008; Fujimura and Usuki, 2020) and Mn-SOD (Kumagai, 2013). MeHg therefore has a compounding effect on the redox system, which does indeed increase ROS (Ali et al., 1992) and can trigger apoptosis (Fujimura and Usuki, 2020). However, as it not selective for GPX1, it may not offer the specificity required to improve treatment in GPX1-overexpressing patients while preventing further damage.

1.4.3.4 Gold compounds

Gold (Au) compounds work in a similar fashion to MeHg, as they both have high affinity for selenols. Gold(I) thioglucose was found to covalently bond to the selenol in the active site of glutathione peroxidase in a reversible fashion, preventing the detoxification of H_2O_2 (Chaudiere and L. Tappel, 1984). Recently, this concept has been applied to create a more specific inhibitor for GPX1, which has both a greater affinity for GPX1 and a greater selectivity. Peptide-Au clusters have been synthesised using molecular dynamic simulations, allowing the peptides within the clusters to bind selectively to amino acids in the GPX1 active site, giving Au direct access to the GPX1 selenocysteine (Liu et al., 2017). When tested in tumour cells, GPX1 activity was successfully reduced by the addition of these clusters, and intrinsic apoptosis was stimulated, indicating these clusters have good potential as a GPX1-specific drug. Indeed, other peptide-Au clusters have exhibited anti-tumour ability in

xenograft experiments (Zhai et al., 2018), signifying that a similar success *in vivo* is foreseeable for the peptide-Au cluster designed by Liu et al.

1.4.3.4 Pentathiepins

Pentathiepins are sulphur-rich heterocyclic compounds, some of which are known to be cytotoxic to cancer cells (Konstantinova et al., 2004; Lee et al., 2002). Recently, a range of pentathiepins were investigated a potential GPX1 inhibitors. These compounds were up to 15 times more effective than MSA at inhibiting bovine GPX, and one compound specifically inhibited GPX1 (Behnisch-Cornwell et al., 2020). This compound was also particularly cytotoxic to cancer cell lines which expressed high levels of GPX1, indicating that pentathiepins may be useful in resensitising GPX1-rich cancer cells to chemotherapeutic drugs. However, there are other effects, such as increased DNA damage and a rapid change to mitochondrial membrane potential, which are yet to be confirmed as GPX1-related. Therefore, further research is needed to fully establish the impact of pentathiepins on cancer cells, ahead of its clinical use.

1.4.3.5 Peroxiplat

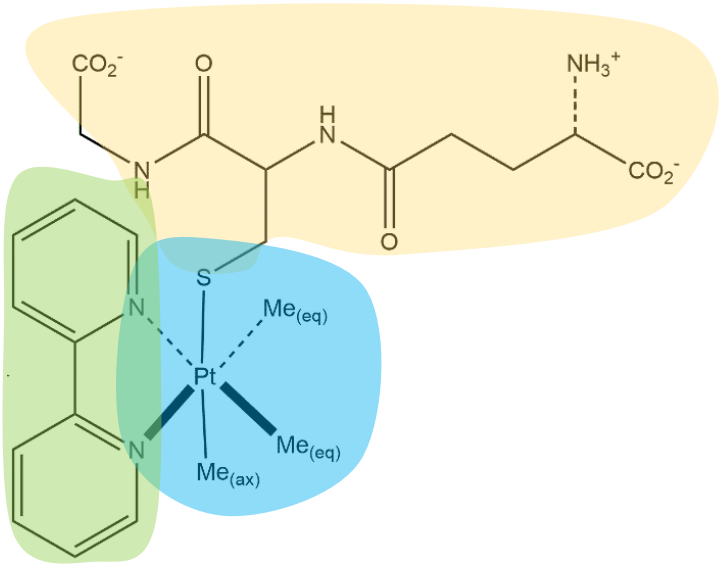

***Figure 1.16: Structure of the photoluminescent compound PeroxiPlat**. S-glutathionyl-fac-trimethyl-2,2'-bipyridylplatinum(IV), otherwise known as Peroxiplat, composed of a platinum core (blue) with a* bipyridine ligand (green) and a glutathionyl group (yellow).

PeroxiPlat (figure 1.16), is a recently synthesised and patented photoluminescent compound (Coogan et al., 2021). Potentially, this compound could be used for imaging as well as inhibition of GPX1, creating exciting possibilities for a dual-action agent for the diagnosis and

treatment of GPX1-overexpressing cancer patients. The structure of Peroxiplat is derived from the original d^6 polypridyl lumophore, $[Ru(bipy)_3]^{2+}$, which has been used extensively for in-cell experiments (Fernández-Moreira et al., 2010). D-block lumophores have biochemical advantages, such as kinetic inertness, along with beneficial physical properties, such as larges Stokes shifts, long luminescence lifetimes and lower photobleaching (Fernández-Moreira et al., 2010). Together, these qualities make d^6 metal complexes ideal for imaging cells, offering bright and clear images without causing instant cytotoxicity.

However, there is potential for selective toxicity in GPX1-rich cells as it is thought to bond to GPX1 using its platinum complex and the associated bioconjugate - a glutathionyl group. It has been proposed that PeroxiPlat is therefore able to interact with the active site of GPX1 in a similar fashion to a GSH substrate, as was discussed previously (figure 1.4). However, this would instead result in a covalent Pt-Se bond, which would occupy the active site and inhibit GPX1 activity (figure 1.17). In theory, this could be an irreversible interaction, indicating that PeroxiPlat has the potential to be a potent GPX1 inhibitor.

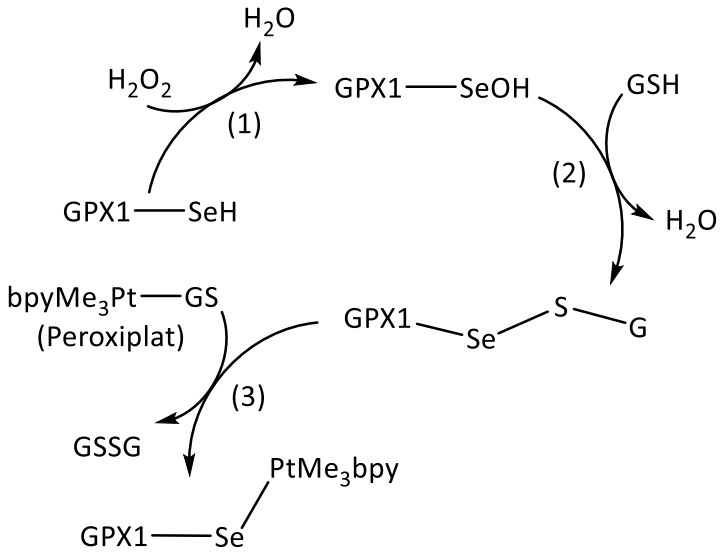

Figure 1.17: Proposed interaction of PeroxiPlat ($PtMe_3$(bpy)GS) with GPX1. *(1) GPX1 is attacked at the selenium of the active site selenocysteine residue, which results in its oxidation to the selenic form and addition of the reduced glutathione (2). This is followed by a dehydration to selenenyl sulphide (2), which opens the Se up to attack by a second reduced glutathione molecule, producing a GSSG product and regenerating the enzyme. (3) This final reduction step is where PeroxiPlat is theorised to substitute for GSH, and where a strong covalent Pt-Se bond is established.*

Indeed, the reaction of PeroxiPlat with a selenocysteine amino acid was revealed by NMR to occur via a Pt-Se bond (Coogan, M, unpublished work). This has been further investigated with the larger molecule diphenyl diselenide, where again spectra indicated a Pt-Se bond, indicating that such a reaction could indeed be possible with more complex selenium-containing compounds, such as GPX1. Not only this, but *in vivo* experiments with HaCaT cells (figure 1.18) have found evidence of the Pt-Se interaction occurring within cells, as lambda scans show comparable emission spectra to the Pt-Se product, and show little emission at 488 nm, the usual excitation frequency of PeroxiPlat. This shift in emission and expression indicates that Peroxiplat has the potential to inhibit GPX1 as well as to provide a means of measuring GPX1 level *in vivo*. PeroxiPlat could therefore be of great clinical use, both for the diagnosis and treatment of cancer, as GPX1 has been linked to poor prognosis and poor response to treatment.

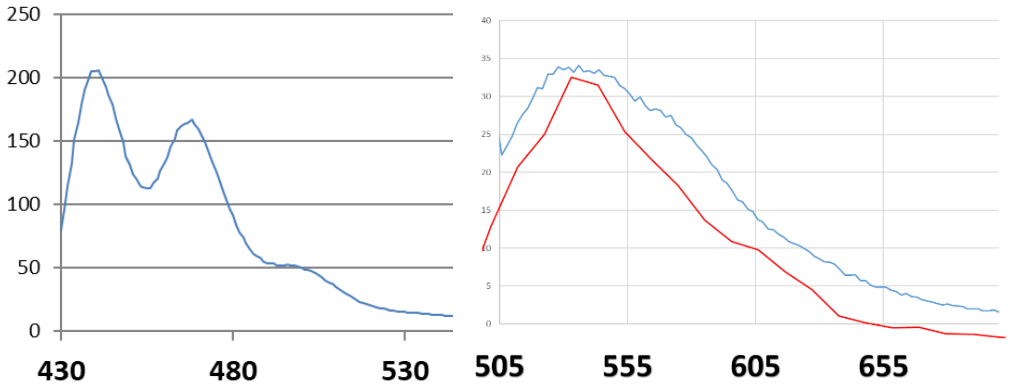

Figure 1.18. Emission spectra of PeroxiPlat in various states. *Peroxiplat excited 405 nm (LHS), and scaled overlay of emission spectrum of Sec-bound Peroxiplat (blue) and lambda scan of free PeroxiPlat in HaCaT cells (red) (RHS). Both charts: x-axis scale: wavelength (nm) y-axis scale: emission intensity (arbitrary units). Figure taken from Coogan, M, unpublished work.*

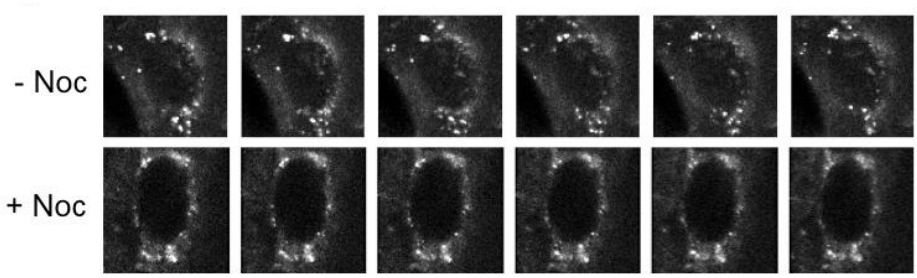

Figure 1.19: Timelapse of HaCaT cells with PeroxiPlat, and with or without Nocodazole (Noc), a microtubule transport inhibitor*. Photographs were taken at 20 second intervals. Figure taken from Coogan, M, unpublished work.*

It has been suggested that Peroxiplat is specific to GPX1. Confocal imaging experiments have illustrated that PeroxiPlat accumulates in the peroxisome, as there was no movement of PeroxiPlat clusters when peroxisome transport is inhibited with Nocodazole (figure 1.19). It also appeared that GPX1 was highly localised to the peroxisomes. However, it should be noted that GPX1 was not the only selenoprotein which could theoretically be targeted, nor has an interaction between PeroxiPlat and GPX1 been directly observed. Furthermore, the method of Peroxiplat uptake remains unknown, as canonical glutathione channels, while able to transport large amounts of GSH into the cell, are unlikely to accommodate Peroxiplat due to the Pt-S bond. Therefore, more research is needed on how PeroxiPlat functions within the cell to determine its theranostic potential.

1.5 Summary

GPX1 is a major selenoprotein in cancer progression. It is a central redox enzyme, not only important for the protection of cells against ROS, but also in modulating cellular signalling. The development of cancer can give GPX1 oncogenic properties, driving the progression of tumours, and increasing their resistance to chemotherapeutic agents. This culminates in worse prognosis for GPX-overexpressing patients in most cases, and therefore GPX1 has become a potential target for inhibitors to improve patient outcome. Its specific structural qualities, such as tetrameric form and its high affinity for GSH can be exploited in designing inhibitors which selectively target GPX1 over other GPXs and selenoproteins. Indeed, many types of GPX1 inhibitor are currently being investigated, including PeroxiPlat, which may double as a diagnostic tool to assess suitability for GPX1-targeted treatment. Although none yet have proven to be high specificity and high efficacy *in vivo,* it is certain that such an inhibitor could be extremely beneficial for treatment of cancer, particularly in MDR tumours. Furthermore, there is immense potential for the eventual use of a GPX1 inhibitor, as these inhibitors move into further rounds of investigation.

1.6 Project Aims

GPX1 is plays a multifaceted role in cancer, and its key function in managing cellular ROS allows GPX1 to both prevent and promote cancer development. As such, this project intends to investigate GPX1 within the cancer context from many angles, from mRNA to protein to network. To achieve this, this project aims to:

- Ascertain whether *GPX1* is overexpressed across a range of cancer types and determine the prognostic effect of *GPX1* expression in cancer patients using bioinformatic-based research
- Assess the importance of mutations to *GPX1* in cancer development using existing cancer databases
- Determine whether the expression patterns of GPX1-related proteins may compound to promote cancer development and progression
- Establish, using the Genomics of Drug Sensitivity in Cancer (GDSC) database, whether *GPX1* expression promotes chemoresistance across a range of cancer cell types
- Determine the effect of supplementation at various concentrations of sodium selenite (Na_2SeO_3) on GPX1 protein levels in cancerous (HeLa and A431) and non-cancerous (HaCaT) cell types, and the longevity of this response
- Investigate whether selenium supplementation with Na_2SeO_3 can impact chemoresistance in HaCaT cells
- Assess the potential of a novel photolumiscent compound, PeroxiPlat, as theranostic agent in cancer

Chapter 2 - Methods

2.1 Bioinformatics

2.1.1 GEPIA

Gene Expression Profiling Interactive Analysis (GEPIA) is an interactive portal which allows the user to generate various plots based on gene expression in cancer types (Tang et al., 2017). The GEPIA database contains 9,716 tumour and 8,587 tissue samples, combining information from both TCGA and GTEx databases. The GEPIA portal was used to generate an expression profile for *GPX1* across tumour and normal samples, and Kaplan-Meier survival plots using expression of *GPX1* as a factor for survival. The plots display overall survival and disease-free survival in a range of cancers, with HR, P and Cox P values labelled. A table defining the abbreviations of the cancer types can be found on pages 6-8.

The GEPIA portal was also used to generate a scatter plot showing *GPX1* against *GPX4* expression in normal and tumour samples. This was generated using the correlation analysis tool and selecting *GPX1* and *GPX4* for comparison using the Pearson coefficient. Samples for comparison were selected from the TCGA datasets and only sample types which were represented in both the tumour and the normal datasets were chosen (BLCA, BRCA, CESC, CHOL, COAD, ESCA, HNSC, KICH, KIRC, KIRP, LIHC, LUAD, LUSC, PAAD, PCPG, PRAD, READ, SARC, SKCM, STAD, THCA, THYM, UCEC).

The multiple gene comparison tool was also used to generate heatmaps of expression across tumour and normal samples. The tissue types selected were ACC, BLCA, BRCA, CESC, CHOL, COAD, ESCA, GBM, HNSC, KICH, KIRC, KIRP, LAML, LGG, LIHC, LUAD, LUSC, OV, PAAD, PCPG, PRAD, READ, SARC, SKCM, STAD, TGCT, THCA, THYM, UCEC, UCS. The sets of genes selected for comparison were GPX1 family proteins (GPXs 1-8) along with SBP2, and a further set of GPX1-related genes (EXOSC2, POLR2L, HSD17B10, TP53, RHOA, KARS, VAMP8, ABL2, CTSD and TXN). This heatmap was created using matched TCGA normal and GTEx data on a log scale (log2(TPM + 1)) and adjusted using Plotly software to improve the visible contrast.

2.1.2 FireBrowse

The FireBrowse Portal (http://firebrowse.org/) uses HG19 TCGA data, and this was employed to produce a boxplot for *GPX1* expression across a range of cancers. This data originates from RNASeq experiments and *GPX1* expression in the plot displayed as RNA-Seq by Expectation-Maximisation (log2).

2.1.3 COSMIC

The Catalogue of Somatic Mutations in Cancer (COSMIC) dataset is a comprehensive resource designed to investigate the effect of somatic mutations in cancer (Tate et al., 2018).

According to cancer.sanger.ac.uk/cosmic, COSMIC is the 'world's largest source of expert manually curated somatic mutation information relating to human cancers.' The data is sourced from large established databases, such as TCGA and ICGC, as well as from peer reviewed genome screening papers. As a result, there are over 37,000 genomes in the COSMIC database. I investigated GPX1 by querying the canonical *GPX1* gene into the portal (ID COSG75375), and curating data from the Gene View and Mutation Distribution sections. This was used to generate charts displaying the distribution of mutations across the gene and the expression and copy number variations seen in tumour samples.

2.1.4 ICGC

The International Cancer Genome Consortium (ICGC) portal allows users to query specific genes in a large dataset of cancer genomes (Zhang et al., 2019). *GPX1* was investigated using this portal, and a mutation distribution map was created from the output given in the 'Protein' tab. Prevalence data was also pulled out from this output. This was generated by interrogating 19,729 samples in the database.

2.1.5 Ensembl

Ensembl is a browser which allows users to investigate genomes, including gene variants, across a range of species (Howe et al., 2020). In this analysis, *GPX1* was queried in the *Homo Sapiens* dataset, where there were 3685 entries for variants of *GPX1*. This was further investigated for the presence of the P77R variant, and information for mutational impact scores were extracted.

2.1.6 GDC

The Genomic Data Commons (GDC) data portal allows the user to browse, analyse and extract data from the TCGA database (Grossman et al., 2016). *GPX1* was queried and of 12,174 somatic samples, 800 were tested for the *GPX1* gene. The mutation distribution map was taken from the 'Protein' tab, which also lists the source of each result.

2.1.7 GDSC

Genomics of Drug Sensitivity in Cancer (GDSC) is a data portal created by Wellcome Sanger Institute and the Cancer Genome Project which allows the user to pull data on drug sensitivity across 1000 human cancer cell lines (Yang et al., 2013). To investigate the connection between *GPX1* expression and resistance to the chemotherapeutic drugs cisplatin, doxorubicin and docetaxel. Each of the drugs were searched and the IC_{50} values were extracted for all available cell lines. Note that some of the cell lines had no *GPX1* expression data and/or no IC_{50} results in the databases. The IC_{50} was plotted on a log scale

against the *GPX1* expression data (RNA-Seq) taken from the from the Cancer Cell Line Encyclopaedia (Broad Institute) and were manually curated and matched to each cell line.

2.2 Cell Culture

2.2.1 Media and Buffers

Name	**Components**
Dulbecco's Modified Eagle's Medium with 4.5 g/L Glucose, with L-glutamine and phenol red (Lonza BioWhittaker™)	Supplemented with 10% FCS (Labtech) and 100 U/mL penicillin and 100 μg/mL streptomycin (Gibco)
10X Tris Glycine SDS PAGE Buffer (National Diagnostics)	0.25 M Tris base, 1.92 M glycine, and 1 % (w/v) SDS
RIPA buffer	25 mM Tris, 150mM NaCl, 0.1 % SDS, 0.5 % sodium deoxycholate, 1 % Triton X 100. Supplemented with cOmplete™ Mini, EDTA-free protease inhibitor cocktail tablets (Roche) and PhosSTOP phosphatase inhibitor cocktail tablets (Roche)
Transfer Buffer	300 mM Tris base (Fisher), 10 μM CAPS (Sigma), 10% (v/v) ethanol (Fisher), 0.05% w/v SDS (Melford).
4X SDS Loading Buffer (pH 6.8)	50 mM Tris-HCl pH 6.8, 2% SDS, 10% glycerol, 0.02 % bromophenol blue, 100mM DTT (added directly before use)
Blocking Buffer	5% milk in 1X TBST (137 mM Sodium Chloride, 20 mM Tris, 0.025% Tween-20. Supplied at pH 7.6, stock 20X Tris buffered saline solution with detergent Tween 20, Severn Biotech)
Incubation buffer	0.5% Bovine Serum Albumin (Sigma) in PBS

Table 2.1: Composition of the media and buffers used throughout the experiments.

2.2.2 Mammalian Cell culture (HaCaT, A431 and HeLa)

Immortalized human HaCaT keratinocyte, A431 and HeLa cells were grown in individual flasks at 37°C with 5% CO_2 in a humidified incubator. Cells were grown in Dulbecco's modified essential medium (DMEM; Lonza, Switzerland) supplemented with 10% heat inactivated foetal calf serum (Invitrogen, Carlsbad, CA) and 100 UmL^{-1} penicillin and 100

µgmL^{-1} streptomycin (Lonza, Switzerland), and were passaged every 3 to 4 days, or when the cells had reached 80-90% confluence.

2.3 Selenium supplementation with Na_2SeO_3

2.3.1 Antibodies

Name	Concentration
GPx-1/2 Mouse Monoclonal Antibody (Santa Cruz Biotechnology sc-133160)	Western Blot 1:1000 Immunofluorescence 1:200
Purified mouse anti-actin Ab-5 monoclonal antibody (BD Bioscience 612656)	Western Blot 1:10000
Anti-mouse IgG, HRP-linked Antibody (Cell Signalling 7076)	Western Blot 1:4000
Goat anti-Mouse IgG (H+L) Cross-Adsorbed Secondary Antibody Alexa Fluor 488 (ThermoFisher A-11029)	Immunofluorescence 1:1000

Table 2.2: Types and concentrations of antibodies used in immunofluorescent and Western Blotting protocols

2.3.2 Stimulating GPX1 activity with Na_2SeO_3

To investigate the effect of selenium stimulation on GPX1 production and determine the optimum concentration to use for maximum GPX1 yield, HaCaT, A431 and HeLa cultures were prepared with varying levels of Na_2SeO_3 for varying incubation times. An appropriate density of cells for each cell type (table 2.3) was suspended in 2 mL of DMEM, FCS, penicillin, and streptomycin (as above) were added to each well in a six well plate. These were left to seed for 2 hours at 37°C with 5% CO_2 in a humidified incubator. To test the optimum concentration for GPX1 production and cell survival, different concentrations of Na_2SeO_3 were tested. Each well was treated with 20 µL of serially diluted Na_2SeO_3 in milliQ water (10 µM, 1 µM, 100 nM, 10 nM, 1 nM, 0 M). As previous work had utilised 6-day incubations to improve GPX1 activity, two plates were made to test the effect of incubation time with Na_2SeO_3 on survival and GPX1 activity (Hazane-Puch et al., 2013). One plate was incubated for 24 hours, and another for 96 hours in the conditions as before. After the incubation period, the medium was removed, and the cells were washed with 10 mL phosphate buffered saline (PBS) per well. Cells were put on ice, and 70 µL ice-cold RIPA buffer (table 2.1) was added to each well before scraping cells to suspend in the buffer. The suspensions

were then centrifuged at 13000 rpm for 5 minutes, and supernatant was taken from each sample.

Cell type	24h (cells/mL)	96h (cells/mL)
HaCaT	$1.5x10^5$	$7.5x10^4$
A431	$1.5x10^5$	$7.5x10^4$
HeLa	$1x10^5$	$5x10^4$

Table 2.3: Seeding density for all cell types used in either 24- or 96-hour supplementation experiments

2.3.3 Determining total protein concentration with Bradford Assay

In order to ensure samples had equal total protein before testing for GPX1 concentration, a Bradford Assay was performed using BSA to create a standard curve. BSA was diluted with PBS into concentrations of 0, 0.25, 0.5, 1 and 2 mg/mL, and 2.5 µL RIPA (Table 2.1) was added to each. On a 96 well plate, 2.5 µL of each BSA concentration were added to 200 µL Bradford Ultra (Expedeon) in separate wells. 10 µL of each sample with varying Na_2SeO_3 concentration and incubation time were added to 200 µL Bradford Ultra. For the samples and the BSA standards, this was repeated to obtain an average absorbance. This was then tested in a TECAN plate reader measuring absorbance at 595 nm. The data for BSA absorbance was plotted and used to determine the total protein (mean) in each of the samples.

2.3.4 Western blotting

Protein samples prepared from cells incubated with varying concentrations of Na_2SeO_3 for 24 and 96 hours were resolved through an SDS-PAGE gel and blotted to test for differences in GPX1 protein level in response to supplementation with selenium. For equal loading of protein, samples were diluted to 30 mg/mL protein in RIPA, and 20 µL 3x Loading Buffer (table 2.1) was added to each. Samples were boiled for 3 minutes at 95°C before loading 15 µL into a gel (4-20% Tris-Glycine Mini Gels WedgeWell™, ThermoFisher) with TGS. 5 µL of PageRuler Plus protein ladder (ThermoFisher) was also added before running the gel at 225 V for 30 minutes. This was transferred onto an Immobilon®-P PVDF membrane (Sigma-Aldrich). This blot was blocked for one hour in 5% milk in TBST, washed and immunostained with anti-mouse IgG secondary antibody (table 2.2) before imaging with the SuperSignal™ West Femto

ECL kit (ThermoFisher). Equal loading and efficient transfer were confirmed with an anti-actin counter stain.

2.3.5 Determining longevity of response

HaCaTs were incubated for 96 hours in the presence of 1 µM Na_2SeO_3 before seeding a 6 well plate with varying cell densities for 24-72 hours (see table 2.4), and a sample was taken of supplemented cells at 0 hours after withdrawal from selenium. The 0 hour samples of approximately $6x10^5$ cells, both with and without selenium were centrifuged at 13000 rpm for 5 minutes, before washing with PBS and centrifuging again. These were lysed in RIPA buffer and centrifuged as before, and the supernatant was collected. After incubating the plate for 24, 36, 48 and 72 hours, a sample was taken from the appropriate well by washing with PBS and scraping cells with 70 µL ice-cold RIPA buffer (Table 2.1), before centrifuging samples at 13000 rpm for 5 minutes, and taking the supernatant.

Incubation time (hours)	24	36	48	72
Seeding cell density (cells/mL)	$1.5x10^5$	$1.25x10^5$	$7.5x10^4$	$3.75x10^4$

Table 2.4: Cell densities used for seeding HaCaTs in Na_2SeO_3 withdrawal experiments.

2.3.6 XTT assay for resistance to chemotherapeutic agents and H_2O_2

To investigate the effect of Na_2SeO_3-dependent elevation in GPX1 on the cellular response to stress, cell survival with varying concentrations of damaging agents (H_2O_2, cisplatin, doxorubicin and docetaxel) was assessed using an XTT assay. HaCaT cells were incubated for 96 hours either in the presence of, or without, 1 µM Na_2SeO_3, before being seeded into 96 well plates at a density of 5000 cells per well. The Na_2SeO_3-treated cells were seeded in medium containing 1 µM Na_2SeO_3. Cells were allowed to rest for 24 hours before chemical treatments were added. 2 mM H_2O_2, 200 µM cisplatin, 20 µM doxorubicin or 10 nM docetaxel was added to the first well in both plates, and double dilutions were performed across the succeeding 6 wells, with no treatments added to the final row of cells. 50 µL of XTT reagent from the XTT Cell Viability Assay Kit (Biotium) was added to each well and incubated for 6 hours before measuring the absorbance at 630 nm (490 nm reference) on a TECAN plate reader.

2.3.7 CyQuant assay for resistance to chemotherapeutic agents and H_2O_2

To investigate the effect of Na_2SeO_3-dependent elevation in GPX1 on the cellular response to stress, cell survival was assessed using the CyQuant assay after the addition of varying concentrations of damaging agents (H_2O_2, cisplatin, doxorubicin and docetaxel). Cells were seeded into two 96 well plates at a density of 1000 cells per well and were left for one hour to settle. After this, the medium was replaced with 200 µL DMEM, with or without 1 µM Na_2SeO_3 supplementation. Cells were allowed to grow for 96 hours before the media was removed and DMEM containing chemical treatments, as well as selenium supplementation for one plate, were added. 2 mM H_2O_2, 200 µM cisplatin, 20 µM doxorubicin or 10 nM docetaxel was added to the first well in both plates, and double dilutions were performed across the succeeding 6 wells, with no treatments added to the final row of cells. The plates were incubated at 37°C and 5% CO_2 for 24 hours. 100 µL of CyQuant reagent was added to each well and this was incubated again for one hour before measuring the fluorescence at 480/535 nm.

2.4 Investigating the interaction of PeroxiPlat with GPX1

2.4.1 GPX assay

To investigate the effect of PeroxiPlat, prepared as in Coogan et al., 2021, on GPX1 activity, and therefore give an indication of its ability to inhibit GPX1, an assay was run using NADPH as a secondary reporter. PeroxiPlat was diluted in assay buffer to produce a 1 mg/mL solution. 5 µL of Bovine GPX1 was diluted with 5 µL of assay buffer. Wells were prepared as follows: 50 µL assay buffer was added to well 1; 5 µL of 1 mg/mL PeroxiPlat and 45 µL assay buffer were added to well 2; 5 µL diluted bovine GPX1 and 45 µL assay buffer were added to well 3; 5 µL diluted bovine GPX1, 5 µL 1 mg/mL PeroxiPlat and 40 µL assay buffer was added to well 4. A reaction mix containing 148.5 µL assay buffer, 13.5 µL, 40 mM NADPH, 9 µL glutathione reductase and 9 µL reduced glutathione was prepared and 40 µL was added to each well. The wells were then preincubated at room temperature for 15 minutes. 10 µL of cumene hydroperoxide was added and the output was measured immediately at two-minute intervals for 10 minutes at 25°C.

2.4.2 FOX assay

Reagent was prepared according to Rhee et al., 2010 to produce 2X FOX reagent for this assay. This contained 200 µM xylenol orange, 500 µM ammonium iron (II) sulphate hexahydrate in H_2SO_4 and 200 nM sorbitol. In order to prevent autoxidation of the ammonium iron (II) sulphate hexahydrate, it must be dissolved prior to its addition to the reagent mixture.

On a 96-well plate, wells were prepared according to table 2.5, volumes were made up to 55 µL with PBS. These were incubated for 10 minutes at room temperature before adding 55 µL FOX reagent and absorbance at 560 nm was measured after a further 10 minutes at room temperature.

Component\Well	1	2	3	4	5	6	7	8	9
Bovine GPX	25 µL	25 µL		25 µL	25 µL			25 µL	
PeroxiPlat (1 mg/ml)		5 µL	5 µL	5 µL					5 µL
Luperox (10 µM)	5 µL	5 µL	5 µL	5 µL	5 µL	5 µL	5 µL	5 µL	5 µL
Glutathione (20 µM)	20 µL	20 µL	20 µL			20 µL		20 µL	
MSA (500 µM)								5 µL	
PBS	5 µL								
FOX	55 µL	55 µL	55 µL	55 µL	55 µL	55 µL	55 µL	55 µL	55 µL

Table 2.5: Well composition for the FOX assay experiment.

2.5 Flow cytometry for GPX1 interactions

2.5.1 Fixing cells

HaCaT cells were grown in a T75 flask for 96 hours with or without supplementation with 1 µM Na_2SeO_3 up to 90% confluency. These cells were then trypsinised before resuspending in 10 mL DMEM (table 2.1) and centrifuging at 300 g for five minutes. The medium was decanted without disturbing the pellet, and cells were washed with 10 mL PBS before centrifuging for another five minutes at 300 g. The PBS was removed, and this wash was repeated with 5 mL PBS, before finally resuspending in 10 mL 4% paraformaldehyde solution in PBS (ChemCruz) and allowing to fix at room temperature for 15 minutes. This was then washed by centrifugation at 300 g for five minutes with excess PBS, and the supernatant was discarded. This was resuspended in 1 mL fresh PBS and 9 mL ice-cold methanol was added dropwise to the cells, and these were vortexed gently to mix. The fixed and permeabilised cells were stored at -20°C until use.

2.5.2 Immunostaining HaCaTs for GPX1

$5x10^5$ fixed cells/mL (section 2.5.1) from both supplemented and unsupplemented flasks were washed in excess PBS and centrifuged at 300 g for five minutes, and supernatant was discarded. After repeating this washing step, cells were resuspended in 100 µL GPX1

antibody (table 2.2) in incubation buffer (table 2.1) and incubated at room temperature for one hour. They were then washed by centrifugation (300 g, 5 min) in excess incubation buffer twice before resuspending in 100 µL Alexa Fluor 448 antibody (table 2.2) in incubation buffer (table 2.1) and incubating at room temperature for 30 minutes. These were washed by centrifugation in excess incubation buffer (300 g, 5 min) before resuspending in 0.5-1 mL PBS and analysing on the CytoFlex flow cytometer. Two samples with and without supplementation were also prepared without addition of the primary antibody, for comparison.

2.5.3 Interaction with PeroxiPlat

$5x10^5$ fixed cells/mL (section 2.5.1) from both supplemented and unsupplemented flasks were washed in excess PBS and centrifuged at 300 g for 5 minutes, and supernatant was discarded. 10 µL 10 mg/ml PeroxiPlat was added to each 1 mL sample and these were left to incubate for 10 minutes at room temperature. The fluorescence was then measured using the Cytoflex flow cytometer.

Chapter 3 - Bioinformatic analysis of the relationship between GPX1 and cancer

3.1 Introduction

The utilisation of bioinformatic analysis has allowed us to make considerable strides in cancer research. The emergence of high throughput RNA sequencing prompted the generation of unprecedented amounts of transcriptomic data in both cancerous and non-cancerous cell lines. Projects such as The Cancer Genome Atlas (TCGA), Genome Data Commons (GDC) (Grossman et al., 2016) and Gene Expression Profiling Interactive Analysis (GEPIA) (Tang et al., 2017) contain thousands of individual samples from hundreds of projects performed globally across decades. These transcriptional profiling databases are invaluable resources for investigating the expression of genes on a large, even pan-cancer scale.

The accessibility and magnitude of these databases has made bioinformatic-based approaches increasingly prevalent in modern cancer research (Cieślik and Chinnaiyan, 2017). Data portals such as the GEPIA and TCGA portals enable the user to easily identify the changes in gene expression that can be associated with development of cancer and look at clusters of expression across a genome which may compound risk (Sun et al., 2017; Hossain et al., 2019). Such methods have been used to identify expression patterns associated with specific cancer-promoting hallmarks, such as immune infiltration (Lv et al., 2020; Cui et al., 2021), across a range of cancer types. Researchers are now able to identify biomarkers which are able to predict prognosis and cancer drug response (Li et al., 2020; Clayton et al., 2020), making it possible to develop personalised medical interventions, improving patient treatment and outcome (Cardoso et al., 2016). Furthermore, these expansive databases are also large enough to not only measure the prevalence of gene variants in cancer samples, but also to create detailed mutational maps, from which residues of interest can be derived.

These tools are therefore ideal for exploring the true impact of *GPX1* in the context of cancer. This research aims to determine if and how *GPX1* and its variants may advance cancer, and how this impacts patient survival. The aims of this bioinformatic-based research were to (1) ascertain whether expression of the *GPX1* gene was elevated in cancer, (2) determine the prognostic effect of GPX1 mRNA expression, (3) assess the importance of mutations to the *GPX1* gene in cancer development, (4) determine whether the expression patterns of GPX1-related proteins may compound to promote cancer and (5) establish whether *GPX1* mRNA expression promotes chemoresistance across a range of cancer cell types.

3.2 *GPX1* expression in cancer

3.2.1 *GPX1* mRNA expression levels are generally higher in tumour than normal samples

To determine a trend of *GPX1* mRNA expression in tumour tissues when compared to the paired normal tissue, samples were taken from the GEPIA and TCGA databases (figures 3.1 and 3.2). The GEPIA database included 18,323 samples for comparison, and the TCGA database contained 12,011 samples. Both plots confirm that, across most cancer types, *GPX1* mRNA expression is higher than in the normal tissue. There is a large amount of scatter in both tumour and normal samples, indicating that *GPX1* mRNA expression varies greatly in cancerous and non-cancerous cells. However, there is generally a larger amount of variance in the tumour samples compared with corresponding normal cell sample. This increase in *GPX1* mRNA expression is also not seen ubiquitously across the samples, with some tumour cell lines having a far greater increase in expression than others. In particular, the samples from Glioblastoma Multiforme (GBM), Kidney Renal Papillary Cell Carcinoma (KIRP), Acute Myeloid Leukaemia (LAML), Brain Lower Grade Glioma (LGG), Ovarian Serous Cystadenocarcinoma (OV), Pancreatic Adenocarcinoma (PAAD), Skin Cutaneous Melanoma (SKCM), Testicular Germ Cell Tumours (TGCT), Thyroid Carcinoma (THCA), Uterine Corpus Endometrial Carcinoma (UCEC) tumours had very high levels of *GPX1* mRNA expression when compared with the normal tissue. Lung Squamous Cell Carcinoma (LUSC) and Pheochromocytoma And Paraganglioma (PCPG) were the only cancer cell lines to show a large loss of *GPX1* expression compared to the normal sample.

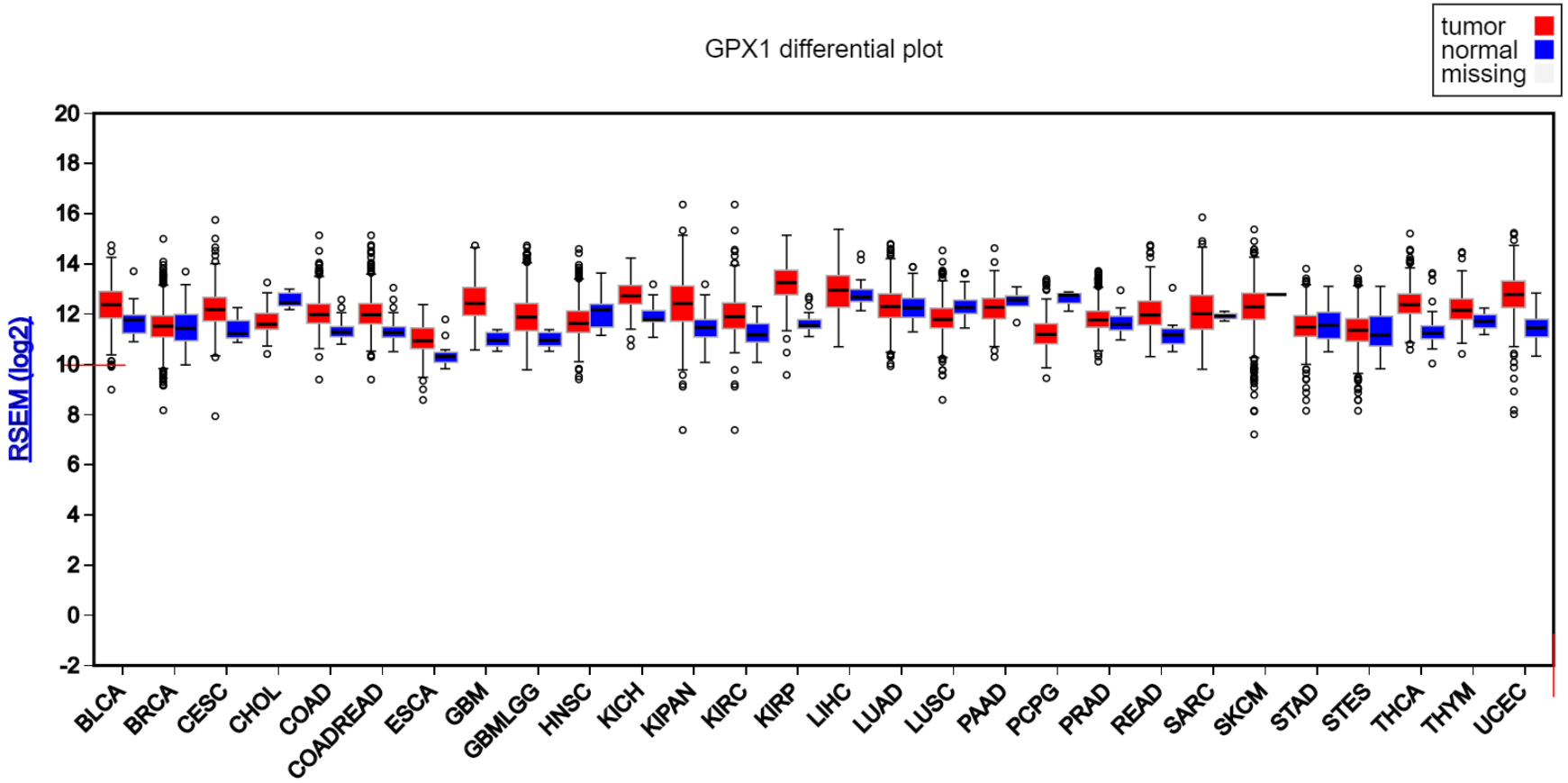

Figure 3.1:* GPX1 *mRNA expression is higher in tumour samples than in the normal samples in the majority of cancer types from Firebrowse data. *Boxplot of* GPX1 *expression found in samples taken from human cancers (red) and normal tissues (blue) based on RNAseq data from TCGA, made with FireBrowse, plotted as RSEM (log2) (RNA-Seq by Expectation-Maximisation).*

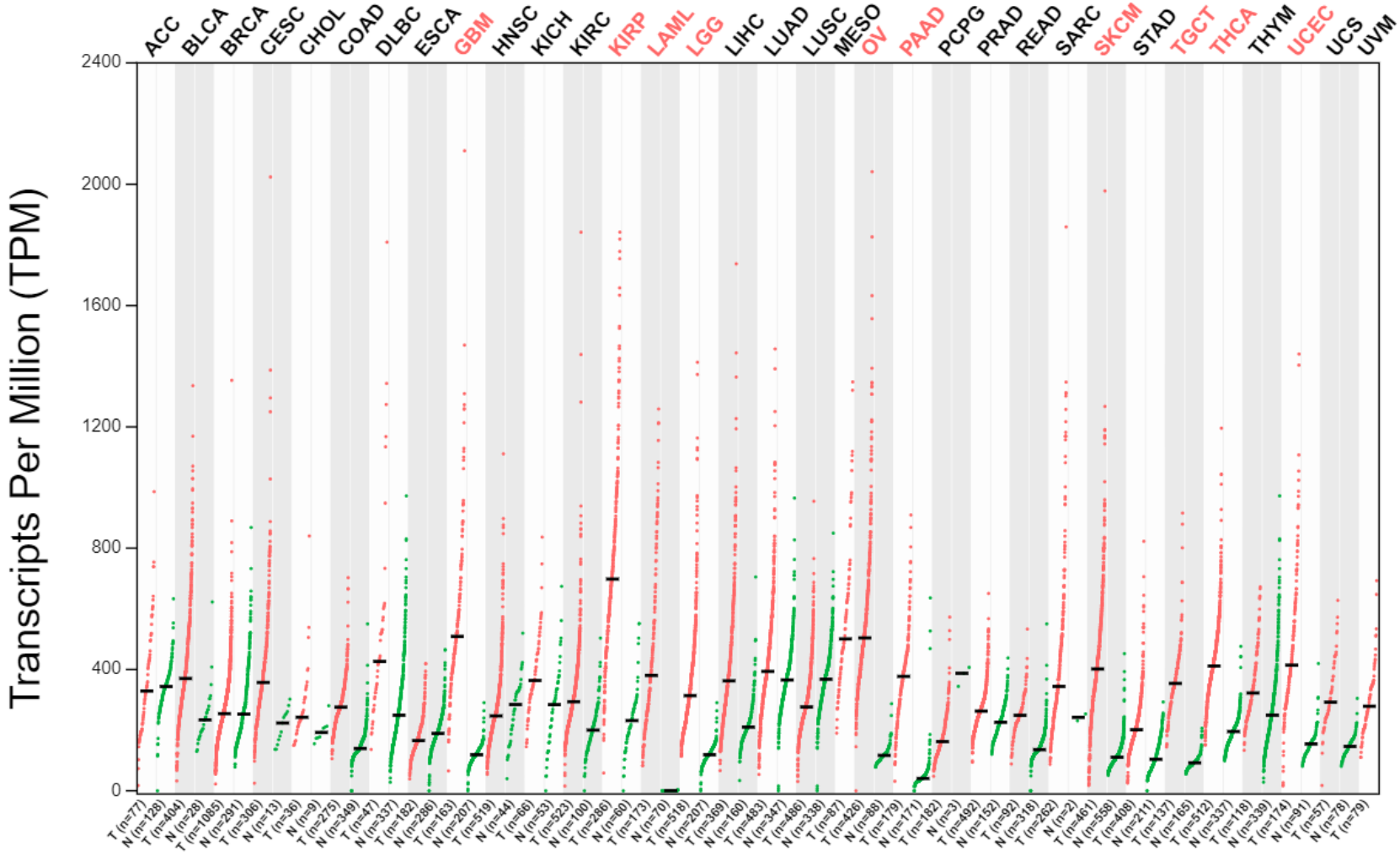

Figure 3.2:* GPX1 *mRNA expression was higher in tumour samples than in the normal samples in the majority of cancer types from GEPIA data. *Gene expression profile comparing tumour samples (red) with normal tissues (green), using RNAseq data from the GEPIA database.*

3.2.2 *GPX1* mRNA expression significantly impacts cancer prognosis in multiple cancer types

After identifying that tumours generally had a larger variation in *GPX1* mRNA expression than normal tissue, Kaplan-Meier plots were generated to determine whether higher *GPX1* mRNA expression in tumour samples correlated with a higher severity of disease. These plots were generated using data from the GEPIA database. In figure 3.3 A (Log-rank P=0.031, HR=2.6) and B (Log-rank P=0.0048, HR=5.4), high expression of *GPX1* was linked to worse overall survival (OS) in uveal melanoma (UVM) patients. In figure 3.3 B, high *GPX1* mRNA expression was defined as the upper quartile of expression in patients, and low *GPX1* mRNA expression as the lower quartile. The effect was more pronounced in this analysis, with no patients surviving past 4 years. However, it should be noted that the sample of UVM patient was fairly small, especially in figure 3.3 B (n(high)=20 and n(low)=20), and therefore the effect may be overestimated.

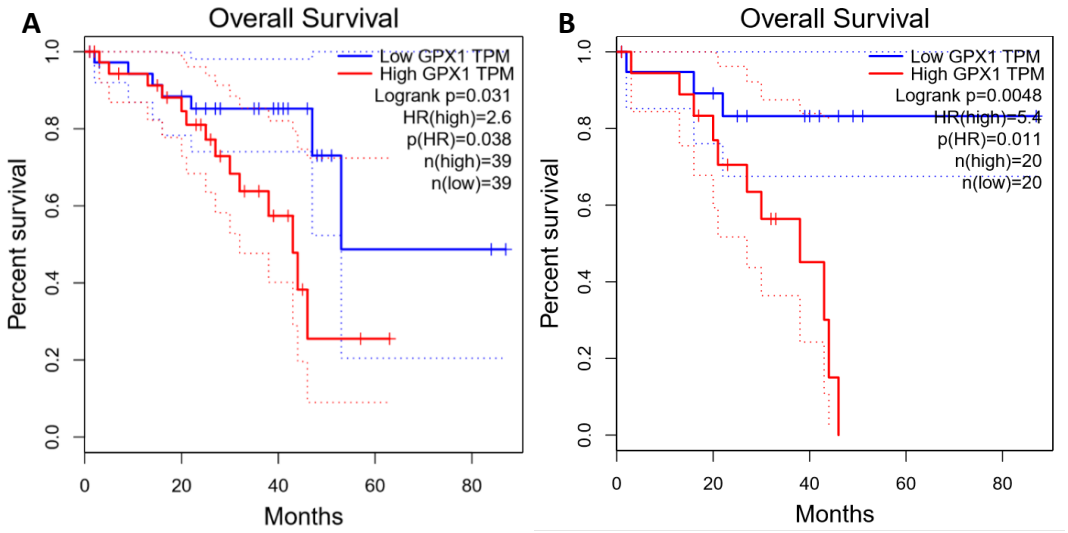

Figure 3.3: Elevated expression of* GPX1 *is associated with decreased overall survival in uveal melanoma (UVM) patients. *Kaplan-Meier plots showing Overall Survival (OS) in UVM patients with low and high* GPX1 *mRNA expression, using* GPX1 *expression and patient survival data from the GEPIA database. (A)* GPX1 *expression level threshold is defined for high and low expression as above and below the median. (B)* GPX1 *expression level threshold is defined for high and low expression as the upper and lower quartiles respectively.*

In figure 3.4 A, B, C and D, *GPX1* mRNA expression above the median was associated with poorer OS and Disease Free Survival (DFS) in Brain Lower Grade Glioma (LGG) (OS Log-rank P=8.4e-05, HR =2.1; DFS Log-rank P=0.001, HR =1.7) and Adenoid cystic carcinoma (ACC) (OS Log-rank P=0.13, HR =1.8; DFS Log-rank P=0.017, HR =2.2) patients.

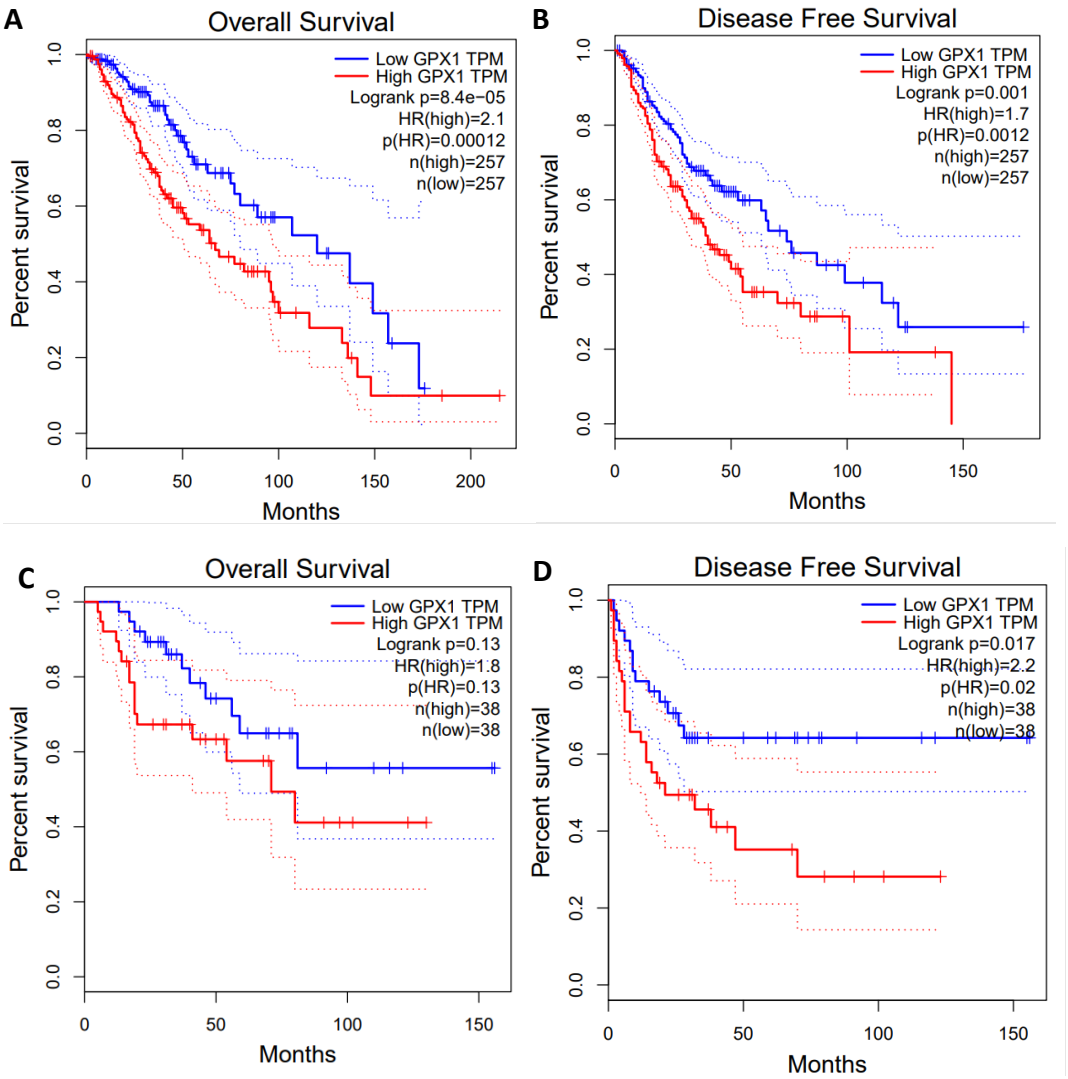

Figure 3.4: Elevated expression of* GPX1 *is associated with decreased overall and disease-free survival in low grade glioma (LGG) and adrenocortical carcinoma (ACC) patients. *(A) Overall survival (OS) and (B) disease free survival (DFS) in LGG patients with low and high* GPX1 *mRNA expression, and survival curves for (C) overall survival and (D) disease free survival in ACC patients with low and high* GPX1 *mRNA expression. The threshold for high and low expression was defined as above and below the median value for* GPX1 *expression.* GPX1 *mRNA expression (RNA seq) and patient survival data were taken from the GEPIA database.*

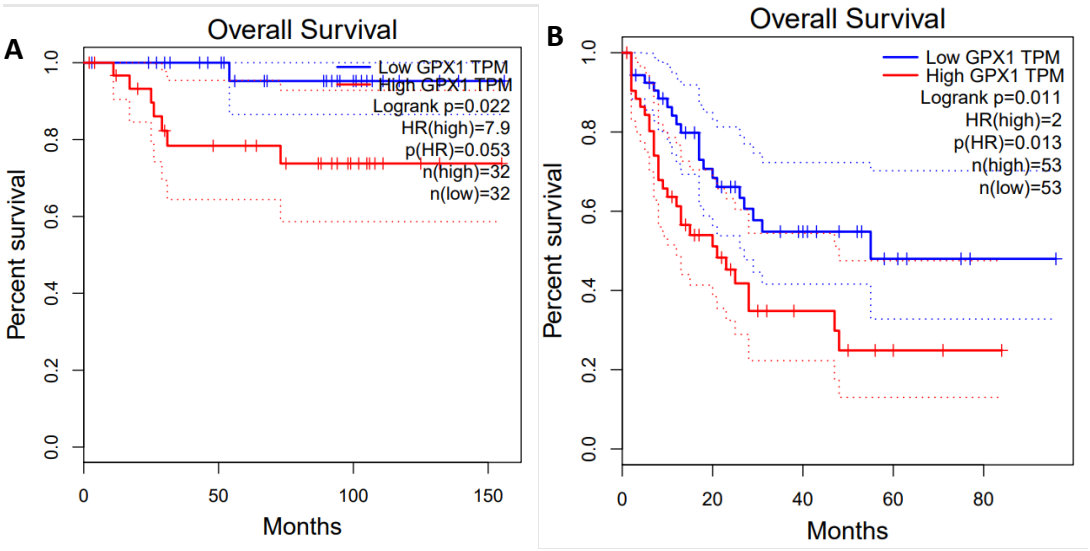

Figure 3.5: Elevated expression of* GPX1 *is associated with decreased overall survival in kidney chromophobe (KICH) and acute myeloid leukaemia (LAML) patients. *Overall survival in (A) KICH, (B) LAML patients with high and low* GPX1 mRNA *expression. The threshold for high and low expression was defined as above and below the median value for* GPX1 *expression.* GPX1 *expression (RNA seq) and patient survival data were taken from the GEPIA database.*

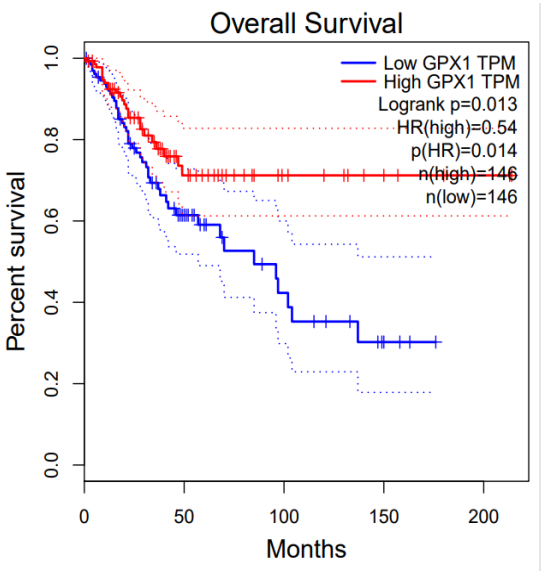

Figure 3.6: Elevated expression of* GPX1 *is associated with increased overall survival in cervical squamous cell carcinoma (CESC) patients. *Overall survival in CESC patients with high and low* GPX1 *mRNA expression. The threshold for high and low expression was defined as above and below the median value for* GPX1 *expression.* GPX1 *expression (RNA seq) and patient survival data were taken from the GEPIA database*

In figure 3.5 A and B, *GPX1* mRNA expression above the median was associated with poorer OS for both in Kidney Chromophobe (KICH) (Log-rank P=0.022, HR =7.9) and LAML (Log-rank P=0.011, HR =2) patients. Note that the largest HR is seen in the KICH group, where patients with high *GPX1* mRNA expression were at a 7.9-fold higher risk than the low *GPX1* mRNA expression group.

Cervical Squamous Cell Carcinoma (CESC) was the only cancer type tested which indicated a positive correlation between *GPX1* mRNA expression and overall survival (Figure 3.6, log-rank P=0.013, HR =0.54).

3.3 GPX1-related protein expression in Cancer

Given that GPX4 can compensate for GPX1 loss in MDR cancer cells (Hall et al., 2014), it was important to determine if the mRNA overexpression of *GPX1* seen in tumour cells is to compensate for loss of GPX4. This is not the case; the relationship between *GPX1* and *GPX4* mRNA expression follows a similar positive trend in both tumour and normal samples (figure 3.7, R= 0.42 and 0.44 respectively). The spread of the data is greater in tumour samples than in normal samples. There is a shift toward overexpression for *GPX1* and *GPX4*. *GPX1* in tumour samples falls within the 7-10 Transcripts per million (TPM) range, compared with 7-9 TPM in normal samples. Thus, mRNA expression has increased in general but this varies greatly between tumour samples. For *GPX4*, tumour samples had between 7 and 10 TPM, whereas normal cells had approx. 7.25-9.5 TPM, and thus there is a greater amount of variance in tumour samples.

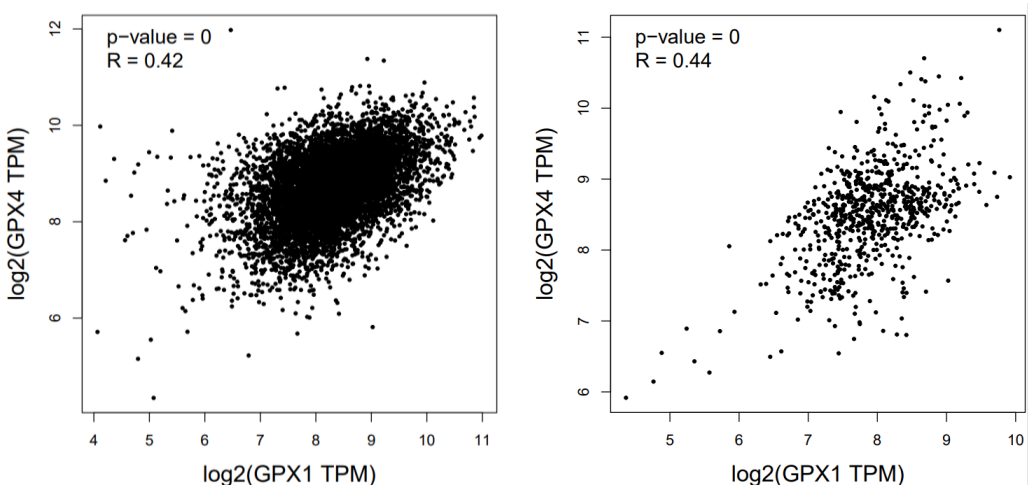

Figure 3.7: Positive correlation is observed between* GPX1 *and* GPX4 *mRNA expression in normal and tumour samples. *Expression in transcripts per million (TPM) of* GPX1 *and* GPX4 *across tumour (left) and normal (right) samples using RNASeq data from the GEPIA database.*

It is already known that GPX family members exhibit some functional redundancy, for example between GPX1 and GPX2 (Esworthy et al., 2000), and can be overexpressed to compensate for the loss of one another. Hence, *GPX1* mRNA overexpression could be accompanied by a loss of other GPXs for whom GPX1 can compensate. Conversely, all GPX members containing selenium use the same translational regulator, the SECIS-SBP2 complex, for selenocysteine incorporation (section 1.2.3.2), and so an upregulation of a member of this complex, such as *SBP2*, will alter the mRNA transcript stability for selenoprotein GPXs, changing the amount of each protein that is produced. To investigate if there was any impact on the expression level of the rest of the GPX family, heatmaps were generated for expression of these proteins in tumours and normal cells.

Previous research from Wei et al. (2020) described a protein-protein interaction network for GPX1, which was created using GENEMANIA. This was generated using gene co-expression, gene co-localisation, gene enrichment and other interactomic data, and suggests the proteins likely to interact with GPX1, even if the relationship between the proteins is currently unknown. This map implicated many other proteins as GPX-related proteins - not only GPX family members, but also SBP2, Exosome component 2 (EXOSC2), RNA polymerase II Subunit L (POLR2L), β-hydroxysteroid 17-beta dehydrogenase X (HSD17B10), Tumour protein 53 (P53), Ras Homolog Family Member A (RHOA), Lysyl-tRNA synthetase (KARS), vesicle-associated membrane protein 8 (VAMP8), Abelson homolog 2 (ABL2), Cathepsin D (CTSD) and thioredoxin (TXN). To investigate how the mRNA expression of these were affected by *GPX1* expression level in cancers, and therefore which GPX1-related processes may be preferentially promoted in GPX1-rich cancers, heatmaps were generated for the GPX1-related protein genes in the same fashion.

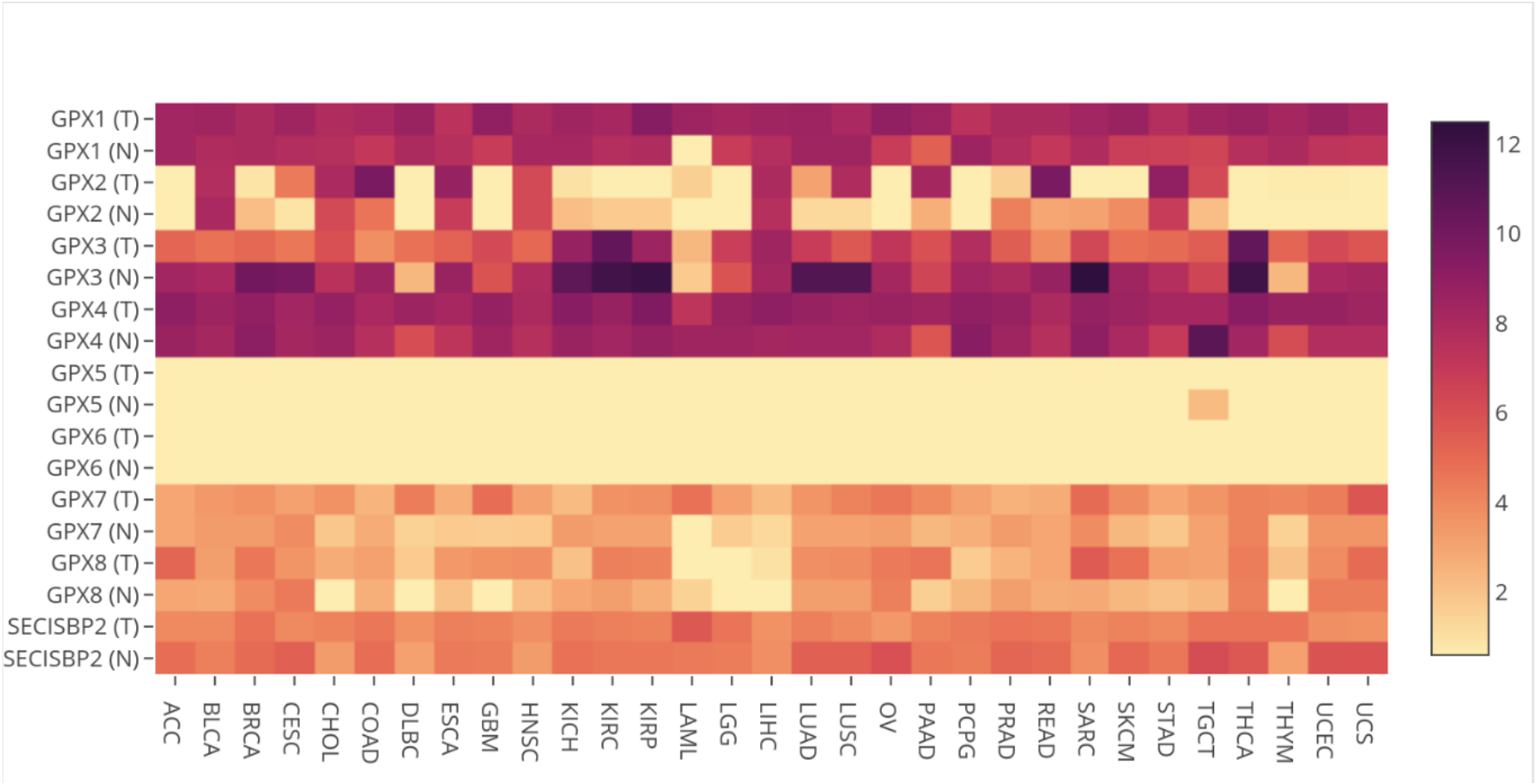

Figure 3.8: Heatmaps of the GPX protein family and SBP2 mRNA expression*. mRNA expression for GPX family proteins and SBP2 (SECISBP2) in TPM in normal (N) and tumour (T) samples across many tumour types. These were generated using the GEPIA gene comparison tool, with data from the GEPIA database.*

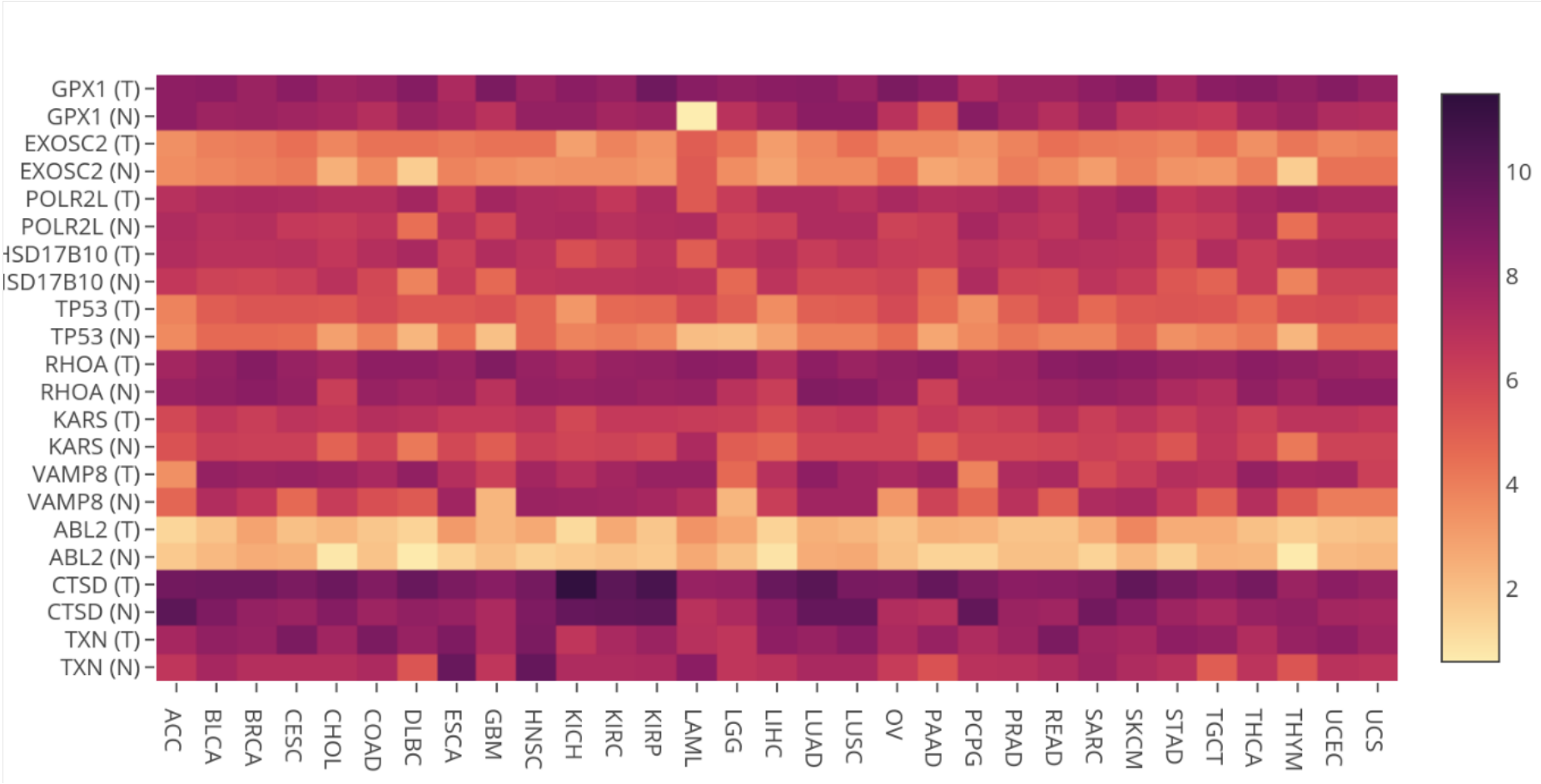

Figure 3.9: Heatmaps of the mRNA expression of GPX1-interacting proteins*. mRNA expression in TPM in normal (N) and tumour (T) samples across many tumour types, for GPX1 and GPX1-interacting proteins indicated by Wei et al., 2020. These were generated using the GEPIA gene comparison tool, with data from the GEPIA database.*

Figure 3.8 indicates that there is no consistent pattern of change to mRNA expression between tumour and normal cell samples for the GPX family as a whole. Although GPX2 has been observed to compensate for loss of GPX1 (and vice versa) *in vivo* (Florian et al., 2010), this pattern is not replicated here. Following lower *GPX1* mRNA expression in tumour cells relative to normal cells, *GPX2* is rarely upregulated, and this pattern is only seen in Esophageal Carcinoma (ESCA) and LUSC samples. Generally, while *GPX1* and *GPX2* mRNA expression is higher in the tumour than the normal samples, *SBP2* mRNA shows the opposite trend. Similarly, in cell lines with both higher *GPX1* and *GPX2* mRNA expression in tumour samples - CESC, CHOL, Colon Adenocarcinoma (COAD), LAML, Liver Hepatocellular Carcinoma (LIHC), PAAD, Rectum Adenocarcinoma (READ), Stomach Adenocarcinoma (STAD) and TGCT - *SBP2* mRNA expression is generally either lower or equal. *GPX3* mRNA expression was generally downregulated in tumour cell samples, although there is no pattern shown that indicates another GPX family member is compensating for this.

GPX4 was commonly upregulated in tumour samples. In the majority of cases, when *GPX1* was upregulated in tumour cells, this was accompanied by an increase in *GPX4* mRNA expression, often to a similar degree. This was seen in Bladder Urothelial Carcinoma (BLCA), CESC, CHOL, COAD, Lymphoid Neoplasm Diffuse Large B-Cell Lymphoma (DLBC), GBM, KICH, Kidney Renal Clear Cell Carcinoma (KIRC), KIRP, LGG, LIHC, OV, PAAD, Prostate Adenocarcinoma (PRAD), Rectum Adenocarcinoma (READ), SKCM, STAD, THCA, Thymoma (THYM), UCEC and UCS samples. *GPX5* and GPX*6* had low and consistent levels of mRNA expression across both tumour and normal samples, with the exception of *GPX5* in tenosynovial giant cell tumour (TGCT), where normal samples showed greater *GPX5* expression compared to tumour samples. *GPX7* and *GPX8* were also commonly overexpressed in the tumour samples, however, these were often expressed in varying degrees, and did not show correlation with *GPX1* mRNA expression comparable with *GPX4*.

In figure 3.9, all of the genes were generally overexpressed in the tumour samples compared with the normal samples. In five tumour types (DLBC, GBM, LIHC, STAD and TGCT), genes for all of the proteins mapped were overexpressed in the tumour sample. Similarly, in five tumour types (BLCA, COAD, PAAD, READ and THYM), all but one of the proteins were overexpressed along with *GPX1*. The most similar mRNA expression profiles to *GPX1* were seen for *POLR2L*, *HSD17B10*, *TP53*, *CTSD*, and, to some extent, VAMP8.

To assess the wider impact GPX1 could be having in the cell via its interaction with the GPX1-related proteins, an Overrepresentation Test on GoPanther was performed (table 3.1). By

inputting the GPX1-related proteins listed in Wei et al, 2020 into GoPanther, only one biological process was found to be significantly enriched; cell activation involved in immune response. This is the only result with both a significant raw P value, and a false discovery rate of below 0.05. The five genes from the inputted set that were associated with this function were *CTSD, KARS, TP53, VAMP8 and RHOA*, some of which had mRNA expression levels which correlated well with *GPX1* (figure 3.9).

GoPanther analysis						
	Number of genes in Homo Sapiens	Number of genes in query	Number expected	Fold enrichment	Raw P value	False Discovery Rate
Leukocyte activation involved in immune response	624	5	0.3	16.71	5.45×10^{-6}	8.67×10^{-2}
> Cell activation involved in immune response	628	5	0.3	16.6	5.62×10^{-2}	4.47×10^{-2}

Table 3.1: Enrichment analysis of GPX1-interacting proteins using GoPanther indicates significant enrichment in cell activation involved in the immune response. *GoPanther output following an Overrepresentation Test of GPX1, SBP2, EXOSC2, POLR2L, HSD17B10, TP53, RHOA, KARS, VAMP8, ABL2, CTSD and TXN.*

3.4 *GPX1* mRNA expression and chemoresistance

As previous work had linked *GPX1* mRNA expression and activity with resistance to anti-cancer drugs (section 1.4.3), this relationship was investigated on a larger scale by comparing *GPX1* mRNA expression (using data from the Broad Institute Cancer Cell Line Encyclopedia) with IC_{50} values for cisplatin, doxorubicin and docetaxel (GDSC) across a range of cancer cell lines. These drugs were selected as two of these (cisplatin and doxorubicin) have already been directly linked to GPX1, and resistance was found across a small number of cancer cell types, and potential mechanisms of action have been explored to explain this effect. Namely, increases in GPX1 activity prevent apoptosis by reducing the level of H_2O_2 and downregulating other key members of the apoptotic pathways (section 1.4.2.5). As docetaxel also uses ROS to initiate apoptosis in target cells (Baş and Naziroğlu, 2019), similar response (GPX1-induced drug resistance) would be expected, thus this was also investigated.

In figures 3.10 A and 3.12 A, cisplatin and doxorubicin showed very little overall correlation between *GPX1* mRNA expression and drug IC_{50}. In figure 3.11 A, docetaxel IC_{50} appeared to

positively correlate with *GPX1* mRNA expression, however this was a very slight correlation. Across all drugs and cancer cell types, there was a large amount of variance in IC_{50}, and therefore a smaller sample of cancer cell types were extracted and plotted (figure 3.10 B, 3.11 B and 3.12 B), to identify cancer cell types of interest. These were selected based on a general positive correlation, however, there is still a large amount of scatter within each cancer type.

The only cancer cell type which was found to have a consistent relationship between *GPX1* mRNA expression and drug IC_{50} was CESC. For cisplatin, the selected cancers were BLCA, CESC, ESCA, HNSC, LGG, OV, and Hodgkin and Burkitt lymphoma (figure 3.10 B). OV appeared to show stronger positive correlation between *GPX1* mRNA expression and drug resistance than other cancer types. In figure 3.11 B, the selected cancers were CESC, MESO, MB, OV. MB appeared to show the strongest correlation; however, this also had a small sample size. In figure 3.12 B, only 3 cancer types were found to have a reasonable correlation: CESC, Hodgkin lymphoma and Burkitt lymphoma. All of these were also identified in the cisplatin dataset, indicating that these cancer types, as opposed to all cancers in the database, may be sensitive to GPX1-induced chemoresistance, and warrant further investigation.

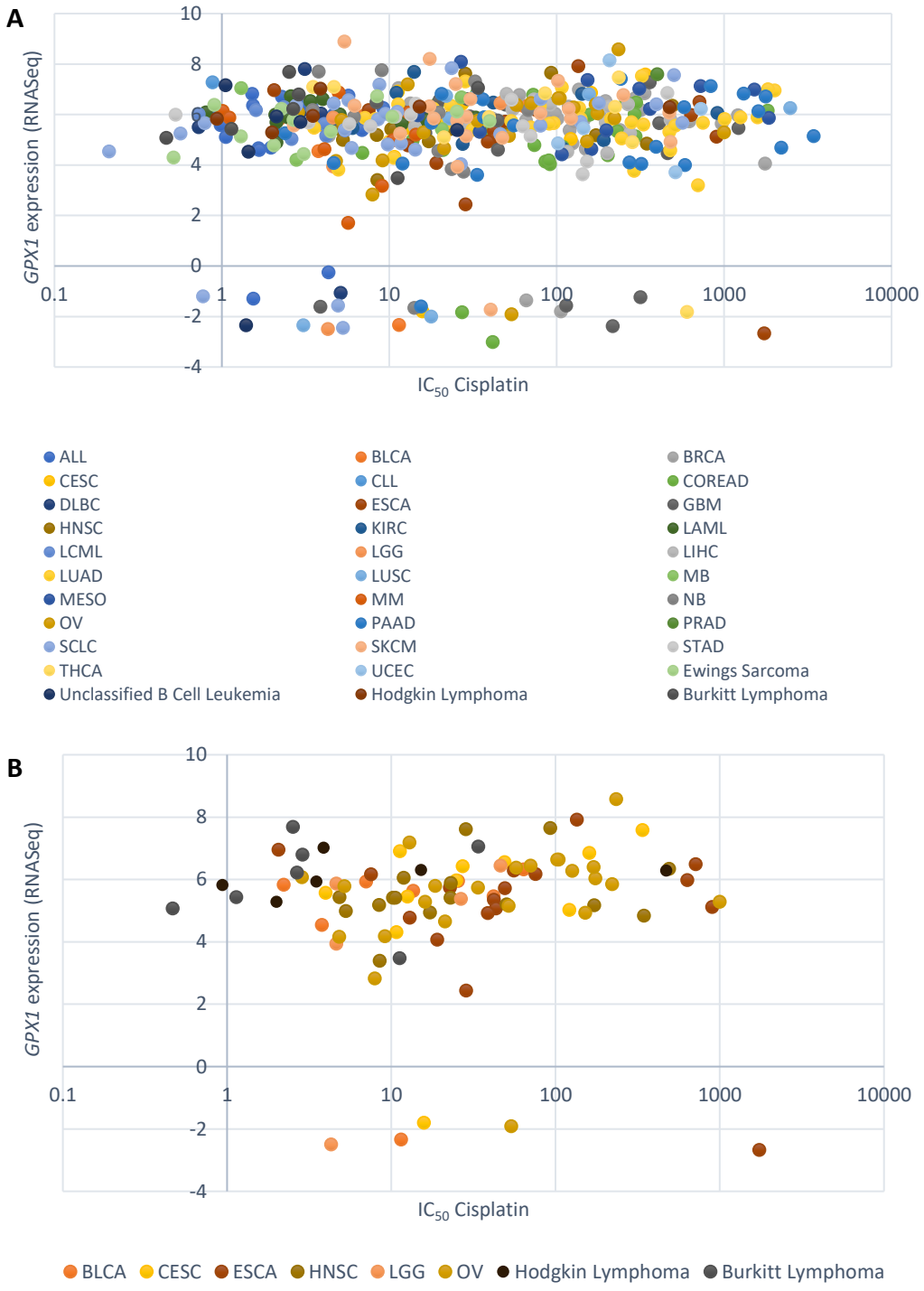

Figure 3.10: Comparison of cisplatin sensitivity with* GPX1 *mRNA expression level. *Cisplatin IC_{50} against* GPX1 *mRNA expression across (A) a range of cancer types and (B) selected cancer types displaying positive correlation. The full dataset contained 528 samples, all of which are represented in figure 3.10 A. These figures were created using GDSC data, matched with expression level of* GPX1 *(RNASeq) taken from the Broad Institute Cancel Cell Line Encyclopaedia*

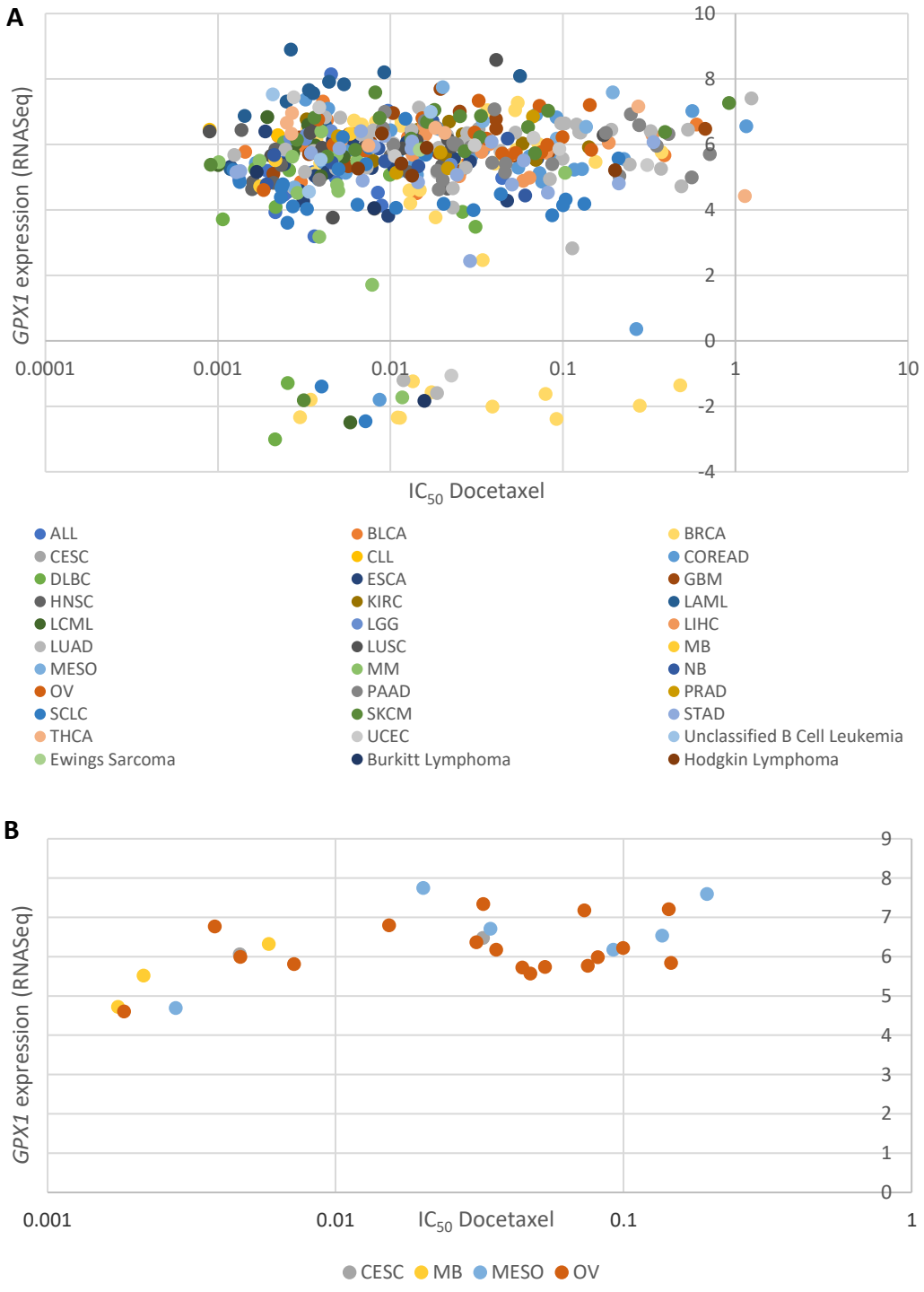

Figure 3.11: Comparison of docetaxel sensitivity with* GPX1 *mRNA expression level. *Docetaxel IC_{50} against* GPX1 *mRNA expression across (A) a range of cancer types and (B) selected cancer types displaying positive correlation. The full dataset contained 527 samples, all of which are represented in figure 3.11 A. These figures were created using GDSC data, matched with expression level of* GPX1 *(RNASeq) taken from the Broad Institute Cancel Cell Line Encyclopaedia.*

Figure 3.12: Comparison of doxorubicin sensitivity with* GPX1 *mRNA expression level. *Doxorubicin IC_{50} against* GPX1 *mRNA expression across (A) a range of cancer types and (B) selected cancer types displaying positive correlation. The full dataset contained 496 samples, all of which are represented in figure 3.12 A. These figures were created using GDSC data, matched with expression level of* GPX1 *(RNASeq) taken from the Broad Institute Cancel Cell Line Encyclopaedia.*

3.5 Expression and Copy Number Variation of *GPX1* in cancer cells

As it was found that *GPX1* was commonly overexpressed in cancer, and was especially detrimental for prognosis, the frequency of overexpression and copy number variation (CNV) for the *GPX1* gene was investigated. In the COSMIC database, *GPX1* expression was compared across 1594 tumour samples, as was CNV, to assess whether duplications of the gene were the source of aberrant *GPX1* expression.

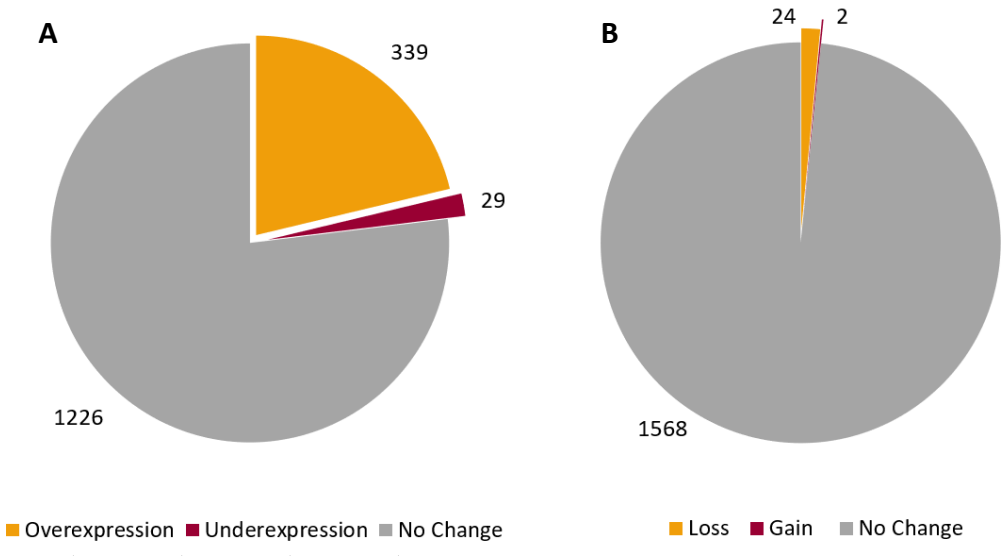

Figure 3.13:* GPX1 *gene expression and gene variation in COSMIC tumour samples. *(A) Graph showing the number of tumour samples in the COSMIC database that show either over- or under-expression of* GPX1*, based on RNAseq data of 1,594 samples. (B) Copy number variation for the GPX1 gene seen in tumour samples from samples in the COSMIC database.*

According to figure 3.13 A, the *GPX1* gene is overexpressed in tumour cell samples far more frequently than it under-expressed. Conversely, figure 3.13 B indicates that the *GPX1* gene is more frequently lost than gained in tumour samples. Overall, this therefore indicates that the overexpression seen in those samples is not due to copy number variations, such as duplications, but is due to other changes that can affect expression level (e.g. mutations or regulatory changes).

3.6 Location of GPX1 mutations and effect on cancer

As little data was available on *GPX1* mutations in cancer cell lines, datamining was performed to identify any mutations which may help to drive cancer development or allows *GPX1* to offer greater protection to cancer cells.

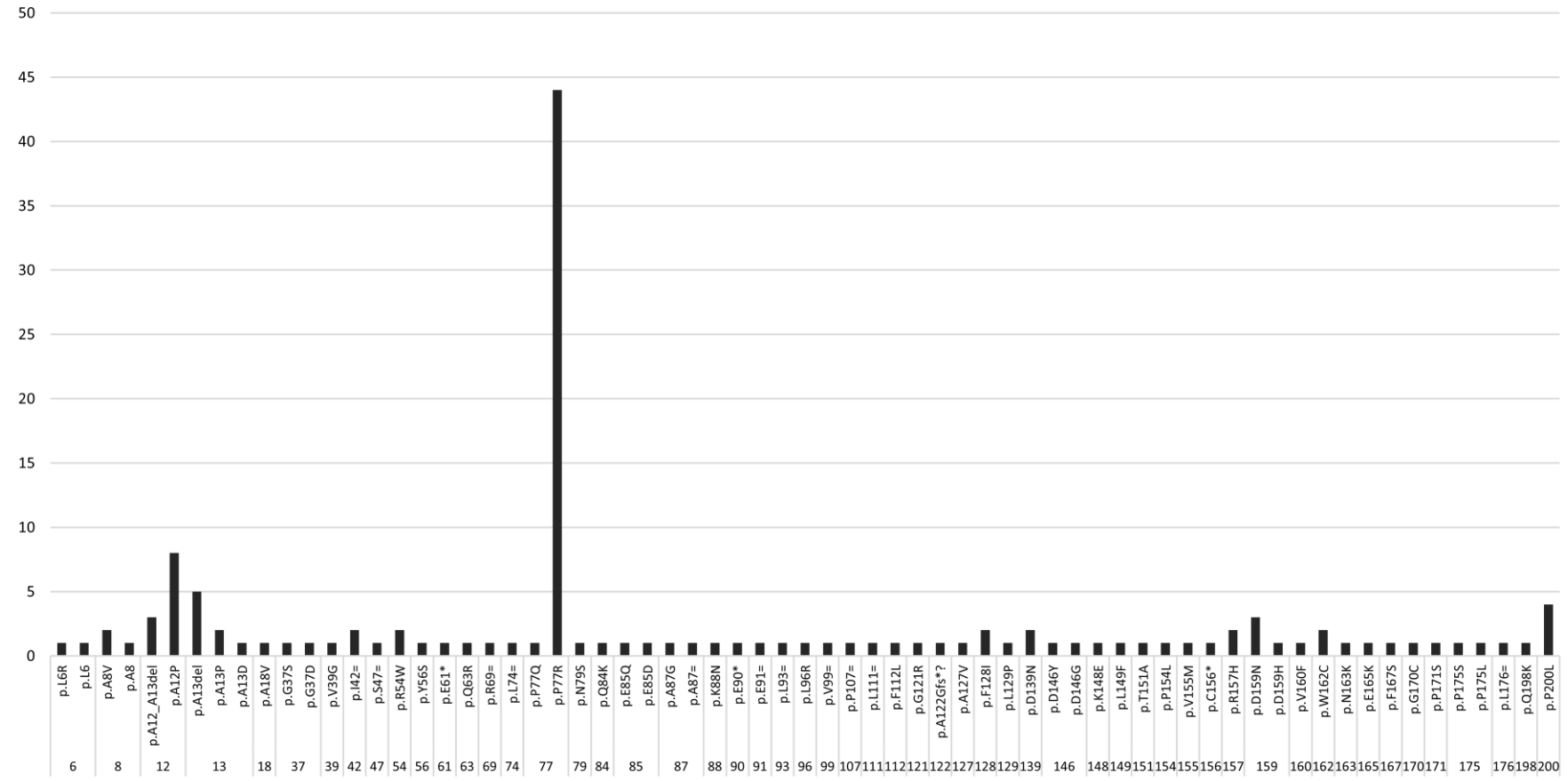

Figure 3.14: GPX1 mutational map generated using COSMIC showing one hotspot at P77R. *Number of mutations (y-axis) vs type and location of mutation observed in samples, mapped to residues in the GPX1 protein (x-axis), using data from the COSMIC database. 389 samples were tested, 155 mutations identified, 136 mapped to a residue*.

COSMIC data from 389 samples (figure 3.14) showed low levels of mutation across much of the protein, aside from a hotspot of mutations at the position P77, the vast majority of which were P77R. Out of 44 samples, 18 were from a single study, McMillan et al., 2018. This data suggests this could be a residue of interest, as it is prevalent in tumour samples. The P77R mutation was further researched in Ensembl to assess the impact of this substitution on protein function (table 3.2). In all tests apart from MetaLR, P77R scored highly for mutational impact. SIFT, Poly-Phen, CADD, REVEL and Mutation Assessor scored indicated that this mutation was not only deleterious with respect to the original amino acid function, but also likely to be pathogenic.

To test whether the same hotspot is present across other datasets, GPX1 mutational maps were also generated using the ICGC and GDC data portal (figure 3.15). Further investigation of mutations in *GPX1* using ICGC and GDC showed no peak at P77R, but generally low levels of mutations throughout the protein, comparable to the COSMIC data. ICGC data also indicated a small number of A12P and D159N mutations, which are also seen in COSMIC. As COSMIC derives some data from this database, it is likely that the mutations shown in the ICGC map are also shown in the COSMIC map.

ENSEMBL analysis						
Mutation	SIFT (how different the AA is likely to be)	Poly-Phen (difference in physical interactions of missense variant)	CADD (cumulative score of deleteriousness)	REVEL (predicts pathogenicity of variant)	MetaLR (predicts pathogenicity of variant)	Mutation Assessor (impact based on evolutionary conservation)
P77R	0 (deleterious)	0.739 (possibly damaging)	31 (likely deleterious)	0.757 (likely disease causing)	0.248 (tolerated)	0.984 (high)

Table 3.2: The P77R mutation is likely to impact the structure and function of GPX1. *Ensembl-generated scores for mutational impact of the P77R* GPX1 *variant, using a range of analyses.*

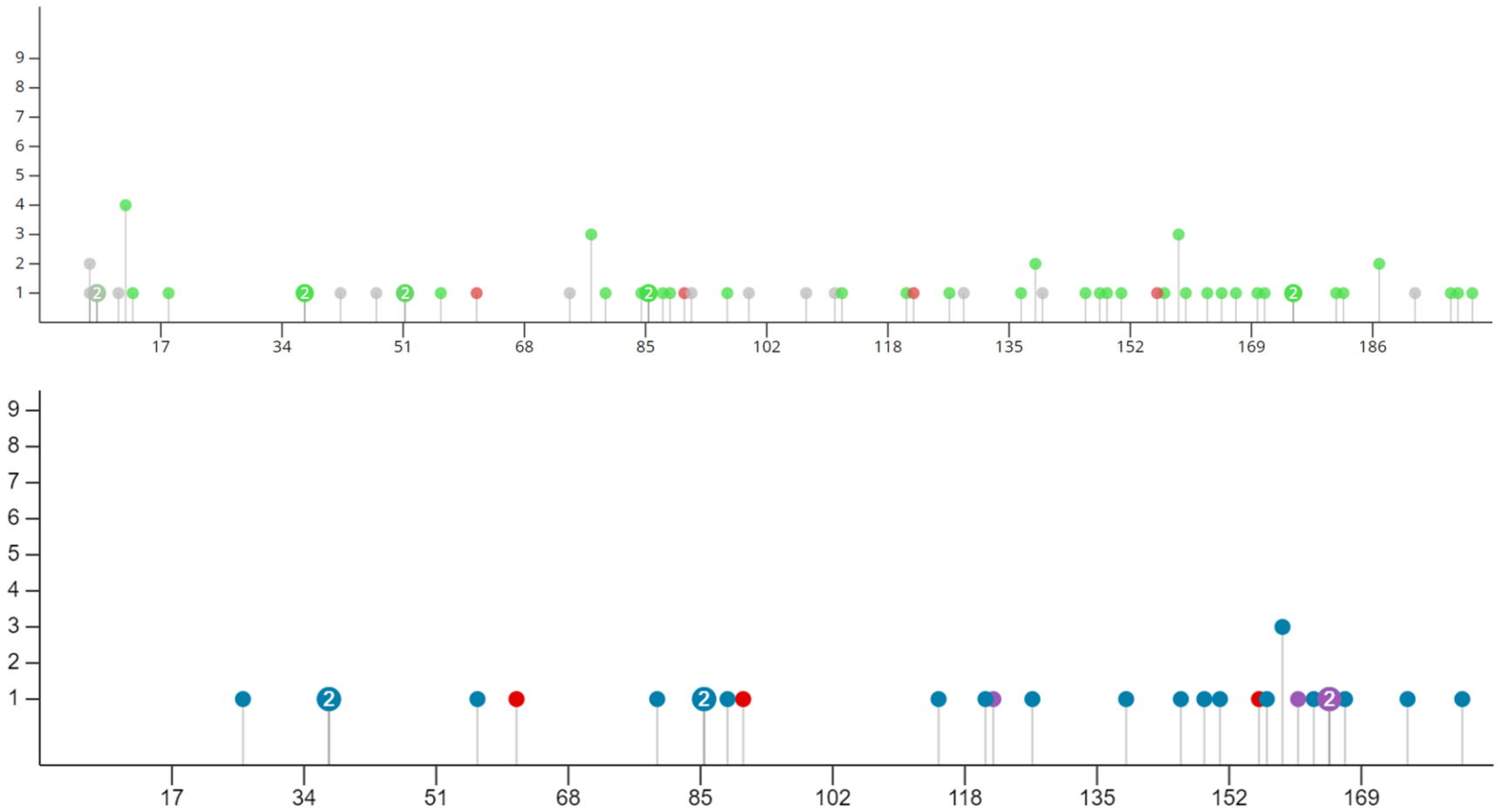

Figure 3.15: GPX1 mutational maps generated using ICGC and GDC show no P77R hotspot. *Number of mutations (y-axis) vs location in the GPX1 protein (x-axis), using data from (top) the ICGC database (19,729 samples tested, 329 mutations identified, 70 mapped to a residue) and (bottom) the GDC database (800 samples tested, and 28 mutations mapped to a residue*).

3.7 Summary

Various bioinformatic approaches were utilised to determine the impact of GPX1 on cancer development and patient survival. *GPX1* mRNA expression in tumour samples was higher than in matched normal samples for most tumour types, using RNASeq data from both GEPIA and TCGA. While in most cancers, there was no significant difference in patient prognosis for patients with high and low *GPX1* mRNA expression, high *GPX1* mRNA expression was found to significantly reduce overall survival in UVM, LGG, KICH and LAML patients, and to significantly reduce disease free survival in ACC and LGG patients. Conversely, high mRNA *GPX1* expression was found to significantly improve overall survival in CESC patients.

Due to its known functional redundancy with regard to other members of the GPX family, as well as a recent review detailing a protein-protein interaction network for *GPX1* (Wei et al., 2020), an investigation was undertaken to determine the expression profiles of these GPX1-related genes across cancer types. Heatmaps from GEPIA indicated that *GPX4* was the only member of the GPX family to be consistently overexpressed with *GPX1* mRNA overexpression. *SBP2*, however, showed the opposite trend. Scatter maps of *GPX1* against *GPX4* mRNA expression for all cancers did not demonstrate a change in the relationship between *GPX1* and *GPX4* mRNA expression between normal and tumour samples, although there was a slight increase in the spread of the mRNA expression for both genes in tumour samples. Heatmaps also indicated that for *POLR2L*, *HSD17B10*, *TP53* and *CTSD*, expression increased with *GPX1* mRNA expression across most cancer types. A GoPanther Overrespresentation Test of the GPX1-related genes was successful in flagging *CTSD*, *KARS*, *TP53*, *VAMP8* and *RHOA* as genes enriching leukocyte activation, involved in immune response.

GPX1 mRNA expression did not appear to correlate with chemoresistance to doxorubicin, docetaxel and cisplatin across the majority of cancer types. CESC was the only cancer type to show positive correlation between *GPX1* mRNA expression and chemoresistance for all drugs investigated. This does not support our current understanding of the role of *GPX1* in chemoresistance, as *GPX1* mRNA overexpression has been associated with chemoresistance *in vitro* across many cancer types (section 1.4.3.1), and an increase in CESC patient survival (figure 3.4).

As very little research had been done on somatic mutations of *GPX1* appearing in cancer, these were investigated using existing cancer databases GEPIA, ICGC and GDC. A hotspot of

mutations was detected using GEPIA analysis - P77R. While Ensembl analysis indicated that the P77R mutation would indeed have a deleterious effect on GPX1 function, further investigation using the ICGC and GDC data portals did not support the presence of this hotspot. As many of the samples which detected the P77R mutation came from a single study only present in GEPIA, it is possible that the P77R has been overrepresented in this database, as there may be differences in curation between databases. This method of data analysis may therefore be unreliable in finding mutations for further investigation.

Chapter 4 - Stimulation of GPX1 production with selenium supplementation

4.1 Introduction

As discussed in section 2.2, GPX1 is a selenoprotein, and as such, requires the rare amino acid selenocysteine for its activity. It is therefore dependent upon selenium for the expression of the *GPX1* gene. *GPX1*, like other selenoprotein genes, is subject to an additional level of regulation at the translational level. The expression of selenoproteins is controlled by a mRNA loop structure called a SECIS element. Folding of the mRNA via the SECIS loop 'recodes' a stop codon to a selenocysteine (Sec) codon, the addition of which is initiated via recruitment of SECIS-binding protein 2 (SBP2) to the loop structure. SBP2 recruits eEFSec-bound Sec-tRNASec to the site, and brings it within close proximity of the ribosome, facilitating the addition of Sec to the amino acid chain.

While the SECIS system increases Sec incorporation efficiency for selenoproteins, this ability is distributed differentially across the selenoproteins, and is dependent upon the SECIS element structure (section 2.2.3). This establishes a selenium hierarchy, under which some selenoproteins are given preferential access to selenocysteine when selenium levels are low. *GPX1* falls at the bottom of this hierarchy, and low levels of GPX1 are produced under selenium-poor conditions. Therefore, while other selenoproteins are constitutively expressed, expression of *GPX1* is highly dependent on selenium level. Providing cells with a selenium supplement is an easy method of theoretically boosting GPX1 production, and this relationship can be exploited experimentally to investigate GPX1 function.

Indeed, previous work has shown increases at the mRNA level following supplementation with selenium (Hazane-Puch et al., 2013; Hazane-Puch et al., 2014). However, this work is limited as it does not confirm whether mRNA overexpression resulted in increased GPX1 at the protein level. Given that *GPX1* expression is also regulated at the translational level, this is an oversight which needs urgent investigation. Furthermore, there is no indication of the longevity of this effect, which would be essential information for contextualising the true impact of selenium in biologically relevant timescales. Given also that *GPX1* overexpression has been linked to chemoresistance, inducing *GPX1* expression with selenium supplementation allows us to investigate these effects within a range of drugs and across cell types. The aims of this work were therefore (1) to investigate the effect of selenium supplementation on GPX1 protein level, (2) to determine the longevity of this effect after selenium withdrawal and (3) to explore the effect of selenium-induced GPX1 production on chemoresistance.

4.2 Stimulating GPX1/2 protein production with sodium selenite (Na_2SeO_3) supplementation

Western blots were performed following supplementation with sodium selenite (Na_2SeO_3) in multiple cell lines to verify that selenium availability can impact GPX1 protein level. The cell lines chosen were HaCaT immortalised keratinocytes, as used in Hazane-Puch et al., 2013, and two cancerous cell lines, A431 (epidermoid squamous cell carcinoma) and HeLa (cervical carcinoma), which can provide information on GPX protein level in the cancer cell context. HeLa cells also belong to the CESC cancer type, which were found in GDSC datamining to have potential for GPX1-induced chemoresistance (figures 3.8, 3.9 and 3.10) and thus deeper understanding of how to manipulate GPX1 level is of great interest.

Na_2SeO_3 increased GPX1/2 protein level in HaCaT cells in a dose- and time-dependent manner (figure 4.1 A and B). The largest increase was seen at 1 µM and 100 nM after 96 hours, and for all concentrations 96-hour incubations yielded a larger increase than 24-hour incubations. However, both 24- and 96-hour experiments saw a similar response to Na_2SeO_3 concentration – similarly high protein level at 1 µM and 100 nM concentrations, with a decrease in GPX1/2 protein yield for each subsequent dilution of Na_2SeO_3.

Similar results were seen in A431 (figure 4.1 C and D) and HeLa cells (figure 4.1 E and F), where 96-hour incubation with Na_2SeO_3 yielded higher GPX1/2 protein than 24-hour, and a similar dose dependency was observed. However, these cancer cell lines appear to be less sensitive to Na_2SeO_3 than HaCaT cells, with both showing a smaller increase in protein level at higher concentrations than is observed in HaCaT cells. For example, the maximum GPX1/2 yield achieved in HaCaTs was 29.4 times the control, although only 2 repeats were performed. However, in HeLa and A431 cells, the peak protein levels achieved were 6 and 3.1 times higher than basal, respectively. HeLa Cells were the most resistant to selenium toxicity, and thus, samples were able to be taken at a higher dose, 10 µM, for both 24 and 96 hours.

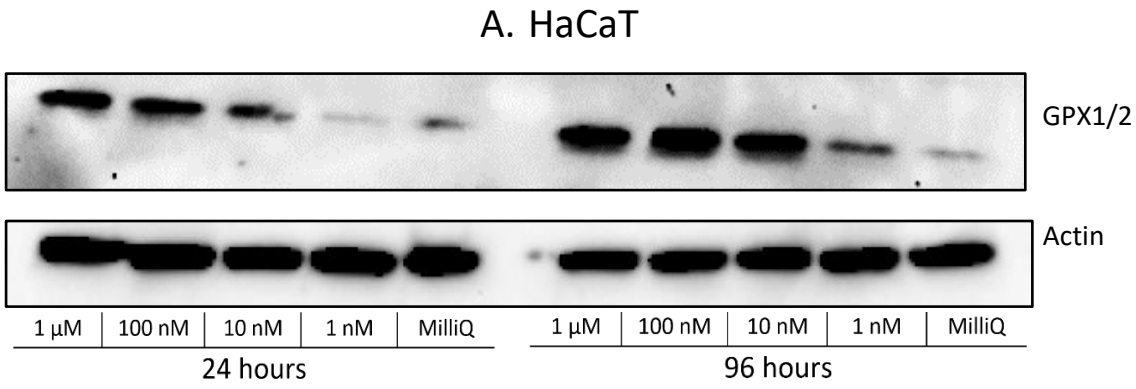
A. HaCaT
GPX1/2
Actin
1 µM
100 nM
10 nM
1 nM
MilliQ
1 µM
100 nM
10 nM
1 nM
MilliQ
24 hours
96 hours

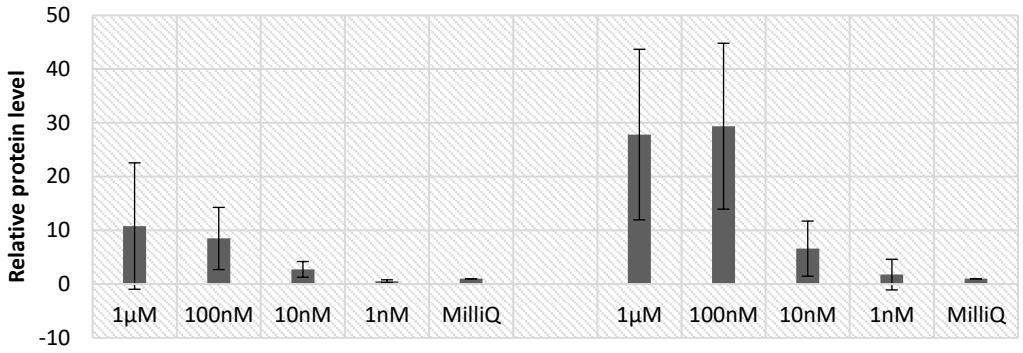
B. HaCaT
Relative protein level
50
40
30
20
10
0
-10
1µM
100nM
10nM
1nM
MilliQ
1µM
100nM
10nM
1nM
MilliQ

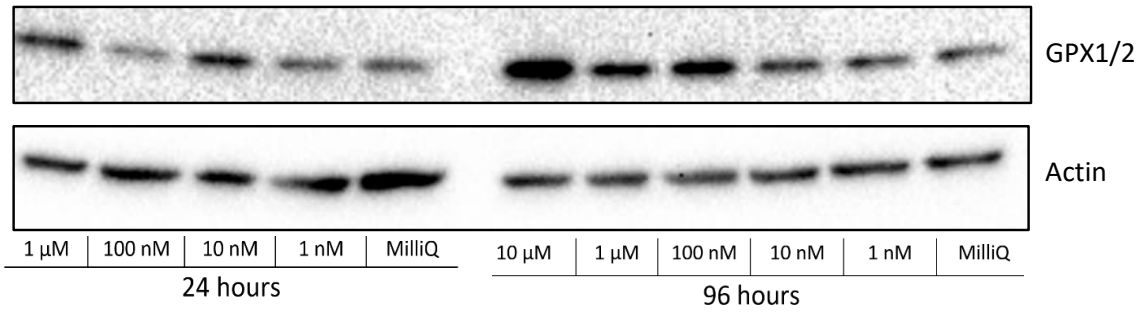
C. A431
GPX1/2
Actin
1 µM
100 nM
10 nM
1 nM
MilliQ
10 µM
1 µM
100 nM
10 nM
1 nM
MilliQ
24 hours
96 hours

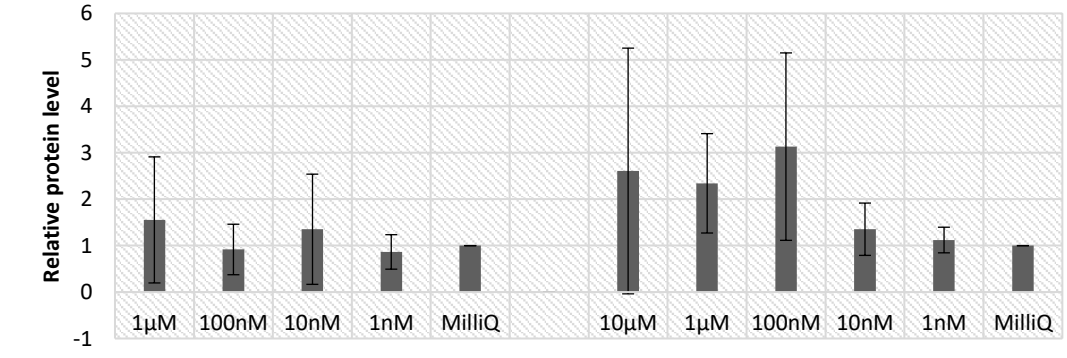
D. A431
Relative protein level
6
5
4
3
2
1
0
-1
1µM
100nM
10nM
1nM
MilliQ
10µM
1µM
100nM
10nM
1nM
MilliQ

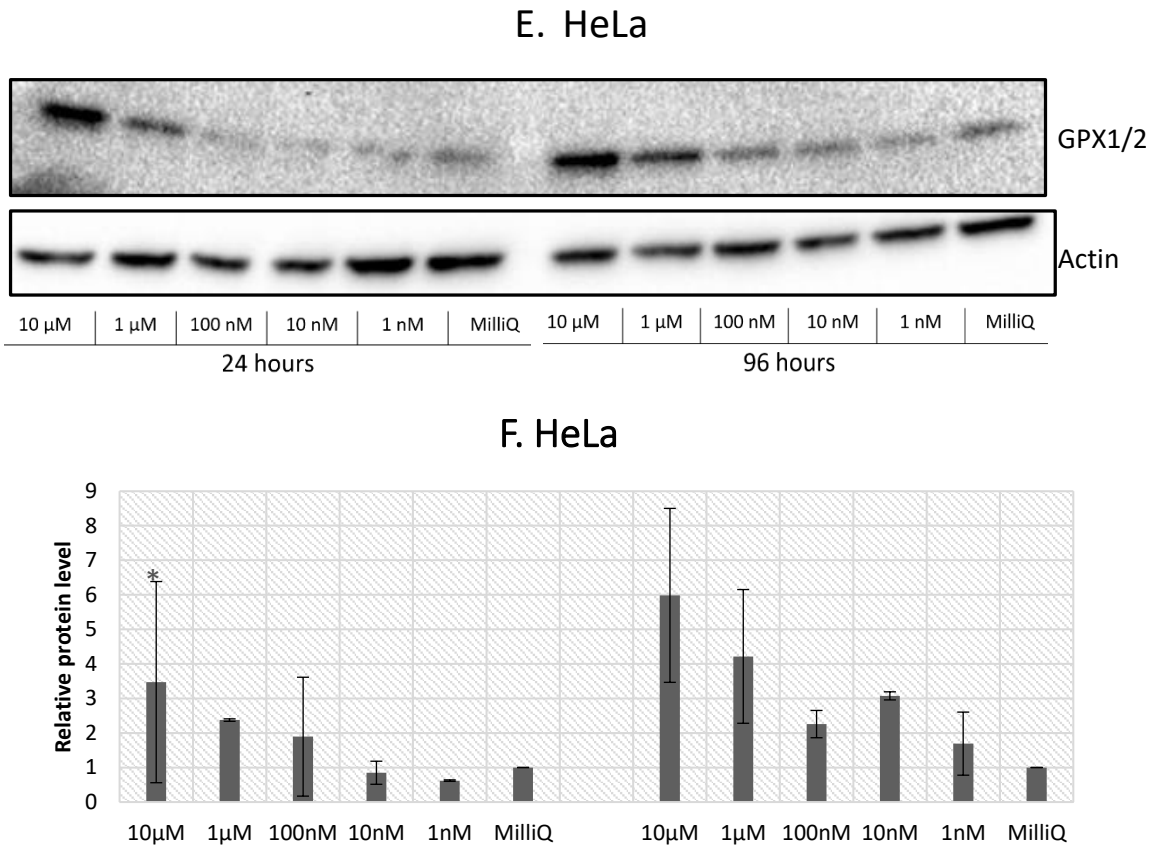

Figure 4.1: GPX1/2 protein levels increase in HaCaT, A431 and HeLa cells following supplementation with varying concentrations of Na_2SeO_3 over 24 and 96 hours. *Western blot of (A) HaCaT, (C) A431 and (E) HeLa extracts taken after 24 or 96 hours, and plots of protein level measured through band intensity normalised to actin (B) HaCaT (n=2 biological replicates), (D) A431 (n=4 biological replicates) and (F) HeLa (n=3, *n=2 biological replicates) after 24 hours (left) and 96 hours (right) of supplementation, with standard deviation bars.*

4.3 Longevity of response following Na_2SeO_3 withdrawal

While there is some previous research detailing the effect of selenium supplementation on a limited number of cell types human cells (Hazane-Puch et al., 2013, Hazane-Puch et al., 2014), there is none that documents the longevity of this response. To fill this gap in our understanding, HaCaT cells were treated with Na_2SeO_3 for 96 hours, before withdrawing the supplementation, and harvesting cells at 0h, 24h, 36h, 48h and 72h after withdrawal. HaCaTs were selected as they had the largest increase in GPX protein level following supplementation, so are not only highly sensitive to selenium levels, but would also presumably have the most noticeable drop in GPX1 level following withdrawal.

In figure 4.2 A and B, peak GPX protein was seen immediately after 96 hours of supplementation, where it was 8.4 times greater than the basal level. The level of GPX then

dropped by 70% within the following 24 hours of Na_2SeO_3 withdrawal to 2.6 times higher than background. GPX protein level slowly decreased for the following 24 hours and remained at a level slightly above basal until between 48 and 72 hours of withdrawal, where

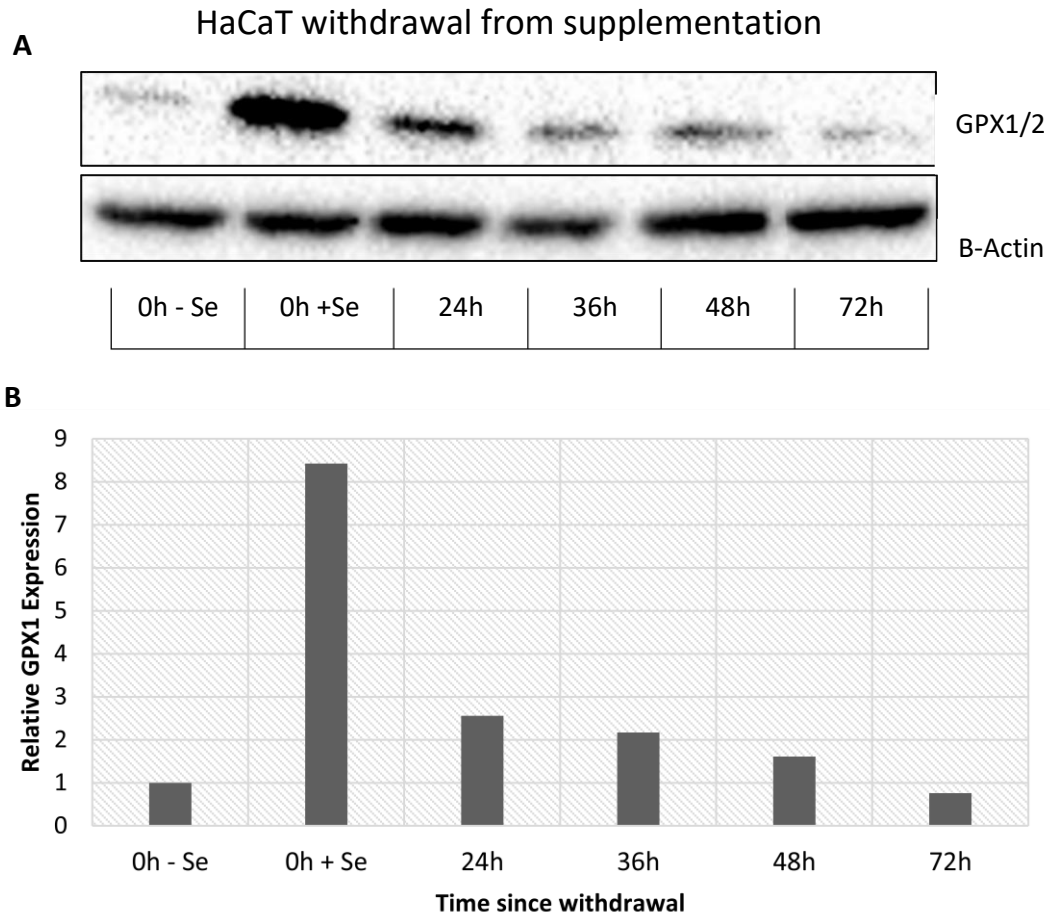

Figure 4.2: GPX1/2 protein level decreases rapidly in HaCaTs following selenium withdrawal. *Western blot (A) and bar chart (B) showing protein level in HaCaT cells following withdrawal from 1 µM Na_2SeO_3. 0 hour -Se represents the cells with no supplementation prior to the withdrawal experiment, and 0h +Se represents cells after 96-hour supplementation with Na_2SeO_3. Each subsequent lane shows the protein level of previously supplemented cells after hours of withdrawal (incubation without supplement).*

it returned to basal levels (as shown in the untreated 0 hours cells).

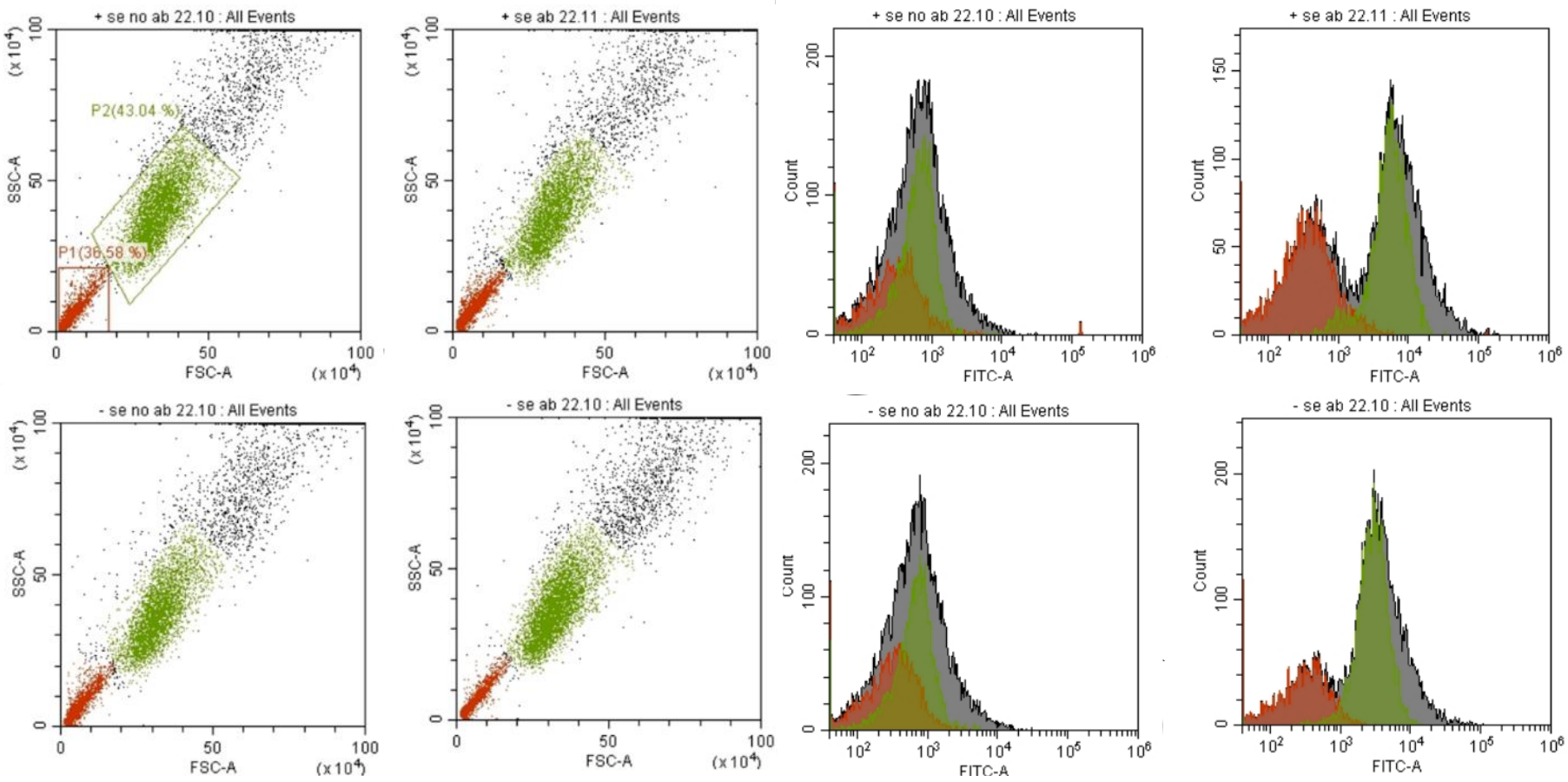

Figure 4.3: Immunofluorescence flow cytometry of HeLa cells indicates 96-hour incubation with Na_2SeO_3 increases GPX1/2 protein level. *Scatter graphs (left) indicate populations of cells grouped through gating. P1 represents cell debris, P2 represents intact cells which have taken up the Alexa Fluor antibody. Histograms (right) indicate the absorbance on FITC-A with P1 in red and P2 in green. Measurements taken on a Cytoflex and labelled using CytExpert software*

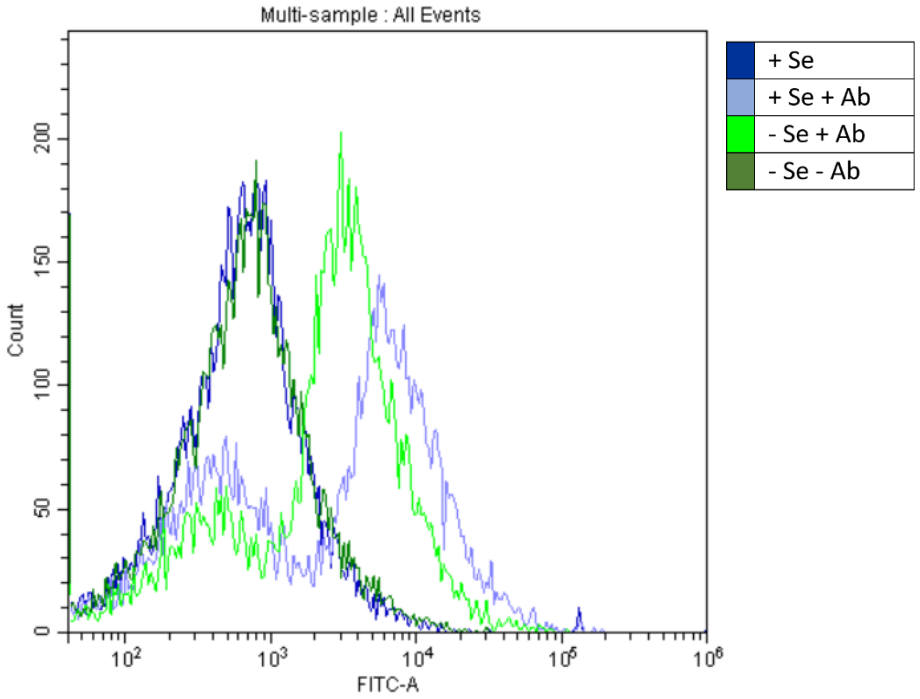

Figure 4.4: Selenium supplementation increases cellular levels of GPX1/2 as measured by flow cytometry. *Histogram overlay of all events measured in the FITC channel. The graphs shown correspond to cells with no primary antibody, both with (dark blue) and without (dark green) selenium supplementation, and cells with primary antibody, with (light blue) and without (light green) selenium supplementation.*

In figures 4.3 and 4.4, the peak is shifted left in cells given the GPX1/2 antibody, indicating that GPX1 is present in the cells with and without supplementation. In the supplemented group, this peak is shifted further left, and is flatter, indicating that more GPX1 was produced. This again suggests that Na_2SeO_3 supplementation promotes GPX1 production in cells, but also indicates that the increase in GPX1 protein level varies from cell to cell, and GPX1 is not homogenously expressed within the cohort.

4.4 Effect of Na_2SeO_3 supplementation on resistance to chemotherapeutic drugs

As discussed in 1.4.3, *GPX1* expression has been previously linked to chemoresistance in a few cancer cell lines. Further research with GDSC did indeed find some cancer cell types that may be more susceptible to GPX-induced chemoresistance, and thus designing a protocol for investigating this relationship is necessary for potentially exploiting this relationship in improving drug response. Therefore, survival assays were performed using the three chemotherapeutics drugs selected earlier (cisplatin, doxorubicin and docetaxel), as well as H_2O_2, as ROS are an important mediator in the induction of apoptotic cell death and are

therefore central to the action of chemotherapeutics.

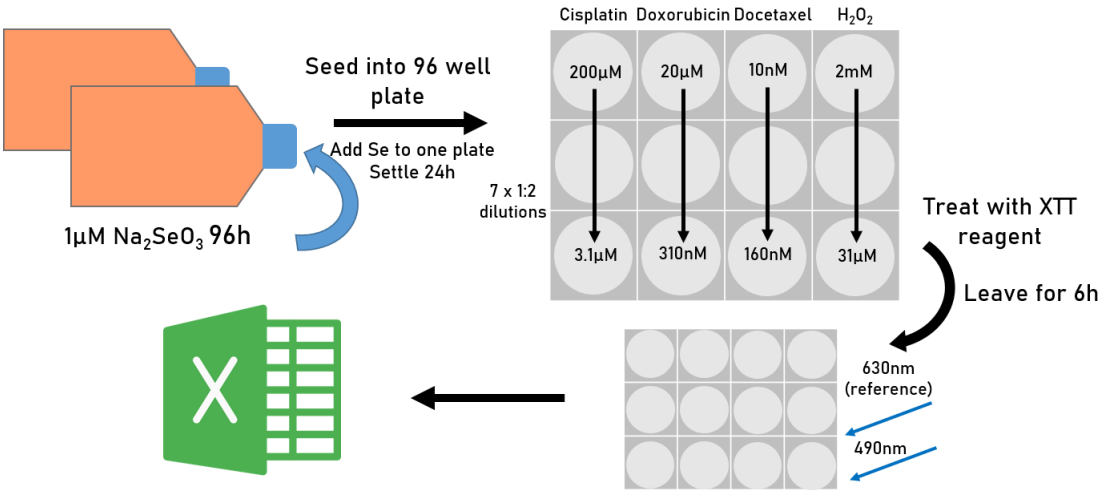

***Figure 4.5: XTT assay protocol for survival in cells after drug treatment**. Cells were incubated with or without sodium selenite after treatment with cisplatin, doxorubicin, docetaxel and hydrogen peroxide (H_2O_2).*

These treatments were performed in HaCaT as not only were these were shown to be very sensitive to selenium-induced overexpression of GPX1 and maintained largely elevated GPX1 protein levels for 24 hours after withdrawal. Although this was originally intended to be repeated in HeLa and UVM cell types, time restrictions prevented this. Survival of the HaCaT cells after exposure to chemotherapeutic drugs or H_2O_2 was measured using two survival assays, XTT and CyQuant, with or without 96 hours of prior incubation with sodium selenite. XTT and CyQuant use distinct methods for measuring survival: the XTT assay uses metabolic activity as a proxy for proliferation, measured via the reduction of a tetrazolium salt, while CyQuant quantifies survival by measuring interaction of fluorescent compounds with cellular nucleic acids. As will be discussed, original XTT experiments used the same media for the full experiment (figure 4.5), whereas later experiments were performed by replacing media with Na_2SeO_3-free DMEM before survival was measured.

Initial XTT data would suggest that there were no surviving selenium-treated cells at any dosage, and the absorbance values of all doses fell either below or near to that of the no cell control (figure 4.6). To illustrate this, only values for absorbance, not survival, were plotted. However, further inspection of the cells on a brightfield microscope showed the cells had similar post-treatment survival to the untreated cells. This therefore indicated that the assay was unable to measure the survival in treated cells. This could have been due to either the presence of selenium in the medium or the shift in redox status in the HaCaTs due to the overexpression of GPX1 which places the cells outside of the dynamic range of the reagent.

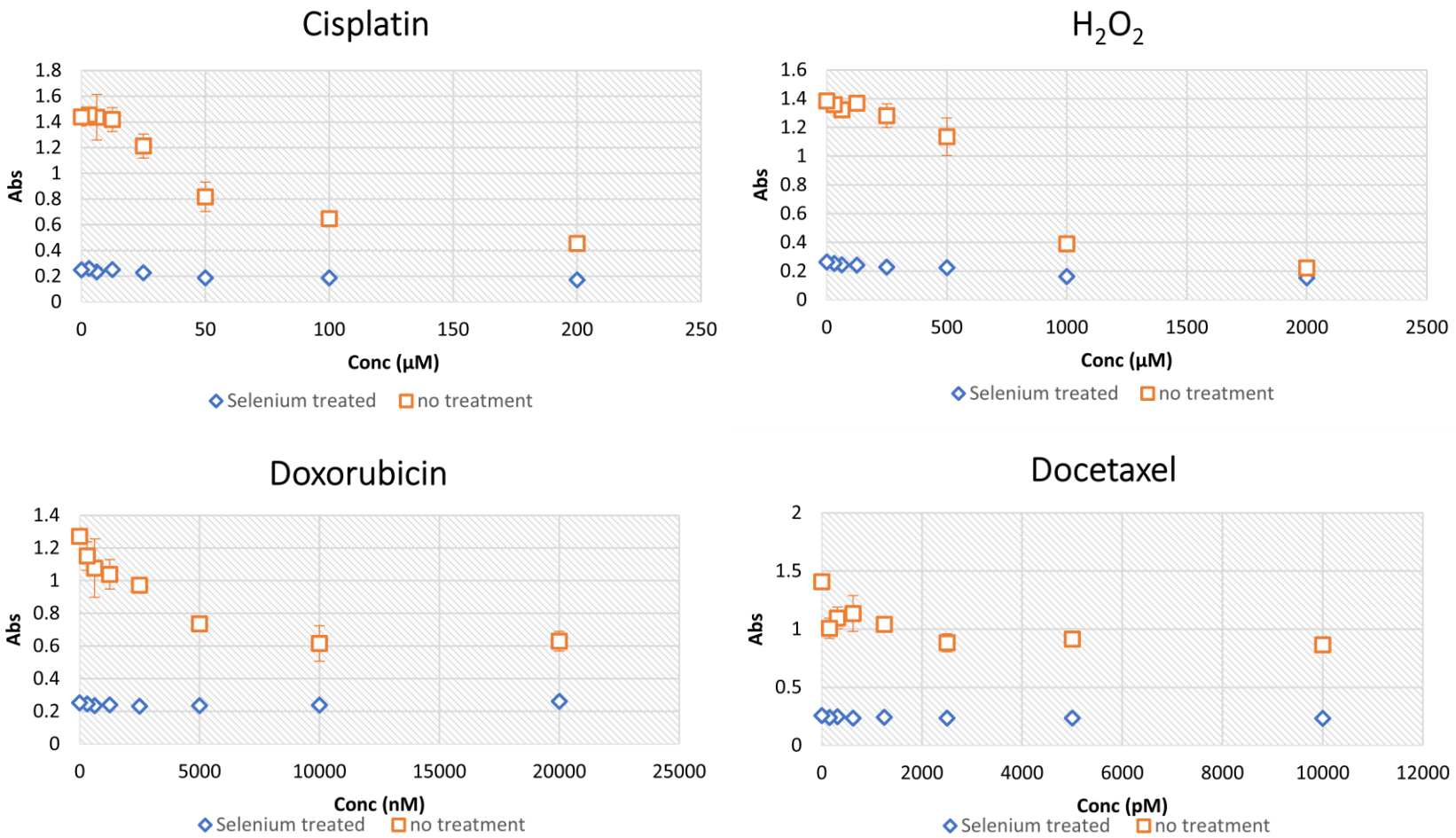

Figure 4.6: XTT does not effectively measure cell viability when measurements are taken in Na_2SeO_3-supplemented media. *Plots of absorbance seen in XTT assay after supplementation of HaCaTs with or without Na_2SeO_3 and treatment with cisplatin, doxorubicin, docetaxel or H_2O_2, when media was not changed before taking the XTT measurement (n=3 technical replicates).*

To determine the cause of this issue, further XTT experiments were performed in which the supplemented media was changed for Na_2SeO_3-free DMEM. In this instance, values for percentage survival were calculated as there was large enough difference seen between the lower and higher doses (figure 4.7). The survival for cells treated with cisplatin and H_2O_2 was significantly different after selenium treatment (paired two tailed T test p=0.0013 and p=0.0027 respectively). For H_2O_2 treatment, selenium treatment improved cell survival modestly, and for cisplatin, the opposite effect was observed. The effects of supplementation on survival after doxorubicin or docetaxel treatment were not found to be significant (p=0.2678 and p=0.0633 respectively). However, the results for the cisplatin, doxorubicin and docetaxel treatments did not meet expectations, as cells in both the unsupplemented and supplemented media were highly resistant to treatment at the doses tested, indicating that these data are unreliable. Conversely, hydrogen peroxide treatment did appear to be toxic to both sets of cells, although selenium treatment provided a small level of protection against this.

These experiments were inconclusive both for determining the cause of the issue in the original experiment and for determining the effect of supplementation on resistance to chemotherapeutic drugs. Hence, a new approach was implemented that did not rely upon metabolic activity for survival determination. This protocol was therefore repeated with the CyQuant assay, which instead uses a florescence-based method of determining cytotoxicity based on interaction with cellular nucleic acids.

Figure 4.8 shows the CyQuant assay results for all drug treatments except docetaxel, as the values for this were highly variable. Generally, selenium supplementation was associated with slightly increased survival after treatment with chemotherapeutic drug or H_2O_2. However, the only drug for which any significant change was observed was doxorubicin, where selenium supplementation provided a small amount of protection against the cell death at most doses (two tailed T-test p=0.0451). For cisplatin, docetaxel and H_2O_2, no significant effect was observed when cells were supplemented with sodium selenite (p=0.3896, p=0.9401 and p=0.0826 respectively). However, it should be noted that, due to time constraints, there are no biological repeats for this experiment, and I was unable to optimise the protocol, and therefore these data may be less reliable than subsequent assay results may have been.

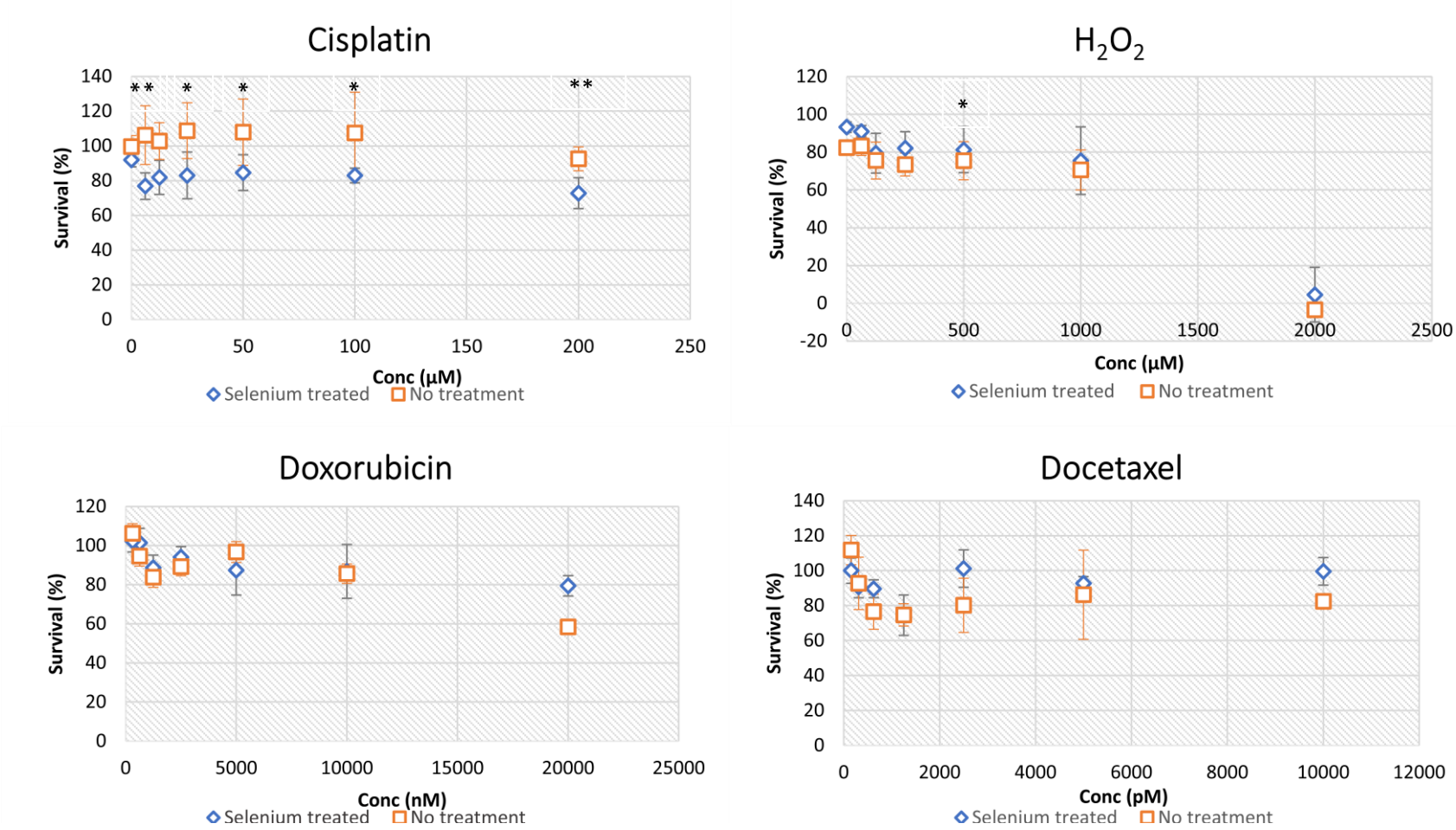

Figure 4.7: Na_2SeO_3 supplementation increased HaCaT survival following treatment with H_2O_2 and decreased HaCaT survival after cisplatin treatment.

*Plots of survival for HaCaTs (XTT assay) after supplementation with or without Na_2SeO_3, and changing the medium before adding treatment with cisplatin, doxorubicin, docetaxel or H_2O_2 (n=3 technical replicates). Asterisks indicate significance using a paired two-tailed t-test, * p<0.05, **p<0.002*

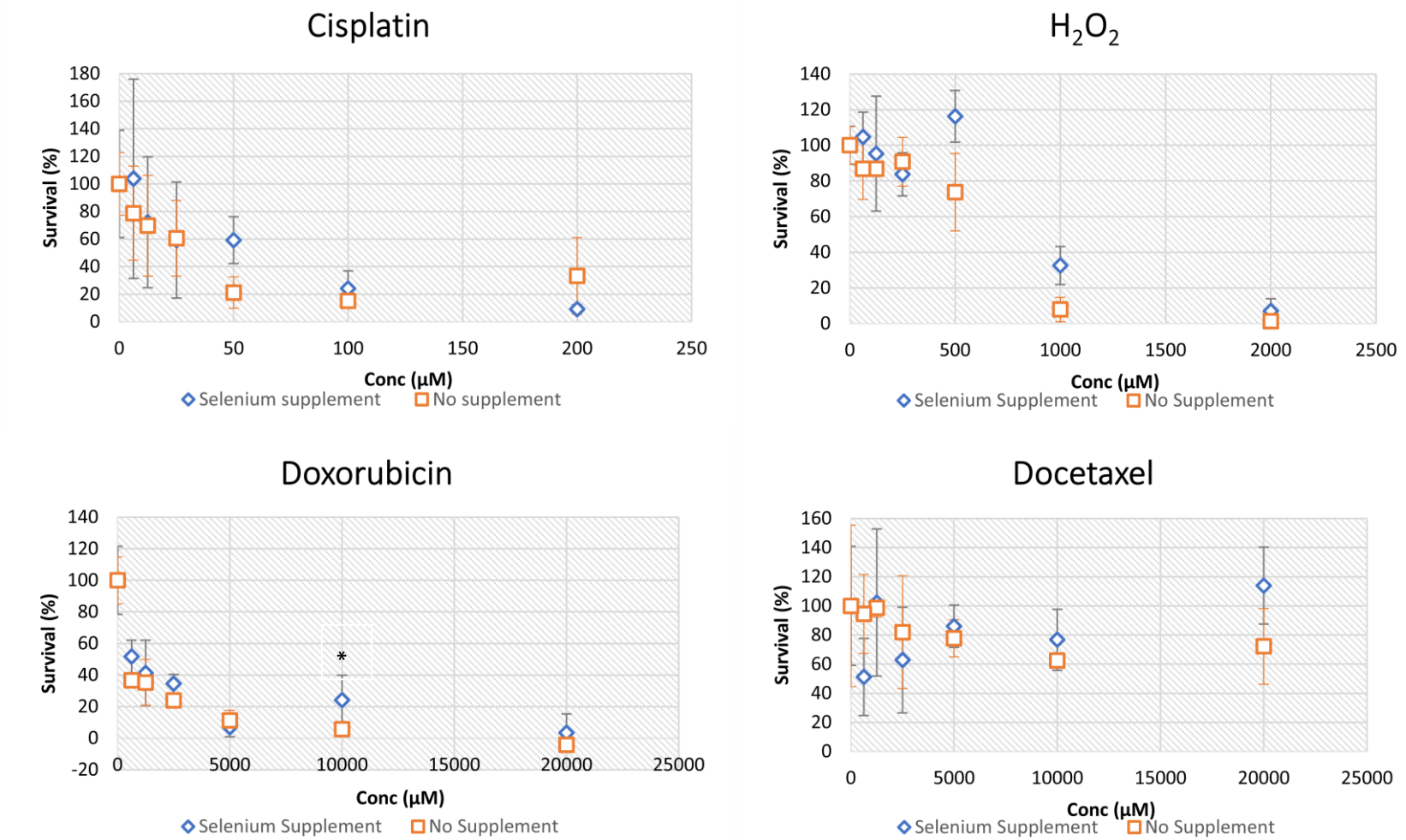

Figure 4.8: Na_2SeO_3 treatment significantly improves survival of HaCaTs following doxorubicin treatment. *Plots of survival for HaCaTs (measured by CyQuant) after supplementation with or without Na_2SeO_3, and changing the medium before treatment with cisplatin, doxorubicin, docetaxel or H_2O_2 (n=3 technical replicates).). Asterisk indicates significant value ($p<0.05$) using a two-tailed t-test, * $p=0.0451$*

4.5 Summary

Selenium supplementation is known to increase *GPX1* expression, however, this has been investigated primarily at the mRNA level. Supplementation with selenium was found to significantly increase GPX1/2 protein level after 24 and 96 hours for HaCaT, A431 and HeLa cells. HaCaTs were the most sensitive to this treatment, having a peak increase of 29 times the basal expression level, compared with 6 and 3.1 times in HeLa and A431 respectively. However, some of these samples only have 2 repeats, and more would be required to produce more accurate data for protein level increase with lower standard deviation. This effect was further observed in HeLa cells through flow cytometry, where it was revealed that, within a cohort of cells, there is variance in GPX1/2 level, even with excess selenium available. The longevity of the selenium-stimulated increase in GPX1/2 protein level was tested in HaCaTs, and was found to be very transient, as it dropped by 70% within 24 hours of selenium withdrawal and returned to near basal levels after 48 hours. Although this was only performed once, this result is consistent with our current understanding of the selenium hierarchy, where GPX1 is ranked last when selenium bioavailability is low (section 1.2.3.3).

Although two types of survival assay were performed, there were many issues with these assays. The XTT assay was performed using two protocols, with and without changing media prior to the addition of XTT reagent. Without changing media, the results were misleading, indicating that all cells were dead. The same assay performed with fresh media indicated that Na_2SeO_3 treatment improved cell survival with H_2O_2, and reduced survival with cisplatin. However, again this result was unreliable, as the toxicity of all treatments but H_2O_2 were shown to be lower than expected. It remains unclear whether the presence of selenium in the media affects the assay itself, or whether the redox status of the treated cells is pushed beyond the detection threshold for the XTT assay. However, the results of the assay using fresh media was closer to the expected outcome. The CyQuant assay indicated that selenium supplementation only significantly improved survival against doxorubicin treatment, although this was only performed once with three technical replicates. Further CyQuant assays using an optimised protocol would likely yield more accurate results.

Chapter 5 - Investigation of novel GPX1 inhibitor PeroxiPlat

5.1 Introduction

Despite its multiple functions in promoting cancer development and protecting cancers against cell death, there is no GPX1 inhibitor that is available for clinic use. As mentioned in section 4.3, there are a range of inhibitors that have been used experimentally as GPX1 inhibitors. However, most of these inhibitors are not specific for GPX1, due to the high structural and functional conservation within the GPX family. Mercaptans, the most widely used inhibitors of GPX1, alter a lysine residue in the active site that is common to other GPX family members (Chaudiere et al., 1984; Hall et al., 2014). Other inhibitors, such as methylmercury and gold(I) thioglucose), have high affinity for selenols, meaning that while they successfully inhibit GPX1, they also inhibit a range of other selenoproteins, both within and beyond the GPX family (Fujimura and Usuki, 2020; Chaudiere and Tappel, 1984). However, pentatheipin GPX1 inhibitors have been able to overcome these challenges and are both more potent and more selective than the most potent mercaptan used in research; MSA (Behnisch-Cornwell et al., 2020). While pentatheipin inhibitors were able to successfully able to kill GPX1-rich cancer cells, there were additional unexpected effects on cell which are not proven to be linked to GPX1 activity. Thus, the need for a potent and well-understood GPX1 inhibitor remains.

PeroixPlat is a luminescent platinum-based compound that, as it contains a GSH bioconjugate, has been theorised to interact with GPX1 as a GSH mimic, acting as a potential GPX1 inhibitor (Coogan et al., 2021). PeroxiPlat is thought to replace the second GSH substrate in attacking the selenenyl sulphide intermediate, irreversibly establishing a strong Pt-Se bond rather than regenerating the enzyme. This Pt-Se bond was observed via NMR when PeroxiPlat reacted with selenocysteine and a larger Sec-containing molecule - diphenyl diselenide (Coogan, M, unpublished work). *In vivo*, lambda scans of HaCaTs after addition of PeroxiPlat detected emission comparable with that of Sec-bound PeroxiPlat, and not of free PeroxiPlat (figure 1.18). Furthermore, confocal imaging has shown PeroxiPlat localising to the peroxisome, suggesting a preferential interaction with GPX1 over other selenoproteins (figure 1.19).

If it is able to inhibit GPX1 successfully, PeroxiPlat has a further advantage over existing GPX1 inhibitors, as it is luminescent, and therefore holds potential as a diagnostic tool as well as an inhibitor. So far, the evidence does indeed suggest that PeroxiPlat is able to bind to the active site of GPX1 in a potentially selective fashion *in vivo*. However, the effect of this interaction on GPX1 activity has not been investigated, nor has the ability of PeroxiPlat to be taken up by and detected within cancer cells. In order to assess the potential of PeroxiPlat

for use as a theranostic agent, many experiments were performed to investigate the interaction of GPX1 and PeroxiPlat. These were designed to (1) measure PeroxiPlat uptake in cells and (2) determine the ability of PeroxiPlat to inhibit GPX1 activity.

5.2 Interaction of PeroxiPlat with GPX1

As a more quantitative method of measuring this interaction, flow cytometry was employed, using Na_2SeO_3 –supplemented and unsupplemented HeLa cells as a means of comparing cellular PeroxiPlat fluorescence with different levels of GPX1. These were also supplemented with Na_2SeO_3 to increase the amount of GPX1 available for PeroxiPlat binding for comparison. Cells were treated with sodium selenite for 96 hours before trypsinisation, resuspension and subsequent treatment with PeroxiPlat at 100 µg/mL for 10 minutes. Cells were then analysed in the PE channel. The flow cytometry showed no indication of PeroxiPlat binding. Figure 5.1 A shows the scatter of HeLa cells (P1) and cell debris (P3) with and without selenium supplementation, and with and without PeroxiPlat. The gating used is labelled on the plots. Another population of cells with comparable side-scattered light (SSC) as the P1 cluster, but lower forward scatter (FSC) was also gated and labelled P2. Levels of PE fluorescence of the P1 and P2 populations were then separately examined in the PE channel (figure 5.1 B), with excitation and emission frequencies that are able to detect PeroxiPlat. While one would expect a greater fluorescence in supplemented cells, as there would be more GPX1 for PeroxiPlat to bind to, the P1 overlay plot (figure 5.1 B) shows no difference in cells with or without supplementation with selenium. Furthermore, there is no difference in the P1 cells with or without PeroxiPlat, regardless of selenium supplementation, indicating that these cells did not take up PeroxiPlat in either condition.

However, as seen in figure 5.1 B, the size of the P2 population for cells given PeroxiPlat was greater than those without, indicating that PeroxiPlat was indeed detected. This peak was further elevated in cells given selenium supplement compared with unsupplemented cells, which could be interpreted to suggest that selenium supplementation was successful in increasing GPX1 and that this was sufficient to increase the uptake of PeroxiPlat by a measurable amount. However, this cluster has a lower FSC than those in P1 and could therefore be debris comprised of PeroxiPlat which was not taken up by HeLa cells, and as there are so few events, this difference could potentially be due to a small error or difference in preparation.

A

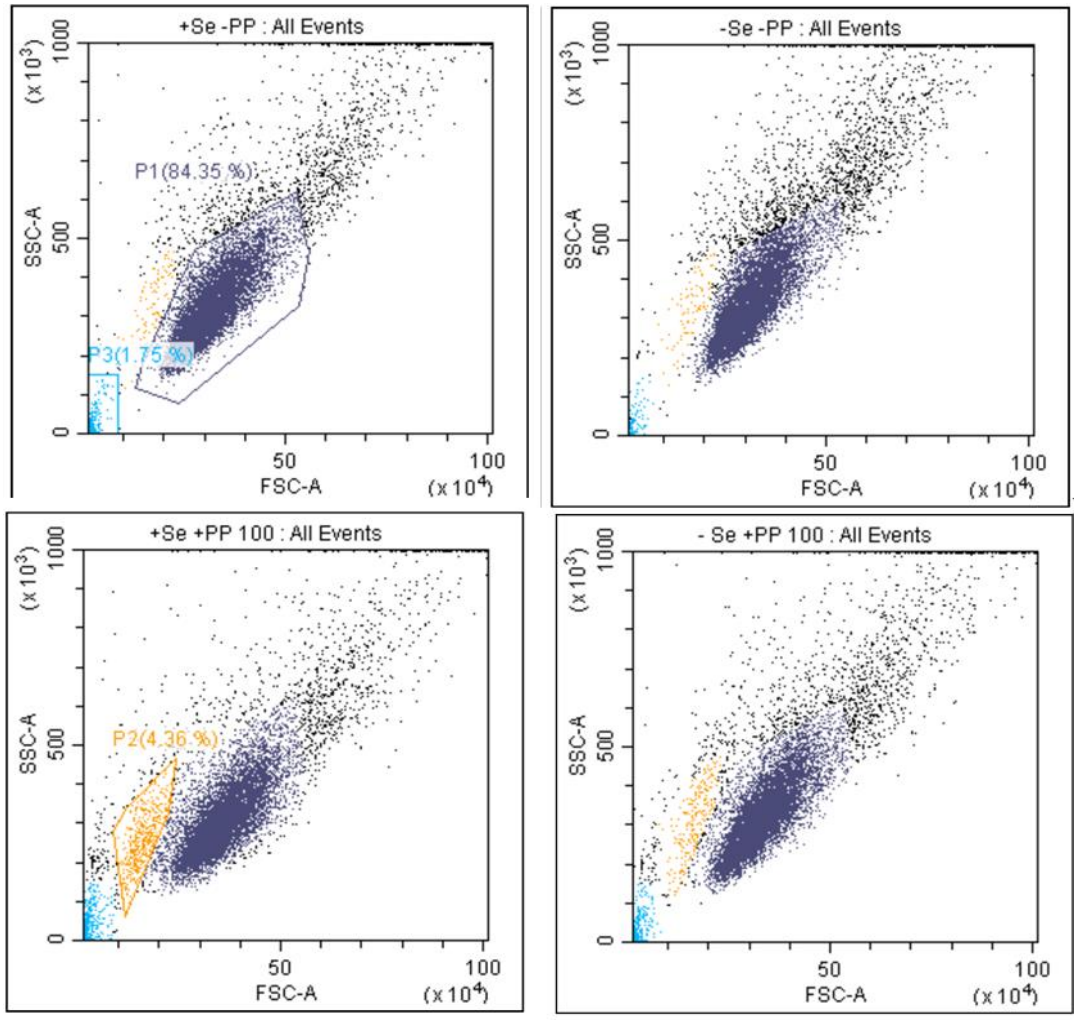

B

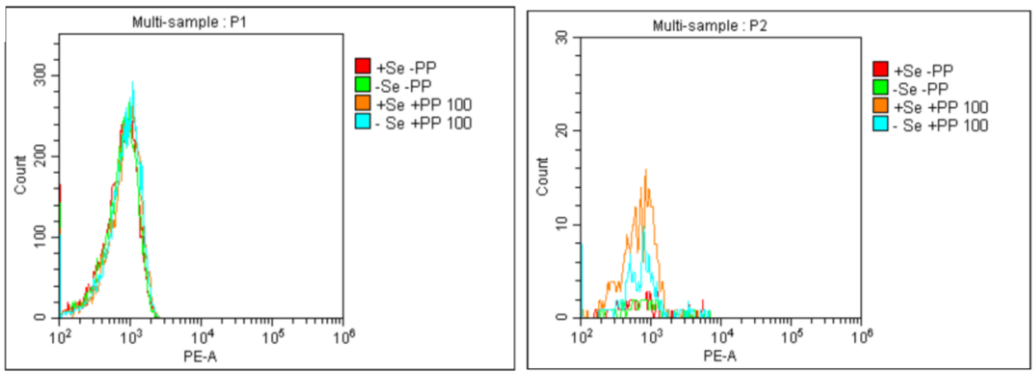

Figure 5.1: Flow cytometry of 100 µg/ml PeroxiPlat in HeLa cells after 96-hour incubation with or without Na_2SeO_3. *(A) Scatter graphs showing cells with (left) or without (right) selenium supplementation with Na_2SeO_3, and with (bottom) or without (top) PeroxiPlat (PP). P1 represents intact cells, P2 represents an unidentified cluster, and P3 represents cell debris. (B) Histogram overlay of (left) P1 and (right) P2 populations with and without selenium supplementation and/or PeroxiPlat, measured on a PE-A filter.*

5.3 Effect of PeroxiPlat on GPX1 activity

To determine whether PeroxiPlat was able to successfully inhibit GPX1, multiple biochemical assays were performed on GPX extracts treated with PeroxiPlat. The glutathione reductase (GR)-coupled GPX assay allows us to observe the function of PeroxiPlat in biochemical conditions similar to GPX's physiological environment. It utilises NADP, NADPH, GSH, GR and a peroxide source for the reaction, which mimics the biological metabolic cycle (figure 1.7). Not only this, but the GPX assay is a time course experiment set over eight minutes, and so the reaction kinetics can be observed in real time, which can give us further information about the efficacy of PeroxiPlat. By contrast, the FOX assay is a single timepoint, simpler system, as the reaction only requires GPX, GSH and a smaller amount of a peroxide source (Luperox). As lower levels of peroxide are present, there is a lower possibility of a cross reaction with PeroxiPlat, which may lead to degradation of PeroxiPlat. Furthermore, this assay is both more sensitive and more direct, as instead of using NADPH absorbance as a proxy to measure activity, it directly uses peroxide level to signal a colour change. This should theoretically allow us to detect low levels of inhibition.

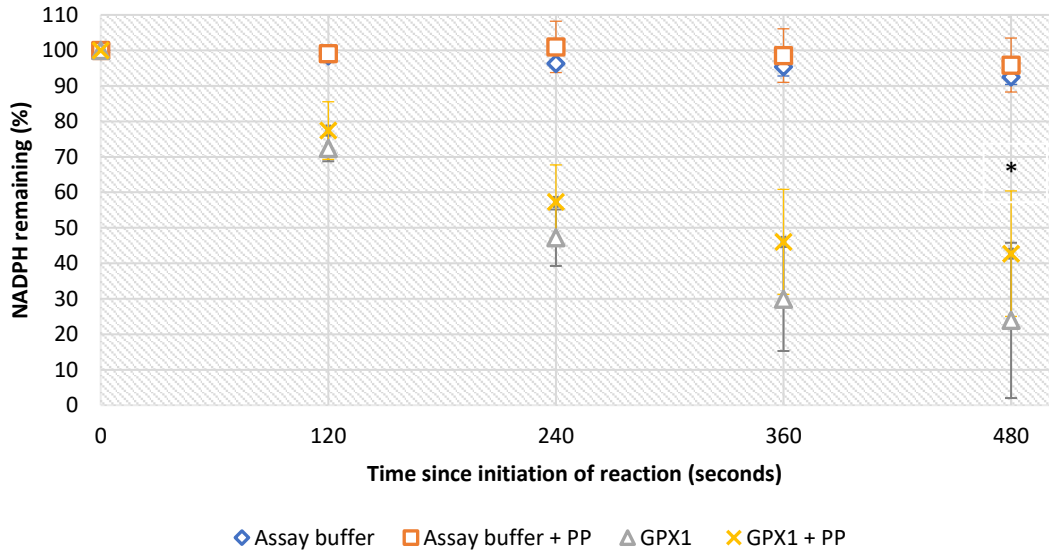

Figure 5.2: GPX1 activity, measured by the GPX assay, is significantly reduced following treatment with PeroxiPlat. *GPX activity as measured via NADPH absorbance through the GPX assay. The absorbance was measured for four samples containing assay buffer with and without PeroxiPlat (PP), and with or without GPX1 (n=2 biological replicates). Asterisk indicates significant value ($p<0.05$) between the paired inhibited and uninhibited GPX1 samples in a paired two-tailed t test, * $p=0.04462$.*

The results of the GR-coupled GPX assay (figure 5.2) suggest that PeroxiPlat is effective at reducing GPX1 activity when compared with the uninhibited GPX1 sample. This was also found to be statistically significant in a paired two-tailed T test (p=0.04462). The inhibitory effect of PeroxiPlat becomes noticeable after 240 seconds, and the difference between the PeroxiPlat-treated and the uninhibited sample increases over the subsequent 240 seconds, reaching 42.7% and 23.9% respectively at the endpoint of 480 seconds. The time taken for 10% of the NADPH to be depleted in PeroxiPlat-treated GPX1 was 45.3 seconds, compared with 37.1 seconds for uninhibited GPX1 indicating an approximate rate reduction of 22% in the initial stages of the reaction. There is also no difference between the samples without GPX1, which eliminates the possibility of PeroxiPlat addition affecting absorbance of NADPH.

As we hypothesised that high glutathione concentration interfered with PeroxiPlat, a more sensitive method of measuring GPX activity was required, which uses a more tolerable level of glutathione. The FOX assay instead measures the concentration of hydrogen peroxide, which is propagated by the FOX assay reagent, giving a more direct and sensitive measurement of GPX activity (Rhee et al., 2010). As this is colorimetric, this can then be easily measured on a plate reader (figure 5.3).

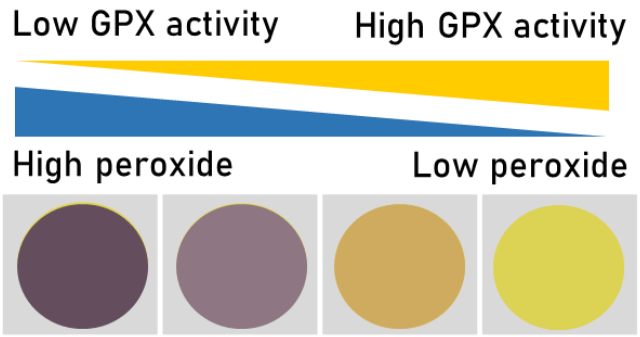

Figure 5.3: Colorimetric reaction observed with peroxide level and GPX activity during the FOX assay

The FOX assay (figure 5.4) also indicated that PeroxiPlat could indeed reduce GPX1 activity, as measured by the percentage turnover of peroxide substrate, from 54% (±7%) to 27% (±14%). This effect was not statistically significant using a two tailed T test (p=0.127), however, as the PeroxiPlat used was kept for up to a month before use, repeats of this experiment with fresh batches of PeroxiPlat may be more effective and give a lower standard deviation. As expected, MSA, a known GPX inhibitor, was highly potent, and inhibited GPX activity significantly (p=0.008). Interestingly, GPX samples with no GSH still retained some activity, which may indicate that the GPX used in these experiments was not

well purified and may contain some GSH substrate. Therefore, it is unclear whether the presence of PeroxiPlat in the absence of GSH affects GPX1 activity.

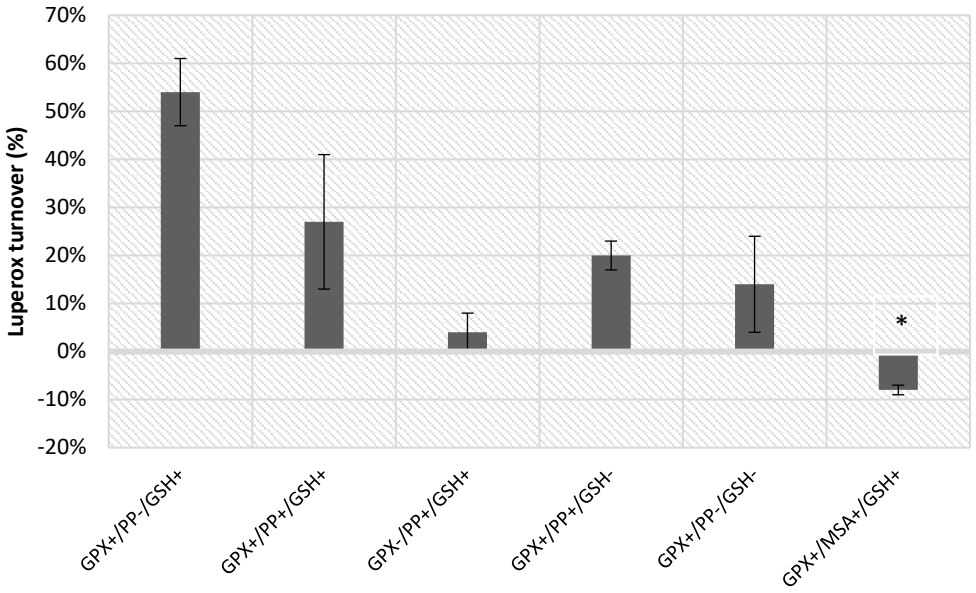

Figure 5.4: GPX1 activity, measured using the FOX assay, is significantly reduced following PeroxiPlat treatment. *GPX activity as measured via the FOX assay, using percentage luperox turnover as a measure of GPX activity. Measurements were made across 6 samples of different composition, including GPX, GSH, PeroxiPlat (PP) and/or MSA (n=3 biological replicates). Asterisk indicates significant value ($p<0.05$) using a two-tailed t test, * $p=0.008$.*

5.4 Summary

The interaction between PeroxiPlat and GPX1 in HaCaTs has been implied after previous experiments using lambda scan confocal microscopy detected a shift in emission frequency, indicating the presence of Sec-bound PeroxiPlat. In this work, flow cytometry was used to attempt detect PeroxiPlat within HeLa cells with and without Na_2SeO_3-stimulated GPX1 overexpression. Flow cytometry data indicated that, for the majority of cells (represented in the P1 population), there was no difference between the supplemented and unsupplemented cells, and those with and without PeroxiPlat, suggesting that PeroxiPlat was not taken up by most cells. However, an additional population was also identified (P3) which exhibited the expected shift in absorbance when PeroxiPlat was added, and this peak was larger in supplemented cells. This therefore strengthens the evidence that PeroxiPlat and GPX1 interact *in vivo*, as the more GPX1 is available, the greater amount of PeroxiPlat is detected. However, this was limited to a small sub-population of the cells, therefore may indicate that PeroxiPlat is not taken up well or has poor reactivity with GPX1 *in vivo*.

The effect of the interaction between PeroxiPlat and GPX1 on GPX1 activity was assessed with two assays. The GPX assay, which gives an indirect measurement of activity based upon NADPH level, evidenced that PeroxiPlat was able to significantly inhibit GPX1 activity. The results of the FOX assay supported this, as PeroxiPlat again inhibited GPX1 activity, although this effect was not significant, and was minimal in comparison to known inhibitor MSA. However, this data had a large amount of variance, which may be due to PeroxiPlat stocks degrading before use and repeats using fresh samples may have shown a more potent and consistent effect. Given what we know of the reaction between GPX1 and PeroxiPlat, it seems likely that PeroxiPlat does react within the active site to inhibit GPX1, although this interaction may be less common in biological conditions than NMR data suggested, as there is only a small cluster of PeroxiPlat-containing events seen in flow cytometry, and both assays indicate a weak inhibitory effect.

Chapter 6 – Discussion

6.1 Introduction

GPX1 is an essential enzyme for removal of H_2O_2 and simple lipid peroxides, and as such is a key protein in the antioxidant response and works within a network of other proteins to regulate cellular redox. This central regulatory role affords GPX1 wider influence over many other pathways, as discussed in section 1.4. Many of these impact cancer progression, as proliferative and apoptotic pathways such as NF-κB and Akt/PI3K can be greatly disrupted by changes in H_2O_2, cell redox status and GPX1 levels. Notably, it has been observed that overexpression of *GPX1* can lead to more aggressive, invasive and metastatic cancers, ultimately resulting in poorer patient prognosis (Cheng et al., 2019; Zhang, Q et al., 2018; Wei et al., 2020). Indeed, *GPX1* expression has been investigated as a promising biomarker for cancer diagnosis. However, while it is clear GPX1 has the potential to offer significant advantages to cancer cells, it remained unclear how often these changes occur, which cancer cell lines GPX1 is advantageous for, and to what extent changes to *GPX1* expression, protein level or structure are responsible for these effects.

Within the antioxidant network are other members of the GPX family (GPXs 1-8) which each have overlapping specificities, allowing for some functional redundancy in function (section 2.1). Despite this, GPX1, being the most catalytically active and most widespread GPX protein, is able to take up specific and distinct functions within the cell, making manipulation of GPX1 an interesting subject for investigation. Increases in *GPX1* expression have been easily achieved in a limited number of cell types by supplementation with a selenium source (Hazane-Puch et al., 2013; Hazane-Puch et al., 2014). This is effective as GPX1 sits at the bottom of the selenium hierarchy, and as such is expressed sparingly with low selenium bioavailability, whilst other selenoproteins, such as GPX4, are given priority. However, when selenium is in excess, GPX1 is produced readily, giving an easy means to investigate the effects of *GPX1* overexpression. However, much of this work has thus far focussed on GPX1 mRNA and not protein level, and so the amount of GPX1 protein produced in the presence of selenium is unknown. This may provide additional context for researching the effect of *GPX1* overexpression in cancer cells. It is also unknown how long this effect is maintained when selenium is withdrawn, which may again offer insights into how selenium withdrawal may be utilised to reduce GPX1 levels in cancers.

While selenium supplementation is an easy method to increase *GPX1* expression, inhibition of GPX1 activity has proved more challenging. At the current time, there is no GPX1-specific inhibitor that is safe and effective in patients. To create GPX1-specific inhibitors, one must

overcome many challenges. Firstly, there is a high degree of similarity between GPX1 and other GPX family members, as they have recently diverged evolutionarily and contain many highly conserved regions (section 1.2). Because of this, many existing inhibitors, such as the mercaptans, exhibit off-target effects on other selenoproteins or GPX family members, or have poor uptake and efficacy. Secondly, the creation of a GSH homologue which has the necessary structural changes to inhibit GPX1 may also preclude its entry to the cell via GSH protein channels, or prevent interaction with GPX1 itself, as is induced by gold and mercury-based inhibitors. PeroxiPlat is a potential inhibitor of GPX1 which is, according to confocal images, able to penetrate the cell and selectively bind to GPX1. However, the nature of this interaction and its efficacy as an inhibitor is yet to be established.

6.2 Data mining

6.2.1 GPX1 is commonly overexpressed in cancers and correlates with worse prognosis

Bioinformatic research from FireBrowse and GEPIA indicated that *GPX1* is overexpressed in most cancer types tested, and only two cancer types were found to lose a large amount of *GPX1* expression with carcinogenesis - LUSC and PCPG (figures 3.1 and 3.2). Some cancers showed particularly high expression compared with the normal tissue (GBM, KIRPL, LAML, LGG, OV, PAAD, SKCM, TGCT, THCA, UCEC). *GPX1* overexpression is a feature of cancer cells in most cases, although the extent varies depending on cancer type. This has also allowed us to identify a subgroup of cancer types which may be particularly susceptible to GPX1-based therapies. This work concurs with Wei et al., 2020, who also used GEPIA to investigate this, although this occurred after this project had completed this work. The inclusion of the FireBrowse plot further strengthens this finding, as it uses another database and yet found the same conclusion.

As also reported in Wei et al., 2020, the Kaplan-Meier plots confirm that this overexpression in some cancers can indeed provide an advantage to cancerous cells, and a disadvantage to patients. UVM appeared to be significantly impacted by *GPX1* overexpression, with the patients in the upper quartile of *GPX1* expression having a 0% survival after approximately 45 months (figure 3.3). This would therefore be an interesting candidate for further investigation, as it appears to rely more heavily on *GPX1* expression for survival. Other cancer types of note are LGG, ACC, KICH and LAML, for whom high *GPX1* expression was well correlated with poor overall survival (figures 3.4 and 3.5). Recently, Cox proportional-hazards models of *GPX1* expression in LGG, LAML and UVM have further confirmed this, as again these were linked with poorer prognosis (Wu et al., 2021).

Of these, LGG and LAML had particularly high gene expression according to GEPIA and would be particularly likely to respond well to therapies reducing GPX1 activity (figure 3.2). Indeed, recent work in T-ALL cells (a LAML cell line) has investigated this relationship, finding that while *GPX1* is overexpressed in T-ALL cells, knockdown of GPX1 induces apoptosis and reduces proliferation (Zhuang et al., 2020). For LGG, data mining has also indicated that increased *GPX1* expression increases immune infiltration of tumours, which allows us to better understand why prognosis is poorer in high *GPX1*-expressing patients (Lv et al. 2020; Wu et al., 2021). Furthermore, according to GDSC analysis, increased GPX1 promotes resistance against cisplatin in LGG cell lines (figure 3.10). While this could indeed compound the effect of GPX1 in cancer cells, the induction of cisplatin resistance in LGG cell lines is yet to be substantiated by lab-based experiments. This would clarify and confirm the extent to which *GPX1* expression provides resistance and may further our understanding of how *GPX1* expression may disadvantage LGG patients.

CESC is the only cell line that increased chemoresistance to all three chemotherapeutic drugs tested via GDSC analysis (figures 3.10, 3.11 and 3.12). This would suggest high *GPX1* expression results in poorer response to treatment, and therefore likely worse prognosis, in CESC patients. However, Kaplan-Meier plots indicated the opposite. In fact, CESC was the only cancer type for which high *GPX1* expression significantly increased overall patient survival (figure 3.6). This analysis has not only a low P value, but also a large sample size, lending a high level of credibility to the survival plot than the GDSC analysis. Additionally, research using Cox propotional-hazard plots showed a slight improvement in prognosis when GPX1 was highly expressed (Wu et al., 2021). It is possible however, that both could be true, and GPX1 works through a non-apoptotic pathway, for example by downregulating inflammatory pathways, to prevent cancer progression and improve patient survival.

It should be noted that the GDSC analysis is limited in its explanation of the relationship between *GPX1* expression and survival, which was observed through the comparative expression analyses (FireBrowse and GEPIA) and in Kaplan-Meier plots. Instead, the GDSC plots indicated that the role of GPX1 in chemoresistance may be minimal (section 3.4). Increasing *GPX1* expression in most cancer cell lines did not appear to increase chemoresistance to cisplatin, docetaxel or doxorubicin. This is in contradiction to existing reports which have not only shown a clear link between GPX expression, cisplatin (Gan et al., 2014) and doxorubicin (Doroshow and Juhasz, 2019) resistance, but have even derived a mechanism-of-action for the induction chemoresistance by GPX1 (Kalivendi et al., 2005), as discussed in section 1.4.3. There are many possible reasons for this discrepancy, for example,

the sample size is too low in many cancer types to draw a conclusion. Secondly, as the samples were tested for *GPX1* expression separately to testing IC_{50}, differences in culture conditions, specifically the selenium level and redox status of the cells, within a cell line could have resulting in a misleading set of values, as the IC_{50} and *GPX1* expression may not represent the true state of the sample at any one time. Therefore, greater credence should be given to the previous data linking GPX1 to chemoresistance, and the plot of *GPX1* expression vs IC_{50} should be remade using more accurately paired data.

6.2.2 GPX1 P77R mutation is a residue of interest

Thus far, there has been very little research into the existence of somatic mutations in *GPX1* in cancer cells. However, there is a known polymorphism of *GPX1* (Pro198Leu) which has been found to increase cancer risk in some cancers (Wang et al., 2017) and decrease GPX1 activity (Jablonska et al., 2009), indicating that the identification of *GPX1* mutants in cancer may be of clinical significance. To this end, data on *GPX1* mutations was extracted and analysed across multiple databases to determine if there were any hotspots which could affect GPX1 function in the cancer cell. P77R was revealed to be such a hotspot through COSMIC analysis (figure 3.14), accounting for 44 of the 155 mutations mapped across the protein, and of 389 samples in total. However, similar maps generated with the ICGC and GDC portals showed no such hotspot (figure 3.15). As these portals share some data sources with COSMIC, this was particularly surprising.

Upon further investigation, it was found that 18 of the samples represented in the COSMIC map were from a single study looking at NSCLCs (McMillan et al., 2018). These samples were not represented in the ICGC database as accessed through the ICGC portal, nor in the TCGA database as accessed via the GDC portal, although both of these databases are used by COSMIC to generate mutational maps. This indicated that either there was a difference in the selection criteria for each portal, which caused some samples to be rejected from analysis, or these samples were added manually to the COSMIC portal and were not available to the other two portals. Regardless, as this is not represented across majority of samples, it is likely that if it is a true mutation, it is only prevalent in NSCLCs.

If the P77R mutation is indeed validated, Ensembl analysis (SIFT, Poly-Phen, CADD, REVEL and Mutation Assessor) suggests this would likely confer significant changes in GPX1 function (table 3.2). P77 sits within a region known as the functional loop (Toppo et al., 2008), which is responsible for the tetramerization of the subunits to form GPX1 (section 1.2.1). If this interaction were impacted, this could alter substrate binding. In GPX1, the tetramerization is

thought to create a shallow cleft which occludes binding of larger lipid peroxide substrates (Flohé et al., 2003). There are many GPX1 homologs within the GPX family which have no functional loop, as they are not tetrameric, but have a similar structure to the GPX1 subunit. It is possible therefore that this mutation would not only change GPX1 quaternary structure but also substrate specificity, removing a larger range of peroxides and aiding cancer cells in resisting cell death. This is speculative, however, and site-directed mutagenesis of *GPX1* at P77R followed by GPX1 activity assays with a range of substrates would ascertain whether this is true.

6.2.3 The role of GPX1 in networks to promote cancer progression

GPX1 expression is often explored within the context of cancer with respect to its function as a remover of oxidative stress. However, its role in redox homeostasis gives it the role of mediator in many other pathways (section 1.4), and therefore *GPX1* overexpression may impact expression of other cancer-driving proteins, or indeed compound the effects of other independently overexpressed genes found in cancer. Additionally, the GPX family is known to have redundancy in function, as well as a hierarchy for expression based on selenium bioavailability (section 1.2.2), and therefore further exploration into the changes in expression for the rest of the family will provide context on the remodelling of redox response in cancer cells.

6.2.3.1 The GPX family

This investigation, using publicly available RNAseq data, demonstrated that *GPX2* was often overexpressed with *GPX1* (figure 3.8). *GPX1* is known to compensate for loss of *GPX2*, as they have some functional redundancy (Florian et al., 2010). Not only do they use similar substrates, they both moderate the inflammatory response, although they have distinct roles (Koeberle et al., 2020; Hiller et al., 2015). In these experiments, however, they were both found to be protective against the development of cancer. Therefore, the revelation that both are fairly commonly overexpressed in cancers raises interesting questions concerning the effect of this on the inflammatory system and on cancer development as a whole. This could be a protective anti-inflammatory response from cells experiencing overactive inflammatory signalling, in order to re-establish a homeostatic state. Conversely, GPX2 has also been found to inhibit apoptosis in the colonic crypts (Florian et al., 2010), and so may act in tandem with GPX1 to increase resistance to apoptosis-inducing chemotherapeutic drugs in cancer cells, potentially worsening patient outcome. Therefore, the full impact of the overexpression of *GPX1* with *GPX2* in the different stages of cancer is unknown and warrants further investigation.

GPX4 was found using GEPIA expression heatmaps to be overexpressed with *GPX1* to a similar degree across many cancers (figure 3.8). However, expression scatter plots of all tumour and normal samples indicated no significant difference in the relationship between the expression of the two proteins overall, indicating this may be specific to the cancer type (figure 3.7). Increases in both *GPX1* and *GPX4* expression has been documented in oral squamous cell carcinoma, although it was found that only *GPX1* overexpression was able to predict poor patient prognosis (Lee et al., 2017), indicating that *GPX1* overexpression was, in this case, more influential than *GPX4* in progressing cancer. Like *GPX2*, *GPX4* overexpression inhibits apoptosis (Ran et al., 2004), but is also able to inhibit cell death via ferroptosis (Kinowaki et al., 2018). The combined action of GPX1 and GPX4 in these *GPX*-overexpressing cancer cells would vastly reduce the ability of cells to undergo ROS-induced apoptosis in response to treatment, as has been observed in doxorubicin resistance (Olsen et al., 2013). Currently, the induction of ferroptosis is being investigated as a way bypass drug resistance in cancer cells (Chen et al., 2021; Hangauer et al., 2017; Wu et al., 2020), however, *GPX1*- and *GPX4*-overexpressing cancers may be invulnerable to such treatment, as they are likely to be more resistant to both forms of cell death.

Surprisingly, *SBP2* was frequently downregulated when *GPX1* was overexpressed (figure 3.8). As SBP2 is required for the selenocysteine insertion stage of translation for selenoproteins (section 1.2.3.2), an increase in SBP2 would be expected with the increased production and activity of GPXs 1, 2 and 4 seen in cancer. This could therefore be a compensatory response to slow the production of GPXs when they have been excessively expressed. However, there is little information on precisely how *SBP2* is regulated, and so the exact mechanism which results in the reduction in *SBP2* expression, and how this may relate to the level of GPX within the cell, requires further investigation.

6.2.3.2 GPX1-interacting proteins

The interaction of GPX1 with a variety of non-GPX proteins was recently suggested by Wei et al using a protein-protein interaction map, providing an insight into the potential role of GPX1 in previously overlooked pathways. After inputting these proteins, *GPX1* overexpression was associated with overexpression of *POLR2L, HSD17B10, P53, CTSD* and, to a lesser extent, VAMP8 across a range of cancers (figure 3.9). Of these, P53 is the only one to have clear interactions with GPX1 already documented, as unphosphorylated p53 binds to the promoter of *GPX1,* inducing its expression (Hussain et al., 2004; Wu et al., 2017). Overexpression of *GPX1* with *P53* has been documented previously in Giant cell tumor of bone (GCTB) and overexpression of *GPX1* was associated with higher recurrence (Okubo et

al., 2013). It appears that this is perhaps a more common event than previously thought, and that P53 may promote cancer recurrence via *GPX1* across a range of cancers.

A GoPanther analysis was performed to determine if the set of GPX1-interacting proteins had common functions which may be enriched, and only one was identified, leukocyte activation (table 3.1). This was enriched by *CTSD, KARS, TP53, VAMP8* and *RHOA*. As three of these are overexpressed alongside *GPX1* in cancer, leukocyte activation may be promoted in cancers with this expression profile. Leukocyte activation is a known driver of tumour growth, as they infiltrate the TME and produce excessive cytokines to stimulate proliferation (Coussens and Werb, 2002; Korniluk et al., 2016). However, leukocytes also produce large amounts of ROS, which may stimulate *GPX1* expression to compensate and prevent cell death to tumour cells (section 1.4). Whether or not this relationship is, as our current understanding suggests, causative would be an interesting topic for further research.

6.3 Selenium supplementation

6.3.1 Selenium supplementation is an efficient but short-lived way to improve GPX1 production

As a selenoprotein, GPX1 must compete for selenium against other selenoproteins when selenium is not in excess. However, selenium is preferentially used to produce some selenoproteins over others. GPX1 has a low ranking in the selenium hierarchy, meaning it is sparingly expressed when selenium bioavailability is low, which allows higher-ranking selenoproteins to be produced. This system has been exploited in previous experiments using long-term selenium supplement (Na_2SeO_3) to increase GPX1 activity (Hazane-Puch et al., 2013; Hazane-Puch et al., 2014), and here GPX1 protein level was found to increase with supplementation, consistent with this previous data (figure 4.1). These results concur with previous experiments detailing a dose-dependent relationship between selenium and GPX1 production, with a toxic outcome at higher doses. The non-toxic working zone varies between cell types; HaCaTs experience cell death with 10 µM Na_2SeO_3, as also found by Hazane-Puch et al., while HeLa and A431 cells seemed to tolerate higher doses. For future research in new cell types, it is advisable that a range of doses are tested for *GPX1* expression, protein level, and toxicity, to ensure maximum yield of GPX1.

Experiments using selenium supplementation have used long-term supplementation – a minimum of six days - to improve GPX1 production (Rafferty et al., 1998; Meewes et al., 2001; Hazane-Puch et al., 2013; Hazane-Puch et al., 2014). However, there was no indication that this effect would not be attainable in a shorter-term experiment. In fact, Na_2SeO_3

supplementation significantly increased GPX1 protein level after 24 and 96 hours for all cells tested (HaCaT, A431 and HeLa) (figure 4.1). In all cells, there was a larger increase in GPX1 protein level after 96 hours than after 24 hours. In HaCaTs, the peak GPX1 protein level at 96 hours was 29 times the basal expression level, compared with six and three times in HeLa and A431 respectively. While there was a benefit to longer-term supplementation in this experiment, 96 hours of treatment was able to yield significantly more GPX1 and is therefore an acceptable time frame for future experiments.

HaCaTs appeared to be the most sensitive to Na_2SeO_3 supplementation, however, it is important to note that there is no data available to compare the basal level between HaCaT, HeLa and A431 cells. It is possible, particularly given that cancer cells overexpress *GPX1* in the majority of cases (section 3.2.1), that HeLa and A431 cells have a higher basal level of GPX1 than HaCaTs. This would mean that while the increases observed may be lower, the absolute level of GPX1 protein may be higher than this data would suggest. Further investigation using Western blotting could address this gap in knowledge.

Nevertheless, a larger difference in GPX1 protein level was observed than the Hazane-Puch et al. (2014) study would suggest, as while this data indicated a 29-fold increase in protein level in HaCaTs, Hazane-Puch et al. observed that GPX1 activity in these cells increased approximately four-fold. There are a few possible explanations for this discrepancy. Firstly, Hazane-Puch et al did not detail whether there was a withdrawal period between selenium supplementation and GPX activity measurement. As my research indicated, selenium stimulated GPX1 overexpression in HaCaTs is very transient, and dropped by 70% within 24 hours of selenium withdrawal (figure 4.2), and therefore any measurement for activity taken after selenium withdrawal is likely to be depreciated from the peak value. Furthermore, as only two repeats were performed for my data, 29-fold could be an overestimate.

Lastly, Hazane-Puch used the glutathione reductase (GSR)-NADPH method (Flohé and Günzler, 1984) for measuring GPX activity, which is not specific to GPX1. As GPX1 sits at the bottom of the selenium hierarchy, addition of selenium would result in a large change to GPX1 protein level but very little change in expression of higher-ranking GPXs. Therefore, the increase in GPX activity, if measured across all members of the GPX family, would be an underestimate for the change in GPX1 activity. Subsequently, this assay is an unreliable method to measure the change to GPX1, and western blotting likely gives a more accurate account. This large increase seen via Western Blotting indicates that HaCaTs are very sensitive to selenium levels, and that, across all cells, GPX1 level is regulated heavily by

selenium bioavailability. This concurs with previous work which not only suggested response to supplementation is cell-line specific, but also that mRNA level did not necessarily reflect the increase in protein observed after supplementation (Touat-Hamici et al., 2018).

Flow cytometry was also used to measure the response of HeLa cells to selenium supplementation (figure 4.3). This allowed us to not only confirm the increase in GPX1 production seen via Western blotting, but also to observe the homogeneity in GPX1 level across a cell cohort, which has not yet been investigated. Measuring GPX1 level in HeLa indicated a large amount of variance in the protein level within a cohort of cells, both with and without excess selenium available. This suggests that *GPX1* expression and protein level, while greatly influenced by selenium bioavailability, is not solely reliant on it, contrary to the conclusion of Touat-Hamici et al. Instead, it is more likely that supplementation alone does not determine expression level, but rather is further influenced by other factors within the cell and is specific to the individual cell context.

This finding reinforces our growing understanding of GPX1 as a multifaceted signalling protein. While it is well known that GPX1 production is heavily reliant on selenium level (section 1.2.3), its position as a key signalling molecule would necessitate additional regulation of *GPX1* expression by other means. GPX1 is a modulator in many major signalling pathways (section 1.4), including the NF-Kβ AKT/PI3K and MAPK/ERK. *GPX1* expression can be influenced by cross-talk with these pathways, and also by glucose and Ca^{2+} level (Ohdate et al, 2010), oxidative stress (via RAR-related orphan receptor alpha (Han et al., 2014) and zinc-finger protein 143 (Lu et al., 2012)) and shear stress (Takeshita et al., 2000), and is upregulated by p53 (Hussain et al., 2004) and TFAP2C (Kulak et al., 2012) in cancer cells. However, it is important to remember that an increase in mRNA level does not necessarily correspond with an increase in selenoprotein level, as selenium is required for the translation of GPX1 mRNA.

HeLa cells having a large variance in GPX1 level within the cohort fits with our current understanding of the regulation of *GPX1* expression and seems to support the idea that these changes in mRNA level do impact GPX1 production with and without excess selenium. While selenium remains a major influence on *GPX1* expression, these alternative regulatory mechanisms may play major roles also. The effect of certain stresses or transcription factors on *GPX1* expression with and without selenium is yet to be established, although such an investigation would make a valuable addition to our understanding of how impactful each of these mechanisms are. Furthermore, these results only indicate the lack of homogeneity in a

cancerous cell line, and therefore a repeat with a non-cancerous cell line, such as HaCaTs, may show a greater regulation via the selenium hierarchy and minimal regulation by other means, as these are highly sensitive to selenium level.

6.3.2 Na_2SeO_3-induced increases in GPX1 may provide significant protection against chemotherapeutic drugs and H_2O_2

Selenium-stimulated GPX1 protein production has already been proven to protect mammalian cells against UV-induced cell death (Rafferty et al., 1998; Meewes et al., 2001; Baliga et al., 2007; Hazane-Puch et al., 2013). Similar findings have been found in cardiac fibroblasts, where cell death after doxorubicin treatment decreased following Na_2SeO_3 supplementation (Doroshow et al., 2020). In my research, mixed data was generated regarding the protection that Na_2SeO_3 provides against cell death via the chemotherapeutic drugs doxorubicin, docetaxel and cisplatin, and via H_2O_2 (section 4.4). While the XTT assay indicated that supplementation provided significant protection against only H_2O_2, the CyQuant assay did not concur with this, instead showing that only doxorubicin-induced cell death was significantly reduced.

These results were inconsistent, although a result indicating increased resistance to chemotherapy would be expected given the work from Doroshow et al and previous studies linking *GPX1* overexpression to chemoresistance (section 1.4.3). Furthermore, selenium supplementation itself has been shown to increase the risk of high-grade prostate cancer among men with high selenium status (Kristal et al., 2014). However, the present research was largely inconclusive due to the unknown effects of selenium on the XTT assay, which may have given unreliable results, and the transience of the Na_2SeO_3-induced increase in GPX1, which posed technical challenges when performing survival assays while at peak GPX1 level, as will be discussed below. As the effect of selenium supplementation on chemoresistance via GPX1 could have major clinical implications for cancer treatment, further optimisation of these protocols is advisable. A conclusive result may bridge the gap in our understanding of how selenium affects cancer response to treatment via GPX1.

6.3.2.1 Experimental difficulties

There were numerous issues with the XTT experiments performed. It was unclear whether the issues were the result of selenium reactivity with the assay, or with the nature of the assay itself. The XTT assay may not be suitable for this experiment, as it relies upon the redox status of the cell for its measurement, which is being altered by the overexpression of *GPX1* (Scudiero et al., 1988). The XTT assay uses metabolic activity as a proxy for proliferation, and this is measured via the reduction of a tetrazolium salt (figure 6.1). GPX1 levels alter the

redox status of the cell, and the mechanism for peroxide detoxification itself relies upon glutathione reductase (GR) activity to regenerate GSH for this purpose. GR uses NADPH as a proton donor to reduce GSSG into GSH, which is used for the next cycle of detoxification via GPX1. However, the XTT assay also relies upon NADPH/$NADP^+$, as an intermediate compound (phenazine methosulfate; PMS) must be reduced itself by NADPH before reducing the XTT salt, creating the coloured formazan product.

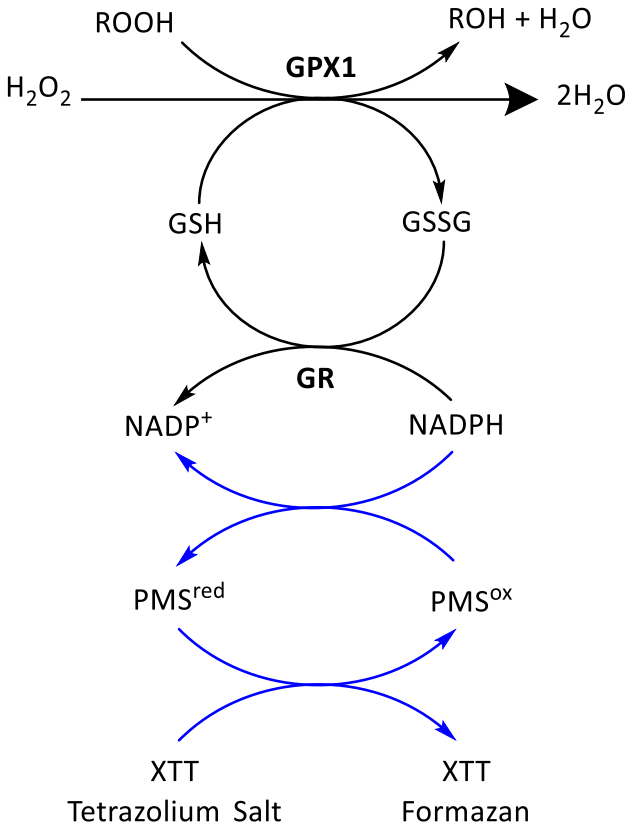

Figure 6.1: Interplay between the GPX1 (black) and XTT (blue) mechanisms*. GPX1 detoxifies peroxides using reduced glutathione (GSH), producing water and, with a lipid peroxide substrate, an alcohol. GSH is regenerated by reducing the GSSG produced from this reaction with NADPH, via GR, leaving oxidised $NADP^+$. NAPDH can also be used to reduce oxidised phenazine methosulfate (PMS), which can in turn reduce the XTT tetrazolium salt to the formazan form.*

Theoretically, as GPX1 activity increases, $NADP^+$ levels increase, leaving less NADPH for the reduction of the XTT salt. This may explain why the XTT data were erratic after supplementation with Na_2SeO_3, especially when supplemented media was not changed before XTT was added, and results indicated all supplemented cells had died. GPX1 activity would be at its peak during this experiment therefore it could easily have prevented XTT

reduction. When media was changed before the measurement, the results were closer to the expected level, although were not fully reliable. As this likely coincides with a drop in GPX1 following selenium withdrawal (section 4.2), this may indeed indicate that significantly increased GPX1 activity disrupts the XTT assay. However, this could also indicate that selenium supplement in the media is the cause of the original anomalous readings. To fully understand this, an experiment should be performed adding XTT and selenium supplement at the final stage, as this would not induce a large change in GPX1 activity, but would allow the reaction, if any, between Na_2SeO_3 and XTT to take place.

6.4 PeroxiPlat and GPX1

As GPX1 has a large influence on cancer progression and patient outcome (section 3.2), there is demand for a selective an effective GPX1 inhibitor. There are a range of inhibitors currently being investigated, although they vary in potency, selectivity and toxicity (section 1.4.3). PeroxiPlat, a luminescent platinum-based compound, is the latest inhibitor to be investigated for this purpose. PeroxiPlat utilises a GSH bioconjugate to replace GSH in the active site and attack the selenenyl sulphide intermediate, creating a covalent Pt-Se bond which irreversibly inhibits the active site. Some of the evidence for this has been established; the Pt-Se bond has been observed via NMR with both selenocysteine and a larger Sec-containing molecule (diphenyl diselenide). Lambda scans of HaCaTs given PeroxiPlat similarly indicated the presence of Sec-bound PeroxiPlat (figure 1.18). Finally, confocal images have also shown PeroxiPlat localising to the peroxisome, where GPX1 can be found (figure 1.19).

6.4.1 PeroxiPlat uptake and interaction with GPX1 remains unclear

While the current data suggests PeroxiPlat does bind to selenocysteine, and can penetrate cells, flow cytometry indicated that the interaction between PeroxiPlat and GPX1 in HeLa cells was, at best, limited (figure 5.1). The vast majority of cells showed no PeroxiPlat present, although a small cluster of events showed a distinct scatter which was largest in the PeroxiPlat-treated and selenium-supplemented group. This could be viewed as evidence of an interaction, as PeroxiPlat detection increased with GPX1 level. However, the number of events was very low, and therefore if it is indeed an event showing PeroxiPlat and GPX1 interaction, it is a rare occurrence. This could also suggest that PeroxiPlat uptake is poor in HeLa cells.

However, this experiment may have reduced uptake compared to a true biological system for many reasons. Firstly, the temperature of the cells was below optimal for uptake, as it was performed at room temperature. Secondly, the PeroxiPlat sample may have degraded in

storage. Furthermore, as HeLa cells are less sensitive to selenium levels than other cell types, and express low GPX1 levels as a baseline, another cell line may be more suitable for this experiment. Not only would the resolution be greater, but the absorbance may improve if there is a greater demand for GSH in the cell from high GPX1 activity.

While there is evidence of PeroxiPlat uptake in HaCaT cells via confocal and lambda scans, it is unclear exactly how successful uptake is. It is also unclear how PeroxiPlat is transported into the cell, as known glutathione transport proteins may not be able to accommodate the PeroxiPlat compound (Nigam et al., 2015), although Organic Anion Transporter 3 has a range of acceptable substrates of varying charge and size (Liu et al., 2016). Inside the cell, GSH must be further trafficked to the peroxisome, although this is also not well understood, and only one known peroxisomal GSH transporter exists in yeast (Elbaz-Alon et al., 2014). Nevertheless, GSH is in high demand, and therefore would have an efficient transport system, of which PeroxiPlat may be able to take advantage.

PeroxiPlat interaction with GPX in a cell-free context is better understood. There is existing evidence of interaction with selenocysteine *in vitro*, which suggests the existence of an interaction. Furthermore, as will be discussed below, PeroxiPlat inhibited GPX in multiple assays after an incubation of just 15 minutes, which further proves that PeroxiPlat targets the active site of bovine GPX (figures 5.2 and 5.4). While this is not human GPX1, the structure is highly conserved between bovine and human GPX1 (see appendix; Toppo et al., 2008), and it is likely PeroxiPlat would interact in an identical manner. The interaction of PeroxiPlat and GPX1 could be further investigated using an ELISA-type pulldown. This experiment was planned to be performed using FLAG-tagged GPX1, however time restrictions prevented this, and the plasmid was never transfected into human cells. This would involve fixing GPX1 to the bottom of a well using FLAG antibodies, before adding PeroxiPlat. After washing, this could then be imaged at the appropriate wavelength to determine whether human GPX1 and PeroxiPlat permanently interact.

6.4.2 Peroxiplat Inhibits GPX1 activity

Previous to this work, inhibition of GPX1 via PeroxiPlat had been predicted but not investigated. As PeroxiPlat was shown to interact with selenocysteine and selenium-containing compounds, it was likely that its interaction with GPX1 would not only be within the active site but would prevent GPX1 activity. Two assays using bovine GPX1 tested the inhibitory potential of PeroxiPlat, and while both indicated that GPX1 was inhibited to some extent, only the GPX assay demonstrated significant inhibition (figure 5.2). However, this

effect may have been underestimated as PeroxiPlat quicky degrades in storage. Furthermore, the FOX assay indicated the GPX samples used contained GSH, which may be competing with PeroxiPlat for GPX (figure 5.4).

In the FOX assay, PeroxiPlat was found to be a fairly weak GPX1 inhibitor; MSA was much more potent than PeroxiPlat. This finding raises concerns over whether PeroxiPlat can match the practicality of other GPX1 inhibitors which have been developed or are undergoing the development process. While MSA is widely used, many of the other GPX1 inhibitors, such as the pentathiepins, are up to 15 times more potent than MSA (section 1.4.3.2). PeroxiPlat is therefore unlikely to exceed the value of existing inhibitors for use on pure GPX1.

However, PeroxiPlat does have the advantage of potentially having high GPX1 selectivity, which is a substantial challenge in developing GPX1 inhibitor. As GPX1 belongs to a family of GPX proteins with highly conserved structural homology, many existing inhibitors have difficulty in reducing off-target effects. MeHg (section 1.4.3.3) targets thiols and selenols, which reduces both GSH availability for use as a GPX1 substrate and inhibits GPX1 activity by directly altering the active site (Fujimura and Usuki, 2020). However, this also affects other selenoproteins and GSH-dependent processes, and so has little GPX1 selectivity. Although it targets the GPX1 active site, MSA also binds with GPX2 and GPX3 in the same manner as with GPX1 (Lubos et al., 2011).

Some inhibitors have overcome this issue of selectivity, however. Perhaps the most selective are Peptide-Au clusters, which were developed using molecular dynamics to use hydrogen binds, hydrophobic interactions and salt bridges to sit within the cleft of the tetrameric GPX1, offering tailor-made inhibition of GPX1 (Liu et al., 2017). One pentathiepin compound was found to be highly selective for GPX1 over other selenoproteins, however no GPX family proteins were tested, and so its true selectivity is unknown (Behnisch-Cornwell et al., 2020). The confocal imaging performed previously does indicate that PeroxiPlat is selective for GPX1, as it accumulates only in the peroxisome, where no other member of the GPX family is known to localise. This could be further investigated using FLAG-tagged GPX1 as mentioned previously, to match the localisation of GPX1 with that of PeroxiPlat on a confocal microscope.

7. Conclusions and Future Work

This study examined GPX1 from multiple perspectives, in order to better understand its role in cancer, and assess the efficacy of a novel photolumiscent compound, PeroxiPlat, as a potential theranostic agent in cancer. GPX1 has been identified as a driver of cancer aggression and drug resistance, and thus further exploration of the role of GPX1 in cancer, and how GPX1 can be inhibited, is necessary. This work combined bioinformatic analysis of vast cancer databases; cell culture, drug treatment and survival assays of a range of cell lines – cancerous and non-cancerous; and biochemical and cell-based assays looking specifically at GPX1 and Peroxiplat. Each arm of this research has its own specific aims, which overall improve our understanding of how GPX1 might impact cancer and how PeroxiPlat may be utilised in this context.

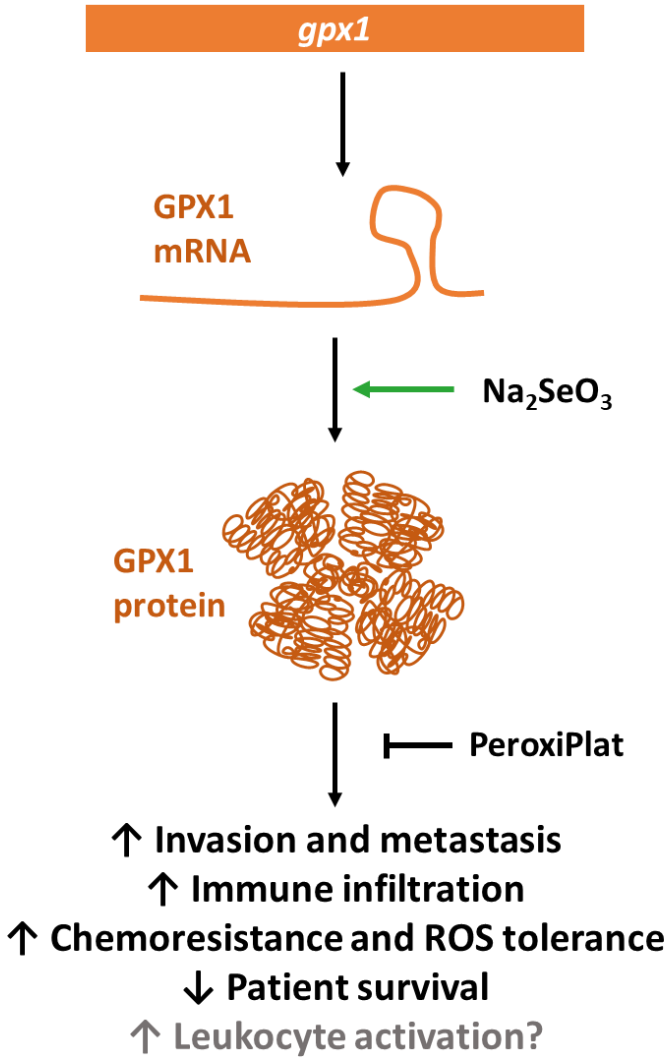

Figure 7.1: Process and manipulation of GPX1 protein production, and the effects on the progression and prognosis of cancer.

The finding that *GPX1* is overexpressed across the majority of cancer types confirms that GPX1 is a valuable subject of research, as findings can be widely applied to many cancer types (section 3.2). Furthermore, *GPX1* expression is associated with significantly lower overall survival in UVM, LGG, KICH and LAML patients and significantly lower disease-free survival in ACC and LGG patients. This cements GPX1 as a protein of concern with regards to cancer progression across a range of cancer types. CESC identified itself as a cancer cell type of interest as it not only showed the opposite trend of increased patient survival with high *GPX1* expression (figure 3.6) but was also the only cell type to show consistent positive correlation between *GPX1* expression and drug resistance across docetaxel, cisplatin and doxorubicin using data from GDSC (section 3.4).

However, the work using GDSC may be fundamentally flawed as this research also shows that cells are highly sensitive to selenium levels in the culture medium, and protein level is regulated at the translation level as well as at the transcriptional level (section 4.2). This work therefore cannot be used disprove the accepted view that high GPX1 activity increases resistance to chemotherapeutic drugs (section 1.4.3). Instead, further research should be performed capturing GPX1 protein level and IC_{50} within one experiment. This would be vital work as it could identify cancer types which are more likely to be successfully targeted for cell death using a GPX1 inhibitor and may potentially create an opportunity for more successful treatment plans to be created for GPX-rich cancer patients by avoiding the use of particular drugs.

Na_2SeO_3 was effective at increasing GPX1 protein level across all cell types tested (HaCaT, A431 and HeLa), with HaCaT being by far the most sensitive to treatment (section 4.2). HaCaTs cells experienced a 29-fold increase in GPX1 protein level, well over the previously reported four-fold increase in GPX1 mRNA under the same conditions (Hazane-Puch et al., 2014). This increase was also short-lived, with the GPX1 level dropping by 70% within the first 24 hours of Na_2SeO_3 withdrawal (section 4.3). Na_2SeO_3 supplementation has revealed itself to be a useful tool for significantly increasing GPX1 levels *in vitro*, but the newly discovered transience of this effect will inform future experiments, ensuring that supplementation is not withdrawn long before measurements are taken.

Similarly, from the survival assays performed, it remains unclear to what extent Na_2SeO_3-induced increases in GPX1 protect against chemotherapeutic drugs. Both assays indicated increased resistance to different agents. While the XTT assay indicated that Na_2SeO_3-induced GPX1 production provided significant protection against H_2O_2 only, whereas the CyQuant

assay showed protection against doxorubicin only (section 4.4). As the XTT assay may have been impacted by the change in redox within the cell or the selenium supplement, and the CyQuant assay had no biological repeats, these results are fairly inconclusive. However, given the previous findings that increased *GPX1* activity promotes chemoresistance in other cell lines (Gouazé et al., 2001; Gan et al., 2014; Chen et al., 2019), further repeats using CyQuant or another survival assay would likely confirm that selenium-induced *GPX1* overexpression decreases cell death in response to treatment with chemotherapeutic agents. This remains a subject of interest, as determining which drugs are effective in GPX1-rich may allow us to improve the treatment efficacy of patients with high GPX1, which, as discussed, suffer low prognoses in many cancer types.

GPX4 was the only member of the GPX family to be consistently overexpressed with *GPX1* overexpression, according to GEPIA data (section 3.3). As both are involved in resistance to cell death, I predict that this may aid *GPX1*- and *GPX4*-overexpressing cancers in reducing the effectiveness of chemotherapeutic agents or agents targeting the ferroptotic system. Such a hypothesis could be easily investigated in further experiments by using drugs to initiate cell death by apoptosis and ferroptosis and manipulating the levels of GPX1 and/or GPX4 by, for example, RNAi, to observe whether the chemoresistant effect is compounded. As ferroptosis is an emerging area of research in cancer therapy (Wang, 2021), understanding the interplay between these GPX proteins is critical for optimising the success of ferroptosis therapies and understanding potential side effects of GPX4 manipulation.

Heatmaps also indicated that for *POLR2L*, *HSD17B10*, *P53* and *CTSD*, expression increased with *GPX1* expression across most cancer types (section 3.3). Apart from *P53*, which directly upregulates *GPX1* (Hussain et al., 2004; Wu et al., 2017), the link between GPX1 and these interacting proteins is uncertain, however, many of these were identified as being involved in leukocyte activation via GoPanther. This information led to the conclusion that some cancer-promoting effects of GPX1, such as immune infiltration (section 1.4.2.2), may be compounded in patients with these expression profiles. The link between many of the other proteins and GPX1, and how they interact in the context of cancer, requires further investigation, as treatments targeting GPX1 may have unexpected side effects due to these proteins. The role of GPX1 as a modulator in many pathways is still being explored, and continuation of this work will likely reveal how these proteins are related and further inform our treatment of GPX1-rich cancers.

GPX1 mutational mapping was inconsistent between databases (section 3.6). While COSMIC data showed a hotspot of mutation at P77R, this was not confirmed using the ICGC and GDC data portals. It was revealed that almost half of the entries containing the P77R appeared to come from one experimental source working with NSCLCs, and thus this may be a more prevalent mutation in this type of cancer than in others. Ensembl analysis indicated this would likely be a deleterious mutation, and as it sits in a loop responsible for tetramerization, the effects may change the structure and function of GPX1. If it can be verified as a common mutation in NSCLCs, this would therefore be an interesting GPX1 mutant to investigate, for example by site-directed mutagenesis, and may tell us more about the structure of GPX1 as well as the function of this variant in NSCLCs.

PeroxiPlat was investigated as a potential theranostic agent for use in cancer cells, as it theoretically would have the ability to fluorescently label and inhibit GPX1, providing a diagnostic and prognostic insight for GPX1-rich cancers, as well as a method of treatment for these more aggressive and chemoresistant cancers. Previous confocal imaging indicates PeroxiPlat can penetrate cells (figure 1.19), and flow cytometry may support this (section 5.2), although it appears to be poorly absorbed in HeLa cells. This poses challenges for diagnostic use, as the uptake would likely be too low to determine whether cells contain high GPX1 levels and inform treatment. However, it is also possible that conditions for uptake were sub-optimal, and different temperatures, fresher PeroxiPlat and increased GPX1 activity may improve absorption of PeroxiPlat. Repeating this experiment with HaCaT cells in optimum conditions may therefore yield more concrete results.

Overall, this work shows that the clinical potential of PeroxiPlat is limited. From our experiments, we can determine that Peroxiplat is an inhibitor of GPX1, although it has low efficacy. Experiments in cell-free assays indicated a weak inhibitory effect of PeroxiPlat (section 6.4.2), which was far lower than that of the existing inhibitor MSA (Behnisch-Cornwell et al., 2019). As some existing inhibitors exceed MSA in GPX1 IC_{50} (section 1.4.3), PeroxiPlat is one of the least potent GPX inhibitors available. However, as discussed, PeroxiPlat is more likely to offer selective inhibition than many existing inhibitors, as it localises to the peroxisome, where GPX1 is usually located. This therefore suggests that PeroxiPlat has potential applications in GPX1- and ROS-related research which other inhibitors do not. Not only can PeroxiPlat fluorescently label GPX1, but it can also provide a small level of inhibition to GPX1 only, which may inform our understanding of GPX family members' ability to compensate for one another, and of the role of GPX1 in redox signalling and in the development of cancer.

8. Overall conclusions

This work adds to the evidence cementing GPX1 as a major protein in cancer development and progression. In this research, both *GPX1* expression and protein level have been found to be very influential for determining cancer outcomes and resistance to treatment, across a range of cancer cell types. Furthermore, it was found that proteins associated with GPX1 have similar expression patterns, and this may compound these effects, thereby highlighting the importance of GPX1 as a modulator through the regulation of H_2O_2, and its influence in many networks. While this data concludes that GPX1 is a strong target for inhibition, a potent inhibitor of GPX1 has not yet been found. However, as Peroxiplat can label and inhibit GPX1 in some conditions, it will likely be useful in future research to determine the full effects of GPX1 in cancer. Overall, this work has opened avenues to investigate specific cell lines which appear to be more sensitive to high levels of *GPX1* expression, and to understand the interactions of GPX1 which influence cancer. Finally, it given insight into how we might inhibit and monitor GPX1, which will inform our future research as we continue to develop a cancer treatment using GPX1 as a target.

9. References

Ali, SF., Le Bel, CP., Bondy, SC., 1992 Reactive oxygen species formation as a biomarker of methylmercury and trimethyltin neurotoxicity. *Neurotoxicology*. 13(3), pp.637-48.

Antunes, F., Han, D. and Cadenas, E., 2002. Relative contributions of heart mitochondria glutathione peroxidase and catalase to H2O2 detoxification in in vivo conditions. *Free Radical Biology and Medicine*, 33(9), pp.1260-1267.

Aoyama, K. and Nakaki, T. (2012). Inhibition of GTRAP3-18 May Increase Neuroprotective Glutathione (GSH) Synthesis. International Journal of Molecular Sciences, 13(12), pp.12017–12035.

Arsova-Sarafinovska, Z., Matevska, N., Eken, A., Petrovski, D., Banev, S., Dzikova, S., Georgiev, V., Sikole, A., Erdem, O., Sayal, A., Aydin, A. and Dimovski, A., 2008. Glutathione peroxidase 1 (GPX1) genetic polymorphism, erythrocyte GPX activity, and prostate cancer risk. *International Urology and Nephrology*, 41(1), pp.63-70.

Baliga, M., Wang, H., Zhuo, P., Schwartz, J. and Diamond, A., 2007. Selenium and GPx-1 overexpression protect mammalian cells against UV-induced DNA damage. *Biological Trace Element Research*, 115(3), pp.227-241.

Baliga, M., Wang, H., Zhuo, P., Schwartz, J. and Diamond, A., 2007. Selenium and GPx-1 overexpression protect mammalian cells against UV-induced DNA damage. Biological Trace Element Research, 115(3), pp.227-241.

Bănescu, C., Iancu, M., Trifa, A., Cândea, M., Benedek Lazar, E., Moldovan, V., Duicu, C., Tripon, F., Crauciuc, A. and Dobreanu, M., 2016. From Six Gene Polymorphisms of the Antioxidant System, Only GPX Pro198Leu and GSTP1 Ile105Val Modulate the Risk of Acute Myeloid Leukemia. *Oxidative Medicine and Cellular Longevity*, 2016, pp.1-10.

Baş, E. and Naziroğlu, M., 2019. Selenium attenuates docetaxel-induced apoptosis and mitochondrial oxidative stress in kidney cells. Anti-Cancer Drugs, 30(4), pp.339-346.

Basnet, H., Tian, L., Ganesh, K., Huang, Y., Macalinao, D., Brogi, E., Finley, L. and Massagué, J., 2019. Flura-seq identifies organ-specific metabolic adaptations during early metastatic colonization. *eLife*, 8(e43627).

Beck, T., Boumber, Y., Aggarwal, C., Pei, J., Thrash-Bingham, C., Fittipaldi, P., Vlasenkova, R., Rao, C., Borghaei, H., Cristofanilli, M., Mehra, R., Serebriiskii, I. and Alpaugh, R., 2019. Circulating tumor cell and cell-free RNA capture and expression analysis identify platelet-associated genes in metastatic lung cancer. *BMC Cancer*, 19(603).

Bedard, K. and Krause, K., 2007. The NOX Family of ROS-Generating NADPH Oxidases: Physiology and Pathophysiology. *Physiological Reviews*, 87(1), pp.245-313.

Beg, A. and Baldwin, A., 1993. The I kappa B proteins: multifunctional regulators of Rel/NF-kappa B transcription factors. *Genes & Development*, 7(11), pp.2064-2070.

Behnisch-Cornwell, S., Bandaru, S., Napierkowski, M., Wolff, L., Zubair, M., Urbainsky, C., Lillig, C., Schulzke, C. and Bednarski, P., 2020. Pentathiepins: A Novel Class of Glutathione Peroxidase 1 Inhibitors that Induce Oxidative Stress, Loss of Mitochondrial Membrane Potential and Apoptosis in Human Cancer Cells. *ChemMedChem*, 15(16), pp.1515-1528.

Behnisch-Cornwell, S., Laubenstein, G. and Bednarski, P., 2019. Studies of the inhibitory activities of tiopronin and mercaptosuccinic acid on glutathione peroxidase and their cytotoxic and antioxidant properties. *Die Pharmazie*, 74(9), pp.536-542.

Bermano, G., Nicol, F., Dyer, J., Sunde, R., Beckett, G., Arthur, J. and Hesketh, J., 1996. Selenoprotein gene expression during selenium-repletion of selenium-deficient rats. *Biological Trace Element Research*, 51(3), pp.211-223.

Berry, M., 2005. Insights into the hierarchy of selenium incorporation. *Nature Genetics*, 37(11), pp.1162-1163.

Berry, M., Banu, L., Chen, Y., Mandel, S., Kieffer, J., Harney, J. and Larsen, P. (1991). Recognition of UGA as a selenocysteine codon in Type I deiodinase requires sequences in the 3' untranslated region. *Nature*, 353(6341), pp.273-276.

Bienert, G., Møller, A., Kristiansen, K., Schulz, A., Møller, I., Schjoerring, J. and Jahn, T., 2006. Specific Aquaporins Facilitate the Diffusion of Hydrogen Peroxide across Membranes. *Journal of Biological Chemistry*, 282(2), pp.1183-1192.

Bjornstedt, M., Xue, J., Huang, W., Akesson, B. and Holmgren, A., 1994. The Thioredoxin and Glutaredoxin Systems Are Efficient Electron Donors to Human Plasma Glutathione Peroxidase. *Journal of Biological Chemistry*, 269(47), pp.29382-29384.

Blum, R. and Kloog, Y., 2014. Metabolism addiction in pancreatic cancer. *Cell Death & Disease*, 5(2), pp.e1065-e1065.

Bozinovski, S., Seow, H., Crack, P., Anderson, G. and Vlahos, R., 2012. Glutathione Peroxidase-1 Primes Pro-Inflammatory Cytokine Production after LPS Challenge In Vivo. *PLoS ONE*, 7(3), pp.e33172.

Breen, A. and Murphy, J., 1995. Reactions of oxyl radicals with DNA. *Free Radical Biology and Medicine*, 18(6), pp.1033-1077.

Breitzig, M., Bhimineni, C., Lockey, R. and Kolliputi, N., 2016. 4-Hydroxy-2-nonenal: a critical target in oxidative stress?. *American Journal of Physiology-Cell Physiology*, 311(4), pp.C537-C543.

Brigelius-Flohé, R. and Kipp, A., 2009. Glutathione peroxidases in different stages of carcinogenesis. *Biochimica et Biophysica Acta (BBA) - General Subjects*, 1790(11), pp.1555-1568.

Brigelius-Flohé, R. and Maiorino, M. (2013). Glutathione peroxidases. *Biochimica et Biophysica Acta (BBA) - General Subjects*, 1830(5), pp.3289-3303.

Bubenik, J. and Driscoll, D., 2007. Altered RNA Binding Activity Underlies Abnormal Thyroid Hormone Metabolism Linked to a Mutation in Selenocysteine Insertion Sequence-binding Protein 2. *Journal of Biological Chemistry*, 282(48), pp.34653-34662.

Budiman, M., Bubenik, J., Miniard, A., Middleton, L., Gerber, C., Cash, A. and Driscoll, D., 2009. Eukaryotic Initiation Factor 4a3 Is a Selenium-Regulated RNA-Binding Protein that Selectively Inhibits Selenocysteine Incorporation. *Molecular Cell*, 35(4), pp.479-489.

Caban, K. and Copeland, P., 2012. Selenocysteine Insertion Sequence (SECIS)-binding Protein 2 Alters Conformational Dynamics of Residues Involved in tRNA Accommodation in 80 S Ribosomes. *Journal of Biological Chemistry*, 287(13), pp.10664-10673.

Caban, K., Kinzy, S. and Copeland, P., 2007. The L7Ae RNA Binding Motif Is a Multifunctional Domain Required for the Ribosome-Dependent Sec Incorporation Activity of Sec Insertion Sequence Binding Protein 2. *Molecular and Cellular Biology*, 27(18), pp.6350-6360.

Cao, M., Mu, X., Jiang, C., Yang, G., Chen, H. and Xue, W., 2013. Single-nucleotide polymorphisms of GPX1 and MnSOD and susceptibility to bladder cancer: a systematic review and meta-analysis. *Tumor Biology*, 35, pp.759-764.

Cardoso, F., van't Veer, L., Bogaerts, J., Slaets, L., Viale, G., Delaloge, S., Pierga, J., Brain, E., Causeret, S., DeLorenzi, M., Glas, A., Golfinopoulos, V., Goulioti, T., Knox, S., Matos, E., Meulemans, B., Neijenhuis, P., Nitz, U., Passalacqua, R., Ravdin, P., Rubio, I., Saghatchian, M.,

Smilde, T., Sotiriou, C., Stork, L., Straehle, C., Thomas, G., Thompson, A., van der Hoeven, J., Vuylsteke, P., Bernards, R., Tryfonidis, K., Rutgers, E. and Piccart, M., 2016. 70-Gene Signature as an Aid to Treatment Decisions in Early-Stage Breast Cancer. *New England Journal of Medicine*, 375(8), pp.717-729.

Carvalho, C., Chew, E., Hashemy, S., Lu, J. and Holmgren, A., 2008. Inhibition of the Human Thioredoxin System. *Journal of Biological Chemistry*, 283(18), pp.11913-11923.

Chan, W., Chen, B., Wang, L., Taghizadeh, K., Demott, M. and Dedon, P., 2010. Quantification of the 2-Deoxyribonolactone and Nucleoside 5'-Aldehyde Products of 2-Deoxyribose Oxidation in DNA and Cells by Isotope-Dilution Gas Chromatography Mass Spectrometry: Differential Effects of γ-Radiation and Fe2+−EDTA. *Journal of the American Chemical Society*, 132(17), pp.6145-6153.

Chaudiere, J. and L. Tappel, A., 1984. Interaction of Gold(I) with the Active Site of Selenium-Glutathione Peroxidase. *Journal of Inorganic Biochemistry*, 20(4), pp.313-325.

Chaudiere, J., Wilhelmsen, E. and Tappel, A., 1984. Mechanism of selenium-glutathione peroxidase and its inhibition by mercaptocarboxylic acids and other mercaptans. *Journal of Biological Chemistry*, 259(2), pp.1043-1050.

Chen, B., Shen, Z., Wu, D., Xie, X., Xu, X., Lv, L., Dai, H., Chen, J. and Gan, X., 2019. Glutathione Peroxidase 1 Promotes NSCLC Resistance to Cisplatin via ROS-Induced Activation of PI3K/AKT Pathway. *BioMed Research International*, 2019(7640547).

Chen, G., Wang, H., Miller, C., Thomas, D., Gharib, T., Misek, D., Giordano, T., Orringer, M., Hanash, S. and Beer, D., 2004. Reduced selenium-binding protein 1 expression is associated with poor outcome in lung adenocarcinomas. *The Journal of Pathology*, 202(3), pp.321-329.

Chen, J., Cao, Q., Qin, C., Shao, P., Wu, Y., Wang, M., Zhang, Z. and Yin, C., 2011. GPx-1 polymorphism (rs1050450) contributes to tumor susceptibility: evidence from meta-analysis. *Journal of Cancer Research and Clinical Oncology*, 137(10), pp.1553-1561.

Chen, S., Su, X., Mi, H., Dai, X., Li, S., Chen, S. and Zhang, S., 2020. Comprehensive analysis of glutathione peroxidase-1 (GPX1) expression and prognostic value in three different types of renal cell carcinoma. *Translational Andrology and Urology*, 9(6), pp.2737-2750.

Chen, X., Kang, R., Kroemer, G. and Tang, D., 2021. Broadening horizons: the role of ferroptosis in cancer. Nature Reviews Clinical Oncology, 18(5), pp.280-296.

Cheng, Q. and Arnér, E., 2017. Selenocysteine Insertion at a Predefined UAG Codon in a Release Factor 1 (RF1)-depletedEscherichia coliHost Strain Bypasses Species Barriers in Recombinant Selenoprotein Translation. *Journal of Biological Chemistry*, 292(13), pp.5476-5487.

Cheng, W., Ho, Y., Valentine, B., Ross,, D., Combs, G. and Lei, X., 1998. Cellular Glutathione Peroxidase Is the Mediator of Body Selenium To Protect against Paraquat Lethality in Transgenic Mice. *The Journal of Nutrition*, 128(7), pp.1070-1076.

Chraa, D., Naim, A., Olive, D. and Badou, A., 2018. T lymphocyte subsets in cancer immunity: Friends or foes. *Journal of Leukocyte Biology*, 105(2), pp.243-255.

Christophersen, B., 1969. Reduction of X-ray-induced DNA and thymine hydroperoxides by rat liver glutathione peroxidase. *Biochimica et Biophysica Acta (BBA) - Nucleic Acids and Protein Synthesis*, 186(2), pp.387-389.

Chu, F., Esworthy, R., Chu, P., Longmate, J., Huycke, M., Wilczynski, S. and Doroshow, J., 2004. Bacteria-Induced Intestinal Cancer in Mice with Disrupted Gpx1 and Gpx2 Genes. *Cancer Research*, 64(3), pp.962-968.

Cieślik, M. and Chinnaiyan, A., 2017. Cancer transcriptome profiling at the juncture of clinical translation. Nature Reviews Genetics, 19(2), pp.93-109.

Cipolla, C. and Lodhi, I., 2017. Peroxisomal Dysfunction in Age-Related Diseases. *Trends in Endocrinology & Metabolism*, 28(4), pp.297-308.

Clayton, E., Pujol, T., McDonald, J. and Qiu, P., 2020. Leveraging TCGA gene expression data to build predictive models for cancer drug response. BMC Bioinformatics, 21(364).

Coogan, M.P., Allinson, S.L., Kania, D.M., Farrow, C.M.A., Harmer, J. and Steel, H.L. (2021) Imaging agent. US202108852

Cook, P., Ju, B., Telese, F., Wang, X., Glass, C. and Rosenfeld, M. (2009). Tyrosine dephosphorylation of H2AX modulates apoptosis and survival decisions. *Nature*, 458(7238), pp.591-596.

Copeland, P., Stepanik, V. and Driscoll, D., 2001. Insight into Mammalian Selenocysteine Insertion: Domain Structure and Ribosome Binding Properties of Sec Insertion Sequence Binding Protein 2. *Molecular and Cellular Biology*, 21(5), pp.1491-1498.

Coussens, L. and Werb, Z., 2002. Inflammation and cancer. *Nature*, 420(6917), pp.860-867.

Cozza, G., Rossetto, M., Bosello-Travain, V., Maiorino, M., Roveri, A., Toppo, S., Zaccarin, M., Zennaro, L. and Ursini, F., 2017. Glutathione peroxidase 4-catalyzed reduction of lipid hydroperoxides in membranes: The polar head of membrane phospholipids binds the enzyme and addresses the fatty acid hydroperoxide group toward the redox center. *Free Radical Biology and Medicine*, 112(2017), pp.1-11.

Cui, J., Zheng, L., Zhang, Y. and Xue, M., 2021. Bioinformatics analysis of DNMT1 expression and its role in head and neck squamous cell carcinoma prognosis. *Scientific Reports*, 11(2267).

Cullen, J., Mitros, F. and Oberley, L., 2003. Expression of Antioxidant Enzymes in Diseases of the Human Pancreas: Another Link Between Chronic Pancreatitis and Pancreatic Cancer. *Pancreas*, 26(1), pp.23-27.

Dai, D., Gan, W., Hayakawa, H., Zhu, J., Zhang, X., Hu, G., Xu, T., Jiang, Z., Zhang, L., Hu, X., Nie, B., Zhou, Y., Li, J., Zhou, X., Li, J., Zhang, T., He, Q., Liu, D., Chen, H., Yang, N., Zuo, P., Zhang, Z., Yang, H., Wang, Y., Wilson, S., Zeng, Y., Wang, J., Sekiguchi, M. and Cai, J., 2018. Transcriptional mutagenesis mediated by 8-oxoG induces translational errors in mammalian cells. *Proceedings of the National Academy of Sciences*, 115(16), pp.4218-4222.

Dalleau, S., Baradat, M., Guéraud, F. and Huc, L., 2013. Cell death and diseases related to oxidative stress:4-hydroxynonenal (HNE) in the balance. *Cell Death & Differentiation*, 20(12), pp.1615-1630.

De Duve, C. and Baudhuin, P. (1966). Peroxisomes (microbodies and related particles). *Physiological Reviews*, 46(2), pp.323-357.

de Haan, J., Bladier, C., Griffiths, P., Kelner, M., O'Shea, R., Cheung, N., Bronson, R., Silvestro, M., Wild, S., Zheng, S., Beart, P., Hertzog, P. and Kola, I., 1998. Mice with a Homozygous Null Mutation for the Most Abundant Glutathione Peroxidase, Gpx1, Show Increased Susceptibility to the Oxidative Stress-inducing Agents Paraquat and Hydrogen Peroxide. *Journal of Biological Chemistry*, 273(35), pp.22528-22536.

de Haan, J., Bladier, C., Lotfi-Miri, M., Taylor, J., Hutchinson, P., Crack, P., Hertzog, P. and Kola, I., 2004. Fibroblasts derived from Gpx1 knockout mice display senescent-like features and are susceptible to H2O2-mediated cell death. *Free Radical Biology and Medicine*, 36(1), pp.53-64.

de Oliveira-Marques, V., Cyrne, L., Marinho, H. and Antunes, F., 2007. A Quantitative Study of NF-κB Activation by H2O2: Relevance in Inflammation and Synergy with TNF-α. *The Journal of Immunology*, 178(6), pp.3893-3902.

Devadas, S., Zaritskaya, L., Rhee, S., Oberley, L. and Williams, M., 2002. Discrete Generation of Superoxide and Hydrogen Peroxide by T Cell Receptor Stimulation:selective regulation of mitogen-activated protein kinase activation and fas ligand expression. *Journal of Experimental Medicine*, 195(1), pp.59-70.

Di Cosmo, C., McLellan, N., Liao, X., Khanna, K., Weiss, R., Papp, L. and Refetoff, S., 2009. Clinical and Molecular Characterization of a Novel Selenocysteine Insertion Sequence-Binding Protein 2 (SBP2) Gene Mutation (R128X). *The Journal of Clinical Endocrinology & Metabolism*, 94(10), pp.4003-4009.

Dittrich, A., Meyer, H., Krokowski, M., Quarcoo, D., Ahrens, B., Kube, S., Witzenrath, M., Esworthy, R., Chu, F. and Hamelmann, E., 2009. Glutathione peroxidase-2 protects from allergen-induced airway inflammation in mice. *European Respiratory Journal*, 35(5), pp.1148-1154.

Donovan, J. and Copeland, P., 2010. Threading the Needle: Getting Selenocysteine Into Proteins. *Antioxidants & Redox Signaling*, 12(7), pp.881-892.

Doroshow, J. and Juhasz, A., 2019. Modulation of selenium-dependent glutathione peroxidase activity enhances doxorubicin-induced apoptosis, tumour cell killing and hydroxyl radical production in human NCI/ADR-RES cancer cells despite high-level P-glycoprotein expression. *Free Radical Research*, 53(8), pp.882-891.

Doroshow, J., Esworthy, R. and Chu, F., 2020. Control of doxorubicin-induced, reactive oxygen-related apoptosis by glutathione peroxidase 1 in cardiac fibroblasts. *Biochemistry and Biophysics Reports*, 21(2020), p.100709.

Elbaz-Alon, Y., Morgan, B., Clancy, A., Amoako, T., Zalckvar, E., Dick, T., Schwappach, B. and Schuldiner, M., 2014. The yeast oligopeptide transporter Opt2 is localized to peroxisomes and affects glutathione redox homeostasis. FEMS Yeast Research, 14(7), pp.1055-1067.

Epp, O., Ladenstein, R. and Wendel, A., 1983. The Refined Structure of the Selenoenzyme Glutathione Peroxidase at 0.2-nm Resolution. *European Journal of Biochemistry*, 133(1), pp.51-69.

Esposito, L., Kokoszka, J., Waymire, K., Cottrell, B., MacGregor, G. and Wallace, D., 2000. Mitochondrial oxidative stress in mice lacking the glutathione peroxidase-1 gene. *Free Radical Biology and Medicine*, 28(5), pp.754-766.

Fagegaltier, D., 2000. Characterization of mSelB, a novel mammalian elongation factor for selenoprotein translation. *The EMBO Journal*, 19(17), pp.4796-4805.

Fang, W., Goldberg, M., Pohl, N., Bi, X., Tong, C., Xiong, B., Koh, T., Diamond, A. and Yang, W., 2010. Functional and physical interaction between the selenium-binding protein 1 (SBP1) and the glutathione peroxidase 1 selenoprotein. *Carcinogenesis*, 31(8), pp.1360-1366.

Faucher, K., Rabinovitch-Chable, H., Cook-Moreau, J., Barrière, G., Sturtz, F. and Rigaud, M., 2005. Overexpression of human GPX1 modifies Bax to Bcl-2 apoptotic ratio in human endothelial cells. *Molecular and Cellular Biochemistry*, 277(1-2), pp.81-87.

Feng, Y., Santoriello, C., Mione, M., Hurlstone, A. and Martin, P., 2010. Live Imaging of Innate Immune Cell Sensing of Transformed Cells in Zebrafish Larvae: Parallels between Tumor Initiation and Wound Inflammation. *PLoS Biology*, 8(12), p.e1000562.

Fernández-Moreira, V., Thorp-Greenwood, F. and Coogan, M., 2010. Application of d6 transition metal complexes in fluorescence cell imaging. *Chem. Commun.*, 46(2), pp.186-202.

Flohé, L. and Günzler, W., 1984. [12] Assays of glutathione peroxidase. *Methods in Enzymology*, pp.114-120.

Florian, S., Krehl, S., Loewinger, M., Kipp, A., Banning, A., Esworthy, S., Chu, F. and Brigelius-Flohé, R., 2010. Loss of GPx2 increases apoptosis, mitosis, and GPx1 expression in the intestine of mice. *Free Radical Biology and Medicine*, 49(11), pp.1694-1702.

Forcina, G. and Dixon, S., 2019. GPX4 at the Crossroads of Lipid Homeostasis and Ferroptosis. *Proteomics*, 19(18), pp.1800311.

Forsberg, L., de Faire, U., Marklund, S., Andersson, P., Stegmayr, B. and Morgenstern, R., 2000. Phenotype Determination of a Common Pro-Leu Polymorphism in Human Glutathione Peroxidase 1. *Blood Cells, Molecules, and Diseases*, 26(5), pp.423-426.

Franco, J., Posser, T., Dunkley, P., Dickson, P., Mattos, J., Martins, R., Bainy, A., Marques, M., Dafre, A. and Farina, M., 2009. Methylmercury neurotoxicity is associated with inhibition of the antioxidant enzyme glutathione peroxidase. *Free Radical Biology and Medicine*, 47(4), pp.449-457.

Fransen, M., Nordgren, M., Wang, B. and Apanasets, O., 2012. Role of peroxisomes in ROS/RNS-metabolism: Implications for human disease. *Biochimica et Biophysica Acta (BBA) - Molecular Basis of Disease*, 1822(9), pp.1363-1373.

Fridman, W., Pagès, F., Sautès-Fridman, C. and Galon, J., 2012. The immune contexture in human tumours: impact on clinical outcome. *Nature Reviews Cancer*, 12(4), pp.298-306.

Fu, Y., Cheng, W., Porres, J., Ross, D. and Lei, X., 1999. Knockout of cellular glutathione peroxidase gene renders mice susceptible to diquat-induced oxidative stress. *Free Radical Biology and Medicine*, 27(5-6), pp.605-611.

Fujimura, M. and Usuki, F., 2020. Methylmercury-Mediated Oxidative Stress and Activation of the Cellular Protective System. *Antioxidants*, 9(10), pp.1004.

Gabaldón, T. (2010). Peroxisome diversity and evolution. *Philosophical Transactions of the Royal Society B: Biological Sciences*, 365(1541), pp.765-773.

Galasso, G., Schiekofer, S., Sato, K., Shibata, R., Handy, D., Ouchi, N., Leopold, J., Loscalzo, J. and Walsh, K., 2006. Impaired Angiogenesis in Glutathione Peroxidase-1–Deficient Mice Is Associated With Endothelial Progenitor Cell Dysfunction. *Circulation Research*, 98(2), pp.254-261.

Gan, X., Chen, B., Shen, Z., Liu, Y., Li, H., Xie, X., Xu, X., Li, H., Huang, Z. and Chen, J., 2014. High GPX1 expression promotes esophageal squamous cell carcinoma invasion, migration, proliferation and cisplatin-resistance but can be reduced by vitamin D. *International Journal of Clinincal and Experimental Medicine*, 7(9), pp.2530-2540.

Giesing, M., Driesel, G., Molitor, D. and Suchy, B., 2012. Molecular phenotyping of circulating tumour cells in patients with prostate cancer: prediction of distant metastases. *BJU International*, 110(11c), pp.E1202-E1211.

Giesing, M., Suchy, B., Driesel, G. and Molitor, D., 2010. Clinical utility of antioxidant gene expression levels in circulating cancer cell clusters for the detection of prostate cancer in patients with prostate-specific antigen levels of 4-10 ng/mL and disease prognostication after radical prostatectomy. *BJU International*, 105(7), pp.1000-1010.

Go, Y., Chandler, J. and Jones, D., 2015. The cysteine proteome. *Free Radical Biology and Medicine*, 84, pp.227-245.

Goerlitz, D., El Daly, M., Abdel-Hamid, M., Saleh, D., Goldman, L., El Kafrawy, S., Hifnawy, T., Ezzat, S., Abdel-Aziz, M., Zaghloul, M., Ali, S., Khaled, H., Amr, S., Zheng, Y., Mikhail, N. and

Loffredo, C., 2011. GSTM1, GSTT1 Null Variants, and GPX1 Single Nucleotide Polymorphism Are Not Associated with Bladder Cancer Risk in Egypt. *Cancer Epidemiology Biomarkers & Prevention*, 20(7), pp.1552-1554.

Gong, G., Méplan, C., Gautrey, H., Hall, J. and Hesketh, J., 2011. Differential effects of selenium and knock-down of glutathione peroxidases on TNFα and flagellin inflammatory responses in gut epithelial cells. *Genes & Nutrition*, 7(2), pp.167-178.

Gonzalez-Flores, J., Gupta, N., DeMong, L. and Copeland, P., 2012. The Selenocysteine-specific Elongation Factor Contains a Novel and Multi-functional Domain. *Journal of Biological Chemistry*, 287(46), pp.38936-38945.

Gouazé, V., Andrieu-Abadie, N., Cuvillier, O., Malagarie-Cazenave, S., Frisach, M., Mirault, M. and Levade, T., 2002. Glutathione Peroxidase-1 Protects from CD95-induced Apoptosis. *Journal of Biological Chemistry*, 277(45), pp.42867-42874.

Gouazé, V., Mirault, M., Carpentier, S., Salvayre, R., Levade, T. and Andrieu-Abadie, N., 2001. Glutathione Peroxidase-1 Overexpression Prevents Ceramide Production and Partially Inhibits Apoptosis in Doxorubicin-Treated Human Breast Carcinoma Cells. *Molecular Pharmacology*, 60(3), pp.488-496.

Greenberg, M., 2011. The Formamidopyrimidines: Purine Lesions Formed in Competition With 8-Oxopurines From Oxidative Stress. *Accounts of Chemical Research*, 45(4), pp.588-597.

Grollman, A. and Moriya, M., 1993. Mutagenesis by 8-oxoguanine: an enemy within. *Trends in Genetics*, 9(7), pp.246-249.

Grossman, R., Heath, A., Ferretti, V., Varmus, H., Lowy, D., Kibbe, W. and Staudt, L., 2016. Toward a Shared Vision for Cancer Genomic Data. New England Journal of Medicine, 375(12), pp.1109-1112.

Guo, D., Wang, Q., Li, C., Wang, Y. and Chen, X., 2017. VEGF stimulated the angiogenesis by promoting the mitochondrial functions. *Oncotarget*, 8(44), pp.77020-77027.

Hall, M., Marshall, T., Kwit, A., Miller Jenkins, L., Dulcey, A., Madigan, J., Pluchino, K., Goldsborough, A., Brimacombe, K., Griffiths, G. and Gottesman, M., 2014. Inhibition of Glutathione Peroxidase Mediates the Collateral Sensitivity of Multidrug-resistant Cells to Tiopronin. *Journal of Biological Chemistry*, 289(31), pp.21473-21489.

Hall, M., Marshall, T., Kwit, A., Miller Jenkins, L., Dulcey, A., Madigan, J., Pluchino, K., Goldsborough, A., Brimacombe, K., Griffiths, G. and Gottesman, M., 2014. Inhibition of

Glutathione Peroxidase Mediates the Collateral Sensitivity of Multidrug-resistant Cells to Tiopronin. *Journal of Biological Chemistry*, 289(31), pp.21473-21489.

Han, Y., Kim, H., Kim, E., Kim, K., Hong, S., Park, H. and Lee, M., 2014. RORα Decreases Oxidative Stress Through the Induction of SOD2 and GPx1 Expression and Thereby Protects Against Nonalcoholic Steatohepatitis in Mice. *Antioxidants & Redox Signalling*, 21(15), pp.2083-2094.

Hanahan, D. and Weinberg, R., 2011. Hallmarks of Cancer: The Next Generation. *Cell*, 144(5), pp.646-674.

Handy, D., Lubos, E., Yang, Y., Galbraith, J., Kelly, N., Zhang, Y., Leopold, J. and Loscalzo, J., 2009. Glutathione Peroxidase-1 Regulates Mitochondrial Function to Modulate Redox-dependent Cellular Responses. *Journal of Biological Chemistry*, 284(18), pp.11913-11921.

Hangauer, M., Viswanathan, V., Ryan, M., Bole, D., Eaton, J., Matov, A., Galeas, J., Dhruv, H., Berens, M., Schreiber, S., McCormick, F. and McManus, M., 2017. Drug-tolerant persister cancer cells are vulnerable to GPX4 inhibition. *Nature*, 551(7679), pp.247-250.

Hansen, R., Sæbø, M., Skjelbred, C., Nexø, B., Hagen, P., Bock, G., Bowitz Lothe, I., Johnson, E., Aase, S., Hansteen, I., Vogel, U. and Kure, E., 2005. GPX Pro198Leu and OGG1 Ser326Cys polymorphisms and risk of development of colorectal adenomas and colorectal cancer. *Cancer Letters*, 229(1), pp.85-91.

Hazane-Puch, F., Champelovier, P., Arnaud, J., Garrel, C., Ballester, B., Faure, P. and Laporte, F., 2013. Long-Term Selenium Supplementation in HaCaT Cells: Importance of Chemical Form for Antagonist (Protective Versus Toxic) Activities. *Biological Trace Element Research*, 154(2), pp.288-298.

Hazane-Puch, F., Champelovier, P., Arnaud, J., Trocmé, C., Garrel, C., Faure, P. and Laporte, F., 2014. Six-day selenium supplementation led to either UVA-photoprotection or toxic effects in human fibroblasts depending on the chemical form and dose of Se. *Metallomics*, 6(9), p.1683.

Hiller, F., Besselt, K., Deubel, S., Brigelius-Flohé, R. and Kipp, A., 2015. GPx2 Induction Is Mediated Through STAT Transcription Factors During Acute Colitis. *Inflammatory Bowel Diseases*, 21(9), pp.2078-2089.

Hirota, Y., Yamaguchi, S., Shimojoh, N. and Sano, K., 1980. Inhibitory effect of methylmercury on the activity of glutathione peroxidase. *Toxicology and Applied Pharmacology*, 53(1), pp.174-176.

Hoepner, S., Loh, J., Riccadonna, C., Derouazi, M., Maroun, C., Dietrich, P. and Walker, P., 2013. Synergy between CD8 T Cells and Th1 or Th2 Polarised CD4 T Cells for Adoptive Immunotherapy of Brain Tumours. *PLoS ONE*, 8(5), p.e63933.

Horiguchi, H., Yurimoto, H., Kato, N. and Sakai, Y., 2001. Antioxidant System within Yeast Peroxisome. *Journal of Biological Chemistry*, 276(17), pp.14279-14288.

Hossain, M., Saiful Islam, S., Quinn, J., Huq, F. and Moni, M., 2019. Machine learning and bioinformatics models to identify gene expression patterns of ovarian cancer associated with disease progression and mortality. *Journal of Biomedical Informatics*, 100(103313).

Howard, M. and Copeland, P., 2019. New Directions for Understanding the Codon Redefinition Required for Selenocysteine Incorporation. *Biological Trace Element Research*, 192(1), pp.18-25.

Howe, K., Achuthan, P., Allen, J., Allen, J., Alvarez-Jarreta, J., Amode, M., Armean, I., Azov, A., Bennett, R., Bhai, J., Billis, K., Boddu, S., Charkhchi, M., Cummins, C., Da Rin Fioretto, L., Davidson, C., Dodiya, K., El Houdaigui, B., Fatima, R., Gall, A., Garcia Giron, C., Grego, T., Guijarro-Clarke, C., Haggerty, L., Hemrom, A., Hourlier, T., Izuogu, O., Juettemann, T., Kaikala, V., Kay, M., Lavidas, I., Le, T., Lemos, D., Gonzalez Martinez, J., Marugán, J., Maurel, T., McMahon, A., Mohanan, S., Moore, B., Muffato, M., Oheh, D., Paraschas, D., Parker, A., Parton, A., Prosovetskaia, I., Sakthivel, M., Salam, A., Schmitt, B., Schuilenburg, H., Sheppard, D., Steed, E., Szpak, M., Szuba, M., Taylor, K., Thormann, A., Threadgold, G., Walts, B., Winterbottom, A., Chakiachvili, M., Chaubal, A., De Silva, N., Flint, B., Frankish, A., Hunt, S., IIsley, G., Langridge, N., Loveland, J., Martin, F., Mudge, J., Morales, J., Perry, E., Ruffier, M., Tate, J., Thybert, D., Trevanion, S., Cunningham, F., Yates, A., Zerbino, D. and Flicek, P., 2020. Ensembl 2021. Nucleic Acids Research, 49(1), pp.884-891.

Hu, Y. and Diamond, A., 2003. Role of Glutathione Peroxidase 1 in Breast Cancer: Loss of Heterozygosity and Allelic Differences in the Response to Selenium. *Cancer Research*, 63(12), pp.3347-3351.

Huang, C., Ding, G., Gu, C., Zhou, J., Kuang, M., Ji, Y., He, Y., Kondo, T. and Fan, J., 2012. Decreased Selenium-Binding Protein 1 Enhances Glutathione Peroxidase 1 Activity and

Downregulates HIF-1α to Promote Hepatocellular Carcinoma Invasiveness. *Clinical Cancer Research*, 18(11), pp.3042-3053.

Huang, Z., Liu, Y., Huang, Z., Li, H., Gan, X. And Shen, Z., 2016. 1,25-Dihydroxyvitamin D3 alleviates salivary adenoid cystic carcinoma progression by suppressing GPX1 expression through the NF-κB pathway. *International Journal of Oncology*, 48(3), pp.1271-1279.

Hussain, S., Amstad, P., He, P., Robles, A., Lupold, S., Kaneko, I., Ichimiya, M., Sengupta, S., Mechanic, L., Okamura, S., Hofseth, L., Moake, M., Nagashima, M., Forrester, K. and Harris, C., 2004. p53-Induced Up-Regulation of MnSOD and GPx but not Catalase Increases Oxidative Stress and Apoptosis. *Cancer Research*, 64(7), pp.2350-2356.

Ighodaro, O. and Akinloye, O., 2018. First line defence antioxidants-superoxide dismutase (SOD), catalase (CAT) and glutathione peroxidase (GPX): Their fundamental role in the entire antioxidant defence grid. *Alexandria Journal of Medicine*, 54(4), pp.287-293.

Jablonska, E., Gromadzinska, J., Peplonska, B., Fendler, W., Reszka, E., Krol, M., Wieczorek, E., Bukowska, A., Gresner, P., Galicki, M., Zambrano Quispe, O., Morawiec, Z. and Wasowicz, W., 2015. Lipid peroxidation and glutathione peroxidase activity relationship in breast cancer depends on functional polymorphism of GPX1. *BMC Cancer*, 15(657).

Jablonska, E., Gromadzinska, J., Reszka, E., Wasowicz, W., Sobala, W., Szeszenia-Dabrowska, N. and Boffetta, P., 2009. Association between GPx1 Pro198Leu polymorphism, GPx1 activity and plasma selenium concentration in humans. *European Journal of Nutrition*, 48(6), pp.383-386.

Jerome-Morais, A., Wright, M., Liu, R., Yang, W., Jackson, M., Combs, G. and Diamond, A., 2011. Inverse association between glutathione peroxidase activity and both selenium-binding protein 1 levels and gleason score in human prostate tissue. *The Prostate*, 72(9), pp.1006-1012.

Jiao, Y., Wang, Y., Guo, S. and Wang, G. (2017). Glutathione peroxidases as oncotargets. *Oncotarget*, 8(45), pp.80093–80102.

Jones, D., Eklöw, L., Thor, H. and Orrenius, S., 1981. Metabolism of hydrogen peroxide in isolated hepatocytes: Relative contributions of catalase and glutathione peroxidase in decomposition of endogenously generated H2O2. *Archives of Biochemistry and Biophysics*, 210(2), pp.505-516.

Jové, M., Naudí, A., Aledo, J., Cabré, R., Ayala, V., Portero-Otin, M., Barja, G. and Pamplona, R., 2013. Plasma long-chain free fatty acids predict mammalian longevity. *Scientific Reports*, 3, 3346.

Kalivendi, S., Konorev, E., Cunningham, S., Vanamala, S., Kaji, E., Joseph, J. and Kalyanaraman, B., 2005. Doxorubicin activates nuclear factor of activated T-lymphocytes and Fas ligand transcription: role of mitochondrial reactive oxygen species and calcium. *Biochemical Journal*, 389(2), pp.527-539.

Kaur, P., Aschner, M. and Syversen, T., 2006. Glutathione modulation influences methyl mercury induced neurotoxicity in primary cell cultures of neurons and astrocytes. *NeuroToxicology*, 27(4), pp.492-500.

Kim, H., Kang, H., You, K., Kim, S., Lee, K., Kim, T., Kim, C., Song, S., Kim, H., Lee, C. and Kim, H., 2006. Suppression of human selenium-binding protein 1 is a late event in colorectal carcinogenesis and is associated with poor survival. *Proteomics*, 6(11), pp.3466-3476.

Kim, H., Lee, A., Choi, E., Kie, J., Lim, W., Lee, H., Moon, B. and Seoh, J., 2014. Attenuation of Experimental Colitis in Glutathione Peroxidase 1 and Catalase Double Knockout Mice through Enhancing Regulatory T Cell Function. *PLoS ONE*, 9(4), p.e95332.

Kinowaki, Y., Kurata, M., Ishibashi, S., Ikeda, M., Tatsuzawa, A., Yamamoto, M., Miura, O., Kitagawa, M. and Yamamoto, K., 2018. Glutathione peroxidase 4 overexpression inhibits ROS-induced cell death in diffuse large B-cell lymphoma. *Laboratory Investigation*, 98(5), pp.609-619.

Klotz, R., Thomas, A., Teng, T., Han, S., Iriondo, O., Li, L., Restrepo-Vassalli, S., Wang, A., Izadian, N., MacKay, M., Moon, B., Liu, K., Ganesan, S., Lee, G., Kang, D., Walmsley, C., Pinto, C., Press, M., Lu, W., Lu, J., Juric, D., Bardia, A., Hicks, J., Salhia, B., Attenello, F., Smith, A. and Yu, M., 2019. Circulating Tumor Cells Exhibit Metastatic Tropism and Reveal Brain Metastasis Drivers. *Cancer Discovery*, 10(1), pp.86-103.

Kodydkova, J., Vavrova, L., Stankova, B., Macasek, J., Krechler, T. and Zak, A., 2013. Antioxidant Status and Oxidative Stress Markers in Pancreatic Cancer and Chronic Pancreatitis. *Pancreas*, 42(4), pp.614-621.

Koeberle, S., Gollowitzer, A., Laoukili, J., Kranenburg, O., Werz, O., Koeberle, A. and Kipp, A., 2020. Distinct and overlapping functions of glutathione peroxidases 1 and 2 in limiting NF-κB-driven inflammation through redox-active mechanisms. *Redox Biology*, 28, pp.101388.

Koeberle, S., Gollowitzer, A., Laoukili, J., Kranenburg, O., Werz, O., Koeberle, A. and Kipp, A., 2020. Distinct and overlapping functions of glutathione peroxidases 1 and 2 in limiting NF-κB-driven inflammation through redox-active mechanisms. *Redox Biology*, 28(101388).

Komatsu, D., Kato, M., Nakayama, J., Miyagawa, S. and Kamata, T., 2008. NADPH oxidase 1 plays a critical mediating role in oncogenic Ras-induced vascular endothelial growth factor expression. *Oncogene*, 27(34), pp.4724-4732.

Konstantinova, L., Rakitin, O. and Rees, C., 2004. Pentathiepins. *Chemical Reviews*, 104(5), pp.2617-2630.

Krhin, B., Goricar, K., Gazic, B., Dolzan, V. and Besic, N., 2016. Functional polymorphisms in antioxidant genes in Hurthle cell thyroid neoplasm - an association of GPX1 polymorphism and recurrent Hurthle cell thyroid carcinoma. *Radiology and Oncology*, 50(3), pp.289-296.

Kristal, A., Darke, A., Morris, J., Tangen, C., Goodman, P., Thompson, I., Meyskens, F., Goodman, G., Minasian, L., Parnes, H., Lippman, S. and Klein, E., 2014. Baseline Selenium Status and Effects of Selenium and Vitamin E Supplementation on Prostate Cancer Risk. JNCI: *Journal of the National Cancer Institute,* 106(3), djt456, pp. 1-8.

Kukreja, R., Kontos, H., Hess, M. and Ellis, E., 1986. PGH synthase and lipoxygenase generate superoxide in the presence of NADH or NADPH. *Circulation Research*, 59(6), pp.612-619.

Kulak, M., Cyr, A., Woodfield, G., Bogachek, M., Spanheimer, P., Li, T., Price, D., Domann, F. and Weigel, R., 2012. Transcriptional regulation of the GPX1 gene by TFAP2C and aberrant CpG methylation in human breast cancer. *Oncogene*, 32(34), pp.4043-4051.

Kumagai, Y., Kanda, H., Shinkai, Y. and Toyama, T., 2013. The Role of the Keap1/Nrf2 Pathway in the Cellular Response to Methylmercury. *Oxidative Medicine and Cellular Longevity*, 2013(848279), pp.1-8.

LaCasse, C., Janikashvili, N., Larmonier, C., Alizadeh, D., Hanke, N., Kartchner, J., Situ, E., Centuori, S., Har-Noy, M., Bonnotte, B., Katsanis, E. and Larmonier, N., 2011. Th-1 Lymphocytes Induce Dendritic Cell Tumor Killing Activity by an IFN-γ–Dependent Mechanism. *The Journal of Immunology*, 187(12), pp.6310-6317.

Lander, H., 1997. An essential role for free radicals and derived species in signal transduction. *The FASEB Journal*, 11(2), pp.118-124.

Landrum, M., Smertenko, A., Edwards, R., Hussey, P. and Steel, P., 2010. BODIPY probes to study peroxisome dynamics in vivo. *The Plant Journal*, 62(3), pp.529-538.

Lee, A., Chan, A. and Li, T., 2002. Acid-accelerated DNA-cleaving activities of antitumor antibiotic varacin. *Chemical Communications*, (18), pp.2112-2113.

Lee, D., Son, D., Park, M., Yoon, D., Han, S. and Hong, J., 2016. Glutathione peroxidase 1 deficiency attenuates concanavalin A-induced hepatic injury by modulation of T-cell activation. *Cell Death & Disease*, 7(4), pp.e2208-e2208.

Lee, E., Choi, A., Jun, Y., Kim, N., Yook, J., Kim, S., Lee, S. and Kang, S., 2020. Glutathione peroxidase-1 regulates adhesion and metastasis of triple-negative breast cancer cells via FAK signaling. *Redox Biology*, 29, p.101391.

Lee, J., Roh, J., Lee, S., Park, Y., Cho, K., Choi, S., Nam, S. and Kim, S., 2017. Overexpression of glutathione peroxidase 1 predicts poor prognosis in oral squamous cell carcinoma. *Journal of Cancer Research and Clinical Oncology*, 143(11), pp.2257-2265.

Legakis, J., Koepke, J., Jedeszko, C., Barlaskar, F., Terlecky, L., Edwards, H., Walton, P. and Terlecky, S., 2002. Peroxisome Senescence in Human Fibroblasts. *Molecular Biology of the Cell*, 13(12), pp.4243-4255.

Lei, X., Evenson, J., Thompson, K. and Sunde, R., 1995. Glutathione Peroxidase and Phospholipid Hydroperoxide Glutathione Peroxidase Are Differentially Regulated in Rats by Dietary Selenium. *The Journal of Nutrition*, 125(6), pp.1438-1446.

Lesoon, A., Mehta, A., Singh, R., Chisolm, G. and Driscoll, D. (1997). An RNA-binding protein recognizes a mammalian selenocysteine insertion sequence element required for cotranslational incorporation of selenocysteine. *Molecular and Cellular Biology*, 17(4), pp.1977-1985.

Li, J. and Shah, A., 2004. Endothelial cell superoxide generation: regulation and relevance for cardiovascular pathophysiology. *American Journal of Physiology-Regulatory, Integrative and Comparative Physiology*, 287(5), pp.R1014-R1030.

Li, Q., Sanlioglu, S., Li, S., Ritchie, T., Oberley, L. and Engelhardt, J., 2001. GPx-1 Gene Delivery Modulates NFκB Activation Following Diverse Environmental Injuries Through a Specific Subunit of the IKK Complex. *Antioxidants & Redox Signaling*, 3(3), pp.415-432.

Li, T., Yang, W., Li, M., Byun, D., Tong, C., Nasser, S., Zhuang, M., Arango, D., Mariadason, J. and Augenlicht, L., 2008. Expression of selenium-binding protein 1 characterizes intestinal cell maturation and predicts survival for patients with colorectal cancer. *Molecular Nutrition & Food Research*, 52(11), pp.1289-1299.

Li, X., Gou, J., Li, H. and Yang, X., 2020. Bioinformatic analysis of the expression and prognostic value of chromobox family proteins in human breast cancer. *Scientific Reports*, 10(17739).

Little, C. and O'Brien, P., 1968. An intracellular GSH-peroxidase with a lipid peroxide substrate. *Biochemical and Biophysical Research Communications*, 31(2), pp.145-150.

Liu, H., Goldenberg, A., Chen, Y., Lun, C., Wu, W., Bush, K., Balac, N., Rodriguez, P., Abagyan, R. and Nigam, S., 2016. Molecular Properties of Drugs Interacting with SLC22 Transporters OAT1, OAT3, OCT1, and OCT2: A Machine-Learning Approach. *Journal of Pharmacology and Experimental Therapeutics*, 359(1), pp.215-229.

Liu, M., Gao, L., Zhao, L., He, J., Yuan, Q., Zhang, P., Zhao, Y. and Gao, X., 2017. Peptide-Au Clusters Induced Tumor Cells Apoptosis via Targeting Glutathione Peroxidase-1: The Molecular Dynamics Assisted Experimental Studies. *Scientific Reports*, 7(131).

Loschen, G. and Flohé, L. (1971). Respiratory chain linked H_2O_2 production in pigeon heart mitochondria. *FEBS Letters*, 18(2), pp.261-264.

Lu, W., Chen, Z., Zhang, H., Wang, Y., Luo, Y. and Huang, P., 2012. ZNF143 transcription factor mediates cell survival through upregulation of the GPX1 activity in the mitochondrial respiratory dysfunction. Cell Death & Disease, 3(11), pp.e422-e422.

Lu, Y., Lou, Y., Yen, P., Newmark, H., Mirochnitchenko, O., Inouye, M. and Huang, M., 1997. Enhanced Skin Carcinogenesis in Transgenic Mice with High Expression of Glutathione Peroxidase or Both Glutathione Peroxidase and Superoxide Dismutase. *Cancer Research*, 57, pp.1468-1474.

Lubos, E., Loscalzo, J. and Handy, D., 2011. Glutathione Peroxidase-1 in Health and Disease: From Molecular Mechanisms to Therapeutic Opportunities. *Antioxidants & Redox Signaling*, 15(7), pp.1957-1997.

Lv, S., Luo, H., Huang, K. and Zhu, X., 2020. The Prognostic Role of Glutathione Peroxidase 1 and Immune Infiltrates in Glioma Investigated Using Public Datasets. *Medical Science Monitor,* 26(e926440).

Maiorino, M., Thomas, J., Girotti, A. and Ursini, F., 1991. Reactivity of Phospholipid Hydroperoxide Glutathione Peroxidase with Membrane and Lipoprotein Lipid Hydroperoxides. *Free Radical Research Communications*, 12(1), pp.131-135.

Mantovani, A., 2014. Macrophages, Neutrophils, and Cancer: A Double Edged Sword. *New Journal of Science*, 2014(271940), pp.1-14.

Marullo, R., Werner, E., Degtyareva, N., Moore, B., Altavilla, G., Ramalingam, S. and Doetsch, P. (2013). Cisplatin Induces a Mitochondrial-ROS Response That Contributes to Cytotoxicity Depending on Mitochondrial Redox Status and Bioenergetic Functions. *PLoS ONE*, 8(11), p.e81162.

Mauri, P., Benazzi, L., Flohé, L., Maiorino, M., Pietta, P., Pilawa, S., Roveri, A. and Ursini, F., 2003. Versatility of Selenium Catalysis in PHGPx Unraveled by LC/ESI-MS/MS. *Biological Chemistry*, 384(4), pp.565-587.

McMillan, E., Ryu, M., Diep, C., Mendiratta, S., Clemenceau, J., Vaden, R., Kim, J., Motoyaji, T., Covington, K., Peyton, M., Huffman, K., Wu, X., Girard, L., Sung, Y., Chen, P., Mallipeddi, P., Lee, J., Hanson, J., Voruganti, S., Yu, Y., Park, S., Sudderth, J., DeSevo, C., Muzny, D., Doddapaneni, H., Gazdar, A., Gibbs, R., Hwang, T., Heymach, J., Wistuba, I., Coombes, K., Williams, N., Wheeler, D., MacMillan, J., Deberardinis, R., Roth, M., Posner, B., Minna, J., Kim, H. and White, M., 2018. Chemistry-First Approach for Nomination of Personalized Treatment in Lung Cancer. *Cell*, 173(4), pp.864-878.e29.

Meewes, C., Brenneisen, P., Wenk, J., Kuhr, L., Ma, W., Alikoski, J., Poswig, A., Krieg, T. and Scharffetter-Kochanek, K., 2001. Adaptive antioxidant response protects dermal fibroblasts from UVA-induced phototoxicity. *Free Radical Biology and Medicine*, 30(3), pp.238-247.

Meng, Q., Xu, J., Liang, C., Liu, J., Hua, J., Zhang, Y., Ni, Q., Shi, S. and Yu, X., 2018. GPx1 is involved in the induction of protective autophagy in pancreatic cancer cells in response to glucose deprivation. *Cell Death & Disease*, 9(1187).

Méplan, C., Dragsted, L., Ravn-Haren, G., Tjønneland, A., Vogel, U. and Hesketh, J., 2013. Association between Polymorphisms in Glutathione Peroxidase and Selenoprotein P Genes, Glutathione Peroxidase Activity, HRT Use and Breast Cancer Risk. *PLoS ONE*, 8(9), p.e73316.

Mills, G. (1957). Hemoglobin Catabolism. *The Journal of Biochemistry*, 299(1), pp.189-197.

Miniard, A., Middleton, L., Budiman, M., Gerber, C. and Driscoll, D., 2010. Nucleolin binds to a subset of selenoprotein mRNAs and regulates their expression. *Nucleic Acids Research*, 38(14), pp.4807-4820.

Mitra, S., Nguyen, L., Akter, M., Park, G., Choi, E. and Kaushik, N. (2019). Impact of ROS Generated by Chemical, Physical, and Plasma Techniques on Cancer Attenuation. *Cancers*, 11(7), p.1030.

Moldovan, L. and Moldovan, N., 2004. Oxygen free radicals and redox biology of organelles. *Histochemistry and Cell Biology*, 122(4), pp.395-412.

Morgan, P., Dean, R. and Davies, M., 2004. Protective mechanisms against peptide and protein peroxides generated by singlet oxygen. *Free Radical Biology and Medicine*, 36(4), pp.484-496.

Müller, C., Wingler, K. and Brigelius-Flohé, R., 2003. 3'UTRs of Glutathione Peroxidases Differentially Affect Selenium-Dependent mRNA Stability and Selenocysteine Incorporation Efficiency. *Biological Chemistry*, 384(1), pp.11-18.

Narayan, V., Ly, T., Pourkarimi, E., Murillo, A., Gartner, A., Lamond, A. and Kenyon, C., 2016. Deep Proteome Analysis Identifies Age-Related Processes in C. elegans. *Cell Systems*, 3(2), pp.144-159.

Neužil, J., Gebicki, J. and Stocker, R., 1993. Radical-induced chain oxidation of proteins and its inhibition by chain-breaking antioxidants. *Biochemical Journal*, 293(3), pp.601-606.

Niedernhofer, L., Daniels, J., Rouzer, C., Greene, R. and Marnett, L., 2003. Malondialdehyde, a Product of Lipid Peroxidation, Is Mutagenic in Human Cells. *Journal of Biological Chemistry*, 278(33), pp.31426-31433.

Nigam, S., Bush, K., Martovetsky, G., Ahn, S., Liu, H., Richard, E., Bhatnagar, V. and Wu, W., 2015. The Organic Anion Transporter (OAT) Family: A Systems Biology Perspective. *Physiological Reviews*, 95(1), pp.83-123.

Ogata, H. and Hibi, T., 2003. Cytokine and Anti-cytokine Therapies for Inflammatory Bowel Disease. *Current Pharmaceutical Design*, 9(14), pp.1107-1113.

Ohdate, T. and Inoue, Y., 2012. Involvement of glutathione peroxidase 1 in growth and peroxisome formation in Saccharomyces cerevisiae in oleic acid medium. *Biochimica et Biophysica Acta (BBA) - Molecular and Cell Biology of Lipids*, 1821(9), pp.1295-1305.

Ohdate, T., Izawa, S., Kita, K. and Inoue, Y., 2010. Regulatory mechanism for expression of GPX1 in response to glucose starvation and Ca2+ in Saccharomyces cerevisiae: involvement of Snf1 and Ras/cAMP pathway in Ca2+signaling. Genes to Cells, 15(1), pp.59-75.

Ohue, Y. and Nishikawa, H., 2019. Regulatory T (Treg) cells in cancer: Can Treg cells be a new therapeutic target?. *Cancer Science*, 110(7), pp.2080-2089.

Okabe, Y., Sano, T. and Nagata, S. (2009). Regulation of the innate immune response by threonine-phosphatase of Eyes absent. *Nature*, 460(7254), pp.520-524.

Okubo, T., Saito, T., Mitomi, H., Takagi, T., Torigoe, T., Suehara, Y., Kaneko, K. and Yao, T., 2013. p53 mutations may be involved in malignant transformation of giant cell tumor of bone through interaction with GPX1. *Virchows Archiv*, 463(1), pp.67-77.

Okubo, T., Saito, T., Mitomi, H., Takagi, T., Torigoe, T., Suehara, Y., Kaneko, K. and Yao, T., 2013. p53 mutations may be involved in malignant transformation of giant cell tumor of bone through interaction with GPX1. Virchows Archiv, 463(1), pp.67-77.

Olsen, C., Berg, K., Selbo, P. and Weyergang, A., 2013. Circumvention of resistance to photodynamic therapy in doxorubicin-resistant sarcoma by photochemical internalization of gelonin. Free Radical Biology and Medicine, 65, pp.1300-1309.

Paz-y-Miño, C., Muñoz, M., López-Cortés, A., Cabrera, A., Palacios, A., Castro, B., Paz-y-Miño, N., Sánchez, M., 2009. Frequency of Polymorphisms pro198leu in GPX-1 Gene and ile58thr in MnSOD Gene in the Altitude Ecuadorian Population With Bladder Cancer. *Oncology Research Featuring Preclinical and Clinical Cancer Therapeutics*, 18(8), pp. 395-400

Pendergrass, K., Boopathy, A., Seshadri, G., Maiellaro-Rafferty, K., Che, P., Brown, M. and Davis, M., 2013. Acute Preconditioning of Cardiac Progenitor Cells with Hydrogen Peroxide Enhances Angiogenic Pathways Following Ischemia-Reperfusion Injury. *Stem Cells and Development*, 22(17), pp.2414-2424.

Perillo, B., Di Donato, M., Pezone, A., Di Zazzo, E., Giovannelli, P., Galasso, G., Castoria, G. and Migliaccio, A., 2020. ROS in cancer therapy: the bright side of the moon. Experimental & Molecular Medicine, 52(2), pp.192-203.

Peter, M., Hadji, A., Murmann, A., Brockway, S., Putzbach, W., Pattanayak, A. and Ceppi, P., 2015. The role of CD95 and CD95 ligand in cancer. *Cell Death & Differentiation*, 22(4), pp.549-559.

Piotrowski, I., Kulcenty, K. and Suchorska, W., 2020. Interplay between inflammation and cancer. *Reports of Practical Oncology & Radiotherapy*, 25(3), pp.422-427.

Pogozelski, W. and Tullius, T., 1998. Oxidative Strand Scission of Nucleic Acids: Routes Initiated by Hydrogen Abstraction from the Sugar Moiety. *Chemical Reviews*, 98(3), pp.1089–1108.

Pore, N., Jiang, Z., Gupta, A., Cerniglia, G., Kao, G. and Maity, A., 2006. EGFR Tyrosine Kinase Inhibitors Decrease VEGF Expression by Both Hypoxia-Inducible Factor (HIF)-1–Independent and HIF-1–Dependent Mechanisms. *Cancer Research*, 66(6), pp.3197-3204.

Pritsos, C., 2000. Cellular distribution, metabolism and regulation of the xanthine oxidoreductase enzyme system. *Chemico-Biological Interactions*, 129(1-2), pp.195-208.

Quiñones, J., Thapar, U., Yu, K., Fang, Q., Sobol, R. and Demple, B., 2015. Enzyme mechanism-based, oxidative DNA–protein cross-links formed with DNA polymerase β in vivo. *Proceedings of the National Academy of Sciences*, 112(28), pp.8602-8607.

Rafferty, T., Mckenzie, R., Hunter, J., Howie, A., Arthur, J., Nicol, F. And Beckett, G., 1998. Differential expression of selenoproteins by human skin cells and protection by selenium from UVB-radiation-induced cell death. *Biochemical Journal*, 332(1), pp.231-236.

Ran, Q., Liang, H., Gu, M., Qi, W., Walter, C., Roberts, L., Herman, B., Richardson, A. and Van Remmen, H., 2004. Transgenic Mice Overexpressing Glutathione Peroxidase 4 Are Protected against Oxidative Stress-induced Apoptosis. *Journal of Biological Chemistry*, 279(53), pp.55137-55146.

Ravn-Haren, G., Olsen, A., Tjønneland, A., Dragsted, L., Nexø, B., Wallin, H., Overvad, K., Raaschou-Nielsen, O. and Vogel, U., 2005. Associations between GPX1 Pro198Leu polymorphism, erythrocyte GPX activity, alcohol consumption and breast cancer risk in a prospective cohort study. *Carcinogenesis*, 27(4), pp.820-825.

Ray, A., Semba, R., Walston, J., Ferrucci, L., Cappola, A., Ricks, M., Xue, Q. and Fried, L. (2006). Low Serum Selenium and Total Carotenoids Predict Mortality among Older Women Living in the Community: The Women's Health and Aging Studies. *The Journal of Nutrition*, 136(1), pp.172-176.

Reich, H. and Hondal, R. (2016). Why Nature Chose Selenium. *ACS Chemical Biology*, 11(4), pp.821-841.

Ren, X., Zou, L., Lu, J. and Holmgren, A. (2018). Selenocysteine in mammalian thioredoxin reductase and application of ebselen as a therapeutic. *Free Radical Biology and Medicine*, 127, pp.238-247.

Rhee, S., Chang, T., Jeong, W. and Kang, D., 2010. Methods for detection and measurement of hydrogen peroxide inside and outside of cells. *Molecules and Cells*, 29(6), pp.539-549.

Rhie, G., Shin, M., Seo, J., Choi, W., Cho, K., Kim, K., Park, K., Eun, H. and Chung, J. (2001). Aging- and Photoaging-Dependent Changes of Enzymic and Nonenzymic Antioxidants in the Epidermis and Dermis of Human Skin In Vivo. *Journal of Investigative Dermatology*, 117(5), pp.1212-1217.

Ribas, V., García-Ruiz, C. and Fernández-Checa, J., 2016. Mitochondria, cholesterol and cancer cell metabolism. *Clinical and Translational Medicine*, 5(1).

Ricciotti, E. and FitzGerald, G., 2011. Prostaglandins and Inflammation. *Arteriosclerosis, Thrombosis, and Vascular Biology*, 31(5), pp.986-1000.

Rodriguez, S. and Huynh-Do, U., 2012. The Role of PTEN in Tumor Angiogenesis. *Journal of Oncology*, 2012, pp.1-11.

Roos, G., Foloppe, N. and Messens, J. (2013). Understanding the pKa of Redox Cysteines: The Key Role of Hydrogen Bonding. *Antioxidants & Redox Signaling*, 18(1), pp.94-127.

Rotruck, J., Pope, A., Ganther, H., Swanson, A., Hafeman, D. and Hoekstra, W. (1973). Selenium: Biochemical Role as a Component of Glutathione Peroxidase. *Science*, 179(4073), pp.588-590.

Rouiller, C. and Bernhard, W. (1956). "Microbodies" and the problem of mitochondrial regeneration in liver cells. The Journal of Cell Biology, 2(4), pp.355-359.

Sarsour, E., Kalen, A. and Goswami, P. (2014). Manganese Superoxide Dismutase Regulates a Redox Cycle Within the Cell Cycle. *Antioxidants & Redox Signaling*, 20(10), pp.1618-1627.

Sattler, W., Maiorino, M. and Stocker, R., 1994. Reduction of HDL- and LDL-Associated Cholesterylester and Phospholipid Hydroperoxides by Phospholipid Hydroperoxide Glutathione Peroxidase and Ebselen (PZ-51). *Archives of Biochemistry and Biophysics*, 309(2), pp.214-221.

Schäfer, G., Cramer, T., Suske, G., Kemmner, W., Wiedenmann, B. and Höcker, M., 2002. Oxidative Stress Regulates Vascular Endothelial Growth Factor-A Gene Transcription through Sp1- and Sp3-dependent Activation of Two Proximal GC-rich Promoter Elements. *Journal of Biological Chemistry*, 278(10), pp.8190-8198.

Schaur, R., 2003. Basic aspects of the biochemical reactivity of 4-hydroxynonenal. *Molecular Aspects of Medicine*, 24(4-5), pp.149-159.

Scheerer, P., Borchert, A., Krauss, N., Wessner, H., Gerth, C., Höhne, W. and Kuhn, H., 2007. Structural Basis for Catalytic Activity and Enzyme Polymerization of Phospholipid Hydroperoxide Glutathione Peroxidase-4 (GPx4). *Biochemistry*, 46(31), pp.9041-9049.

Schoenmakers, E., Agostini, M., Mitchell, C., Schoenmakers, N., Papp, L., Rajanayagam, O., Padidela, R., Ceron-Gutierrez, L., Doffinger, R., Prevosto, C., Luan, J., Montano, S., Lu, J., Castanet, M., Clemons, N., Groeneveld, M., Castets, P., Karbaschi, M., Aitken, S., Dixon, A., Williams, J., Campi, I., Blount, M., Burton, H., Muntoni, F., O'Donovan, D., Dean, A., Warren, A., Brierley, C., Baguley, D., Guicheney, P., Fitzgerald, R., Coles, A., Gaston, H., Todd, P., Holmgren, A., Khanna, K., Cooke, M., Semple, R., Halsall, D., Wareham, N., Schwabe, J., Grasso, L., Beck-Peccoz, P., Ogunko, A., Dattani, M., Gurnell, M. and Chatterjee, K., 2010. Mutations in the selenocysteine insertion sequence–binding protein 2 gene lead to a multisystem selenoprotein deficiency disorder in humans. *Journal of Clinical Investigation*, 120(12), pp.4220-4235.

Schreck, R., Rieber, P. and Baeuerle, P., 1991. Reactive oxygen intermediates as apparently widely used messengers in the activation of the NF-kappa B transcription factor and HIV-1. *The EMBO Journal*, 10(8), pp.2247-2258.

Schulz, R., Emmrich, T., Lemmerhirt, H., Leffler, U., Sydow, K., Hirt, C., Kiefer, T., Link, A. and Bednarski, P., 2012. Identification of a glutathione peroxidase inhibitor that reverses resistance to anticancer drugs in human B-cell lymphoma cell lines. *Bioorganic & Medicinal Chemistry Letters*, 22(21), pp.6712-6715.

Scudiero, D., Shoemaker, R., Paull, K., Monks, A., Tierney, S., Nofziger, T., Currens, M., Seniff, D. and Boyd, M., 1988. Evaluation of a soluble tetrazolium/formazan assay for cell growth and drug sensitivity in culture using human and other tumor cell lines. Cancer Research, 48(17), pp.4827-4833.

Sen, C., Khanna, S., Babior, B., Hunt, T., Ellison, E. and Roy, S., 2002. Oxidant-induced Vascular Endothelial Growth Factor Expression in Human Keratinocytes and Cutaneous Wound Healing. *Journal of Biological Chemistry*, 277(36), pp.33284-33290.

Seyedali, A. and Berry, M., 2014. Nonsense-mediated decay factors are involved in the regulation of selenoprotein mRNA levels during selenium deficiency. *RNA*, 20(8), pp.1248-1256.

Sham, D., Wesley, U., Hristova, M. and van der Vliet, A., 2013. ATP-Mediated Transactivation of the Epidermal Growth Factor Receptor in Airway Epithelial Cells Involves DUOX1-Dependent Oxidation of Src and ADAM17. *PLoS ONE*, 8(1), p.e54391.

Shi, X., Huang, L., Lilley, D., Harbury, P. and Herschlag, D., 2016. The solution structural ensembles of RNA kink-turn motifs and their protein complexes. *Nature Chemical Biology*, 12(3), pp.146-152.

Sies, H., 2017. Hydrogen peroxide as a central redox signalling molecule in physiological oxidative stress: Oxidative eustress. *Redox Biology*, 11, pp.613-619.

Sies, H., Gerstenecker, C., Menzel, H. and Flohé, L., 1972. Oxidation in the NADP system and release of GSSG from hemoglobin-free perfused rat liver during peroxidatic oxidation of glutathione by hydroperoxides. *FEBS Letters*, 27(1), pp.171-175.

Simonović, M. and Puppala, A., 2018. On elongation factor eEFSec, its role and mechanism during selenium incorporation into nascent selenoproteins. *Biochimica et Biophysica Acta (BBA) - General Subjects*, 1862(11), pp.2463-2472.

Singh, A., Dhaunsi, G., Gupta, M., Orak, J., Asayama, K. and Singh, I., 1994. Demonstration of Glutathione Peroxidase in Rat Liver Peroxisomes and Its Intraorganellar Distribution. *Archives of Biochemistry and Biophysics*, 315(2), pp.331-338.

Singh, A., Kukreti, R., Saso, L. and Kukreti, S., 2019. Oxidative Stress: Role and Response of Short Guanine Tracts at Genomic Locations. *International Journal of Molecular Sciences*, 20(17), p.4258.

Singh, A., Rangasamy, T., Thimmulappa, R., Lee, H., Osburn, W., Brigelius-Flohé, R., Kensler, T., Yamamoto, M. and Biswal, S., 2006. Glutathione Peroxidase 2, the Major Cigarette Smoke–Inducible Isoform of GPX in Lungs, Is Regulated by Nrf2. *American Journal of Respiratory Cell and Molecular Biology*, 35(6), pp.639-650.

Sjöstrand, F. and Rhodin, J. (1954). The ultrastructure of the proximal convoluted tubules of the mouse kidney as revealed by high resolution electron microscopy. *Experimental Cell Research*, 4(2), pp.426-456.

Song, J., Yu, Y., Xing, R., Guo, X., Liu, D., Wei, J. and Song, H., 2014. Unglycosylated recombinant human glutathione peroxidase 3 mutant from Escherichia coli is active as a monomer. *Scientific Reports*, 4(1), pp.1-5.

Sultan, C., Saackel, A., Stank, A., Fleming, T., Fedorova, M., Hoffmann, R., Wade, R., Hecker, M. and Wagner, A., 2018. Impact of carbonylation on glutathione peroxidase-1 activity in human hyperglycemic endothelial cells. *Redox Biology*, 16(2018), pp.113-122.

Sun, C., Yuan, Q., Wu, D., Meng, X. and Wang, B., 2017. Identification of core genes and outcome in gastric cancer using bioinformatics analysis. *Oncotarget*, 8(41), pp.70271-70280.

Sung, J., DeMott, M. and Demple, B., 2005. Long-patch Base Excision DNA Repair of 2-Deoxyribonolactone Prevents the Formation of DNA-Protein Cross-links with DNA Polymerase β. *Journal of Biological Chemistry*, 280(47), pp.39095-39103.

Szatrowski, T. and Nathan, C., 1991. Production of Large Amounts of Hydrogen Peroxide by Human Tumor Cells. *Cancer Research*, 51(3), pp.794-798.

Takebe, G., Yarimizu, J., Saito, Y., Hayashi, T., Nakamura, H., Yodoi, J., Nagasawa, S. and Takahashi, K., 2002. A Comparative Study on the Hydroperoxide and Thiol Specificity of the Glutathione Peroxidase Family and Selenoprotein P. *Journal of Biological Chemistry*, 277(43), pp.41254-41258.

Takeshita, S., Inoue, N., Ueyama, T., Kawashima, S. and Yokoyama, M., 2000. Shear Stress Enhances Glutathione Peroxidase Expression in Endothelial Cells. *Biochemical and Biophysical Research Communications*, 273(1), pp.66-71.

Takeuchi, A., Schmitt, D., Chapple, C., Babaylova, E., Karpova, G., Guigo, R., Krol, A. and Allmang, C., 2009. A short motif in Drosophila SECIS Binding Protein 2 provides differential binding affinity to SECIS RNA hairpins. *Nucleic Acids Research*, 37(7), pp.2126-2141.

Tan, M., Li, S., Swaroop, M., Guan, K., Oberley, L. and Sun, Y., 1999. Transcriptional Activation of the Human Glutathione Peroxidase Promoter by p53. *Journal of Biological Chemistry*, 274(17), pp.12061-12066.

Tang, Z., Li, C., Kang, B., Gao, G., Li, C. and Zhang, Z., 2017. GEPIA: a web server for cancer and normal gene expression profiling and interactive analyses. Nucleic Acids Research, 45(W1), pp.W98-W102.

Tate, J., Bamford, S., Jubb, H., Sondka, Z., Beare, D., Bindal, N., Boutselakis, H., Cole, C., Creatore, C., Dawson, E., Fish, P., Harsha, B., Hathaway, C., Jupe, S., Kok, C., Noble, K., Ponting, L., Ramshaw, C., Rye, C., Speedy, H., Stefancsik, R., Thompson, S., Wang, S., Ward, S., Campbell, P. and Forbes, S., 2018. COSMIC: the Catalogue Of Somatic Mutations In Cancer. Nucleic Acids Research, 47(D1), pp.D941-D947.

Toppo, S., Flohé, L., Ursini, F., Vanin, S. and Maiorino, M., 2009. Catalytic mechanisms and specificities of glutathione peroxidases: Variations of a basic scheme. *Biochimica et Biophysica Acta (BBA) - General Subjects*, 1790(11), pp.1486-1500.

Toppo, S., Vanin, S., Bosello, V. and Tosatto, S. (2008). Evolutionary and Structural Insights Into the Multifaceted Glutathione Peroxidase (Gpx) Superfamily. *Antioxidants & Redox Signaling*, 10(9), pp.1501-1514.

Tosatto, S., Bosello, V., Fogolari, F., Mauri, P., Roveri, A., Toppo, S., Flohé, L., Ursini, F. and Maiorino, M., 2008. The Catalytic Site of Glutathione Peroxidases. *Antioxidants & Redox Signaling*, 10(9), pp.1515-1526.

Touat-Hamici, Z., Bulteau, A., Bianga, J., Jean-Jacques, H., Szpunar, J., Lobinski, R. and Chavatte, L., 2018. Selenium-regulated hierarchy of human selenoproteome in cancerous and immortalized cells lines. *Biochimica et Biophysica Acta (BBA) - General Subjects*, 1862(11), pp.2493-2505.

Trifa, A., Bănescu, C., Dima, D., Bojan, A., Tevet, M., Moldovan, V., Vesa, Ș., Murat, M., Pop, I., Skrypnyk, C. and Popp, R., 2016. Among a panel of polymorphisms in genes related to oxidative stress, CAT-262 C>T, GPX1 Pro198Leu and GSTP1 Ile105Val influence the risk of developing BCR-ABL negative myeloproliferative neoplasms. *Hematology*, 21(9), pp.520-525.

Ursini, F., Heim, S., Kiess, M., Maiorino, M., Roveri, A., Wissing, J. and Flohé, L., 1999. Dual Function of the Selenoprotein PHGPx During Sperm Maturation. *Science*, 285(5432), pp.1393-1396.

van der Vliet, A. and Janssen-Heininger, Y., 2014. Hydrogen Peroxide as a Damage Signal in Tissue Injury and Inflammation: Murderer, Mediator, or Messenger?. *Journal of Cellular Biochemistry*, 115(3), pp.427-435.

VanderVeen, L., Hashim, M., Shyr, Y. and Marnett, L., 2003. Induction of frameshift and base pair substitution mutations by the major DNA adduct of the endogenous carcinogen malondialdehyde. *Proceedings of the National Academy of Sciences*, 100(24), pp.14247-14252.

Voitkun, V. and Zhitkovich, A., 1999. Analysis of DNA–protein crosslinking activity of malondialdehyde in vitro. *Mutation Research/Fundamental and Molecular Mechanisms of Mutagenesis*, 424(1-2), pp.97-106.

Volinsky, R. and Kinnunen, P., 2013. Oxidized phosphatidylcholines in membrane-level cellular signaling: from biophysics to physiology and molecular pathology. *FEBS Journal*, 280(12), pp.2806-2816.

Wang, C., Zhang, R., Chen, N., Yang, L., Wang, Y., Sun, Y., Huang, L., Zhu, M., Ji, Y., & Li, W., 2017. Association between glutathione peroxidase-1 (GPX1) Rs1050450 polymorphisms and cancer risk. *International Journal of Clinical and Experimental Pathology*, 10(9), pp.9527–9540.

Wang, D., Yu, W., Lian, J., Wu, Q., Liu, S., Yang, L., Li, F., Huang, L., Chen, X., Zhang, Z., Li, A., Liu, J., Sun, Z., Wang, J., Yuan, W. and Zhang, Y., 2020. Th17 cells inhibit CD8+ T cell migration by systematically downregulating CXCR3 expression via IL-17A/STAT3 in advanced-stage colorectal cancer patients. *Journal of Hematology & Oncology*, 13, pp.1-15.

Wang, H., Cheng, Y., Mao, C., Liu, S., Xiao, D., Huang, J., & Tao, Y. (2021). Emerging mechanisms and targeted therapy of ferroptosis in cancer. Molecular therapy : the journal of the American Society of Gene Therapy, S1525-0016(21)00151-9.

Wang, H., Schoebel, S., Schmitz, F., Dong, H. and Hedfalk, K., 2020. Quantitative analysis of H2O2 transport through purified membrane proteins. *MethodsX*, 7, p.100816.

Wauchope, O., Mitchener, M., Beavers, W., Galligan, J., Camarillo, J., Sanders, W., Kingsley, P., Shim, H., Blackwell, T., Luong, T., deCaestecker, M., Fessel, J. and Marnett, L., 2018. Oxidative stress increases M1dG, a major peroxidation-derived DNA adduct, in mitochondrial DNA. *Nucleic Acids Research*, 46(7), pp.3458-3467.

Wei, R., Qiu, H., Xu, J., Mo, J., Liu, Y., Gui, Y., Huang, G., Zhang, S., Yao, H., Huang, X. and Gan, Z., 2020. Expression and prognostic potential of GPX1 in human cancers based on data mining. *Annals of Translational Medicine*, 8(4), pp.124-124.

Wei, R., Qiu, H., Xu, J., Mo, J., Liu, Y., Gui, Y., Huang, G., Zhang, S., Yao, H., Huang, X. and Gan, Z., 2020. Expression and prognostic potential of GPX1 in human cancers based on data mining. *Annals of Translational Medicine*, 8(4), pp.124-124.

Wong, H., Dighe, P., Mezera, V., Monternier, P. and Brand, M. (2017). Production of superoxide and hydrogen peroxide from specific mitochondrial sites under different bioenergetic conditions. *Journal of Biological Chemistry*, 292(41), pp.16804-16809.

Wu, W., Li, D., Feng, X., Zhao, F., Li, C., Zheng, S. and Lyu, J., 2021. A pan-cancer study of selenoprotein genes as promising targets for cancer therapy. *BMC Medical Genomics*, 14(78).

Wu, Y., Lee, S., Bobadilla, S., Duan, S. and Liu, X., 2017. High glucose-induced p53 phosphorylation contributes to impairment of endothelial antioxidant system. Biochimica et Biophysica Acta (BBA) - *Molecular Basis of Disease*, 1863(9), pp.2355-2362.

Wu, Y., Yu, C., Luo, M., Cen, C., Qiu, J., Zhang, S. and Hu, K., 2020. Ferroptosis in Cancer Treatment: Another Way to Rome. *Frontiers in Oncology*, 10, p.1924.

Xia, C., Meng, Q., Liu, L., Rojanasakul, Y., Wang, X. and Jiang, B., 2007. Reactive Oxygen Species Regulate Angiogenesis and Tumor Growth through Vascular Endothelial Growth Factor. *Cancer Research*, 67(22), pp.10823-10830.

Yang, W., Soares, J., Greninger, P., Edelman, E., Lightfoot, H., Forbes, S., Bindal, N., Beare, D., Smith, J., Thompson, I., Ramaswamy, S., Futreal, P., Haber, D., Stratton, M., Benes, C., McDermott, U. and Garnett, M., 2013. Genomics of Drug Sensitivity in Cancer (GDSC): a resource for therapeutic biomarker discovery in cancer cells. Nucleic Acids Research, 41(D1), pp.D955-D961.

Zahia, T., Bulteau, A., Bianga, J., Jean-Jacques, H., Szpunar, J., Lobinski, R. and Chavatte, L., 2018. Selenium-regulated hierarchy of human selenoproteome in cancerous and immortalized cells lines. *Biochimica et Biophysica Acta (BBA) - General Subjects*, 1862(11), pp.2493-2505.

Zambrano, S., De Toma, I., Piffer, A., Bianchi, M. and Agresti, A., 2016. NF-κB oscillations translate into functionally related patterns of gene expression. *eLife*, 5(e09100).

Zarkovic, N., Cipak, A., Jaganjac, M., Borovic, S. and Zarkovic, K., 2013. Pathophysiological relevance of aldehydic protein modifications. *Journal of Proteomics*, 92, pp.239-247.

Zhai, J., Jia, Y., Zhao, L., Yuan, Q., Gao, F., Zhang, X., Cai, P., Gao, L., Guo, J., Yi, S., Chai, Z., Zhao, Y. and Gao, X., 2018. Turning On/Off the Anti-Tumor Effect of the Au Cluster via Atomically Controlling Its Molecular Size. *ACS Nano*, 12(5), pp.4378-4386.

Zhang, J., Bajari, R., Andric, D., Gerthoffert, F., Lepsa, A., Nahal-Bose, H., Stein, L. and Ferretti, V., 2019. The International Cancer Genome Consortium Data Portal. Nature Biotechnology, 37(4), pp.367-369.

Zhang, J., Wang, X., Vikash, V., Ye, Q., Wu, D., Liu, Y. and Dong, W., 2016. ROS and ROS-Mediated Cellular Signaling. *Oxidative Medicine and Cellular Longevity*, 2016(4350965).

Zhang, Q., Xu, H., You, Y., Zhang, J. and Chen, R., 2018. High Gpx1 expression predicts poor survival in laryngeal squamous cell carcinoma. *Auris Nasus Larynx*, 45(1), pp.13-19.

Zhang, X., Gao, P., Yang, X., Cai, J., Ding, G., Zhu, X., Ji, Y., Shi, G., Shen, Y., Zhou, J., Fan, J., Sun, H., Yang, L. and Huang, C., 2018. Reduced selenium-binding protein 1 correlates with a poor prognosis in intrahepatic cholangiocarcinoma and promotes the cell epithelial-mesenchymal transition. *Am J Transl Res*, 10(11), pp.3567-3578.

Zhao, H., Liang, D., Grossman, H. and Wu, X., 2005. Glutathione peroxidase 1 gene polymorphism and risk of recurrence in patients with superficial bladder cancer. *Urology*, 66(4), pp.769-774.

Zhuang, M., Chaolumen, Q., Li, L., Chen, B., Su, Q., Yang, Y. and Zhang, X., 2020. MiR-29b-3p cooperates with miR-29c-3p to affect the malignant biological behaviors in T-cell acute lymphoblastic leukemia via TFAP2C/GPX1 axis. *Biochemical and Biophysical Research Communications*, 527(2), pp.511-517.

Zinoni, F., Heider, J. and Bock, A. (1990). Features of the formate dehydrogenase mRNA necessary for decoding of the UGA codon as selenocysteine. *Proceedings of the National Academy of Sciences*, 87(12), pp.4660-4664.

Zmijewski, J., Zhao, X., Xu, Z. and Abraham, E., 2007. Exposure to hydrogen peroxide diminishes NF-κB activation, IκB-α degradation, and proteasome activity in neutrophils. *American Journal of Physiology-Cell Physiology*, 293(1), pp.255-266.

Zoidis, E., Seremelis, I., Kontopoulos, N. and Danezis, G., 2018. Selenium-Dependent Antioxidant Enzymes: Actions and Properties of Selenoproteins. *Antioxidants*, 7(5), p.66.

Appendix

```
BOVINE GPX1 RTVYAFSARPLAGGEPFNLSSLRGKVLLIENVASLUGTTVRDYTQMNDLQRRLGPRGLVV  76
HUMAN GPX1  QSVYAFSARPLAGGEPVSLGSLRGKVLLIENVASLUGTTVRDYTQMNELQRRLGPRGLVV  72

BOVINE GPX1 LGFPCNQFGHQENAKNEEILNCLKYVRPGGGFEPNFMLFEKCEVNGEKAHPLFAFLREVL  136
HUMAN GPX1  LGFPCNQFGHQENAKNEEILNSLKYVRPGGGFEPNFMLFEKCEVNGAGAHPLFAFLREAL  132

BOVINE GPX1 PTPSDDATALMTDPKFITWSPVCRNDVSWNFEKFLVGPDGVPVRRYSRRFLTIDIEPDIE  196
HUMAN GPX1  PAPSDDATALMTDPKLITWSPVCRNDVAWNFEKFLVGPDGVPLRRYSRRFQTIDIEPDIE  192

BOVINE GPX1 TLLSQGAS  204
HUMAN GPX1  ALLSQGLS  200
```

Figure A.1: BLAST alignment of Bovine and human GPX1, with areas of conservation highlighted in yellow.